

Concept design of a multipurpose fatigue testing rig for spreader components

ANDERS BRANDT

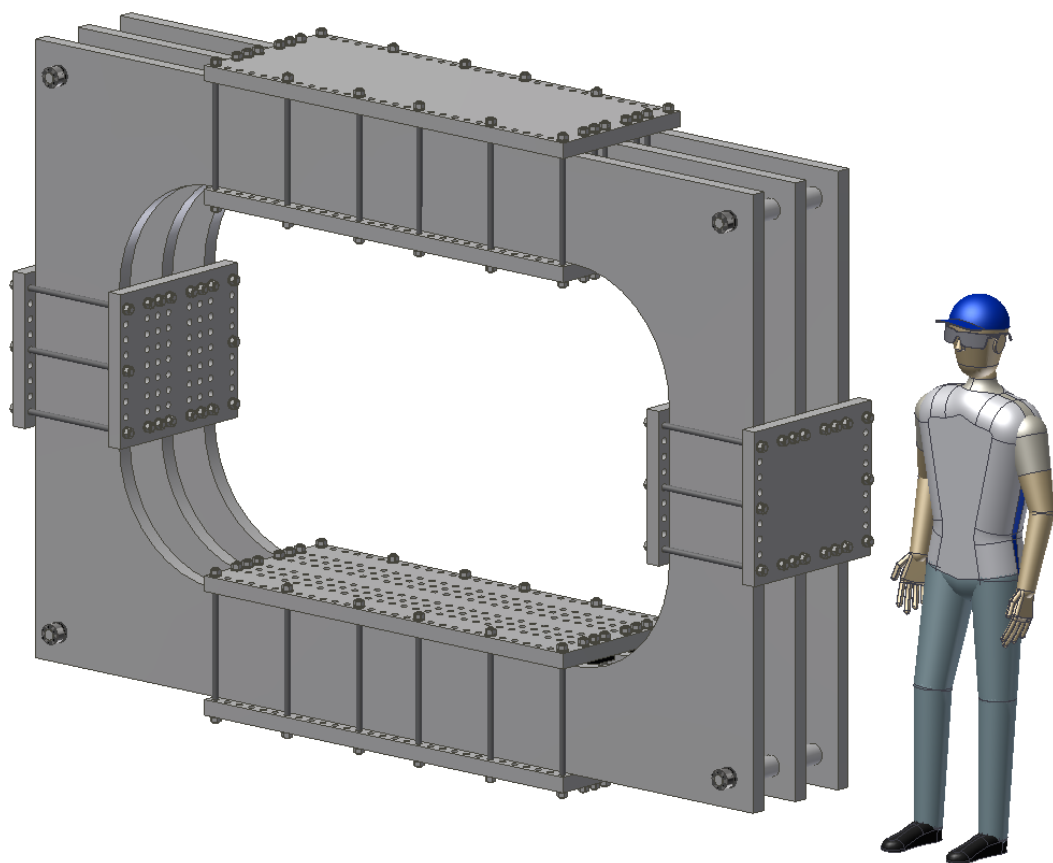


**KTH Industrial Engineering
and Management**

Master of Science Thesis
Stockholm, Sweden 2014

Concept design of a multipurpose fatigue testing rig for spreader components

Anders Brandt



Master of Science Thesis MMK 2014:11 MKN 103
KTH Industrial Engineering and Management
Machine Design
SE-100 44 STOCKHOLM



KTH Industriell teknik
och management

Examensarbete MMK 2014:11 MKN 103

Konceptdesign av en multifunktionell testrigg för utmattningsprovning av lyftokskomponenter

Anders Brandt

Godkänt 2014-05-23	Examinator Ulf Sellgren	Handledare Ulf Sellgren
	Uppdragsgivare Bromma Conquip	Kontaktperson Jerker Lindström

Sammanfattning

Som ett av världens ledande företag inom lyftok har Bromma Conquip skapat sig ett gott rykte när det kommer till tillförlitliga, högpresterande lyftok. Deras framgång har till stor del berott på deras satsningar inom hållfasthetsberäkning (FEM) under utvecklingen av deras lyftok. För att ytterligare kunna förbättra sina lyftok samt verifiera sina beräkningsmodeller, vill de nu utföra riktiga utmattningstester på vissa utvalda komponenter av lyftoket. Det som startade som ett behov från företagets sida, utvecklades med tiden till ett examensarbete där uppgiften blev att designa och dimensionera en testrigg som ska användas för att utmattningstesta tre utvalda lyftokskomponenter.

Fokus för examensarbetet låg på att designa och dimensionera den huvudsakliga stålstrukturen för testriggen och inspänningsverktygen till de tre utvalda lyftokskomponenterna. Avgränsningar gjordes så att varken hydraulsystemet eller styrsystemet för testriggen skulle omfattas i arbetet.

Examensarbetet grundar sig på en informationssökning där viktiga aspekter gällande utmattning utreds och där olika typer av standardiserade utmattningsriggar undersöks. För att skaffa ytterligare kunskap om testriggar för just komponentprovning, gjordes flertalet studiebesök till olika testcenter inom större svenska tillverkningsföretag, där värdefull information kunde inhämtas gällande utmattningsriggarnas utformning samt hur prover installerades i riggarna och hur företagets testprocedurer såg ut.

Under ett brainstorming möte togs flera olika koncept av testriggen fram, där alla utmattningsaspekter från informationsinhämtningen beaktades. Med hjälp av Pugh's matris kunde ett koncept väljas ut som bygger på stora gasskurna plåtar som sätts samman med skruvförband. Dess modulära design och enkelheten i tillverkning av konceptet gjorde att det fick betydligt högre betyg än de andra koncepten. Initiala tester av konceptet visade att dess geometri skulle behöva ändras pga. spänningskoncentrationer i testriggen, men även pga. fysiska begränsningar inne i testriggen.

Designen av det slutgiltiga konceptet för testriggen gjordes samtidigt som designen av fixeringsverktygen för att kunna säkerställa att deras gränssnitt matchar varandra. För att minska belastningen på testriggen utformades ett av fixeringsverktygen så att verktyget i sig blev lastupptagande. Den slutgiltiga dimensioneringen av testriggen påvisar att den klarar av en ekvivalent spänning på 48 MPa, två gånger högre än den belastning testriggen kommer att utsättas för.

Nyckelord: *Lyftok, Utmattning, Utmattningsrigg, Utmattningstester av komponenter*



KTH Industrial Engineering
and Management

Master of Science Thesis MMK 2014:11 MKN 103

Concept design of a multipurpose fatigue testing rig for spreader components

Anders Brandt

Approved 2014-05-23	Examiner Ulf Sellgren	Supervisor Ulf Sellgren
	Commissioner Bromma Conquip	Contact person Jerker Lindström

Abstract

As one of the world leaders in crane spreaders, Bromma Conquip has a high reputation for reliable, high performing crane spreaders. Their success has largely been due to their emphasis on finite element analysis (FEA) during the development of their spreaders. In order to further improve their spreaders as well as verifying their FEA, they have a desire to perform more real testing on certain spreader components. This desire evolved in to a master thesis project where the task was to design and dimension a fatigue testing rig, which could perform fatigue testing on three selected spreader components.

The focus of the thesis was on the design and dimensioning of the main steel structure of the fatigue testing rig and the fixation tools for the three selected spreader components. Limitations were made so that the hydraulic system and control system for the test rig would not be covered in this thesis.

The thesis is founded on an information retrieval where important aspects concerning fatigue are established and where different types of standardized fatigue testing machines are studied. To gain further knowledge about component fatigue testing, several study visits were carried at the fatigue testing laboratories within bigger Swedish manufacturing companies, from which vital information concerning the structure of a test rig as well as test setup and test procedure was retrieved.

Several different concepts for the test rig were generated during a brainstorming session, where all the aspects from the information retrieval were taken into consideration. With the use of Pugh matrix, a concept based on gas cut steel plates that mounts together with bolted joints was selected. Its modular design and the ease of manufacturing made it score well above the other concepts. Initial tests of the concept's revealed that the geometry of the test rig needed to be changed, due to stress concentrations and geometric constraints.

The design of the final concept was made simultaneously as the design the fixation tools, in order to ensure that all the interfaces matched up. To reduce the stress on the test rig, one of the fixation tools was designed basically as an independent load bearing structure within itself. The final dimensioning of the test rig shows that it could withstand an equivalent stress of 48 MPa, twice the stress that it is subjected to.

Keywords: *Spreader, Fatigue, Fatigue testing rig, Component fatigue testing*

FOREWORD

On a more personal note, I would first of all like to thank my industrial supervisor Jerker Lindström and Bromma Conquip in Akalla for enabling this thesis. I'm very pleased that we through close and continuous discussions during the autumn of 2013 managed to form a thesis out of what initially could be seen as a loosely formulated idea. I particularly appreciate that I was given a great deal of influence in defining the thesis, which gave me the possibility to better adapt it more towards my field of study.

I would like to thank Thomas Bergman from HIAB, Joakim Hedegård and Henrik Östling from swerea|KIMAB, Nenad Mrden from Volvo Construction Equipment and Hannes Berg from Scania for sharing your experience concerning fatigue testing, and especially component fatigue testing during the study visit at your fatigue testing laboratories. The knowledge I gained from these visits formed a larger part of the basis for the frame of reference, from which the concepts for the fatigue testing rig could be developed from.

Special thanks go out to my desk neighbor and structural analysis guru Erik Brodin, for the endless support and valuable advices concerning the fatigue dimensioning of the test rig. I'm very grateful that you were always willing to help me out, even during times of doubt. Your input has led me to achieve a higher quality of the thesis.

I would also like to thank the mechanical engineers within the R&D team at Bromma for their valuable input at the "Brainstorming session" during the concept generation. This session helped me widen my views of how a fatigue testing rig could be put together. An extra thanks to those individuals that I could discuss solutions to minor design issues with, during the development of the final concept.

A general thanks to the whole R&D team on the 2nd floor for providing a good atmosphere at the workplace, as well as the morality raising Wednesday-lunch workouts that brought new energy to the thesis during the afternoons.

I want to conclude this section by gently admitting that the scale of the thesis became significantly larger than first anticipated. Due to the extent of the thesis, it went the scheduled time plan, as seen in *Appendix A*. It should however be pointed out the quality of the thesis haven't been compromised, despite the greater work load. Lastly but not least, I want to thank my supervisor at KTH, Ulf Sellgren, for, in hindsight, initially helping me additionally limiting the work for the thesis before the start. As a young and ambitious student, it can sometimes be hard to see ones limitations. I further want to thank Ulf for his support and great patience during the length of the thesis.

Anders Brandt

Kista, May 2014

NOMENCLATURE

The nomenclature is a collection of used symbols and abbreviations within the master thesis. Index “i” is used when notations uses different index throughout the documentation, exact definitions are found in respective section.

Notations

Symbol	Description
---------------	--------------------

A	Amplitude ratio
A_i	Cross section area (m ²)
a_o	Crack initiation (m)
a_r	Critical crack size (m)
b	Width (m)
D	Accumulated damage for Palmgren-Miner (Pa)
D_h	Diameter of the clearance hole for a certain size of (m)
d_i	Diameter (m)
d_p	Pitch diameter of the threads on a bolt (m)
δ	Elongation (m)
Δl	Elongation (m)
E_i	Young’s modulus (Pa)
f	Deflection (m)
FAT	Fatigue class
F_i	Force (N)
H	Head size of a hexagonal bolt (m)
h	Height (m)
I_i	Area moment of inertia (mm ⁴)
k_i	Stiffness (N/m)
k_m	Stress intensity factor
l	Length (m)
L_i	Length (m)
m	Exponent of the S-N curve
M_i	Torque (Nm)
M_{max}	Maximum torque (Nm)
n_i	Estimated number of cycles for each load in each load case
n_t	Sum of all the number of cycle for all the load cases at all loads
N	Number of load cycles

N_s	Number of bolts in a bolted joint
N_t	Dimensioning number of cycles before fatigue failure
$N_{t_{sum}}$	Sum of the estimated amount of cycles for all loads in all load cases
P	Pressure (Pa)
P_k	Force at which a simply supported column risks to buckle (N)
R	Stress ratio
σ_i	Stress (Pa)
σ_a	Stress amplitude (Pa)
σ_e	Fatigue strength (Pa)
σ_m	Mean stress (Pa)
σ_{max}	Maximum stress (Pa)
σ_{min}	Minimum stress (Pa)
σ_r	Stress range (Pa)
σ_u	Ultimate strength (Pa)
σ_{up}	Allowed stress amplitude for a bolt (Pa)
σ_y	Yield strength (Pa)
$\Delta\sigma_i$	Stress range (Pa)
$\Delta\sigma_{Rd}$	Maximum allowed stress range (Pa)
$\Delta\sigma_{ref}$	Reference value of the stress range (Pa)
$\Delta\sigma_{eq,S,d}$	Equivalent constant amplitude stress range (Pa)
s_m	Allowable design stress intensity value
t_f	Thickness of flange (m)
t_w	Thickness of web (m)
τ	Ratio of each estimate amount of cycles for each load in each load case divided by the sum of the estimated amount of cycles for all loads in all load cases
φ_e	Stress alternating factor
φ_m	Material thickness
φ_t	Thickness factor
γ_m	Partial factor of safety
$ z _i$	Absolute distance from the central plane of the cross section of a beam to where the stress/torque acts on the beam (m)

Abbreviations

<i>ANSYS</i>	Finite Element Analysis Software
<i>BSK</i>	Boverkets handbok om stålkonstruktioner (The National Board of Housing's handbook on steel structures)
<i>CAD</i>	Computer Aided Design
<i>FEA</i>	Finite Element Analysis
<i>HCF</i>	High cycle fatigue
<i>HEB</i>	Standardized H-beam
<i>IIW</i>	International Institute of Welding
<i>IPE</i>	Standardized I-beam
<i>KTH</i>	Kungliga Tekniska Högskolan (Royal Institute of Technology)
<i>LCF</i>	Low cycle fatigue
<i>LVDT</i>	Linear variable differential transformer
<i>MATLAB</i>	Multi-paradigm numerical computing software
<i>R&D</i>	Research and Development
<i>S-N</i>	Stress range – Number of cycles

TABLE OF CONTENTS

SAMMANFATTNING (SWEDISH)	i
ABSTRACT	iii
FOREWORD	v
NOMENCLATURE	vii
TABLE OF CONTENTS	xi
1 INTRODUCTION	1
1.1 Background	1
1.2 Purpose	2
1.3 Delimitations	2
1.4 Method	3
2 FRAME OF REFERENCE	4
2.1 Spreaders	4
2.2 Fatigue	6
2.3 Fatigue testing machines	14
3 DESIGN PROCESS	27
3.1 Fatigue loads for the three spreader components	27
3.2 Requirements specification	29
3.3 Concept generation	30
3.4 Concept selection	38
3.5 Concept testing	42

4	FINAL CONCEPT	57
4.1	General design and dimensioning process	57
4.2	Main steel structure	63
4.3	Fixation tools for the three selected spreader components	67
4.4	Final dimensioning	80
5	DISCUSSION AND CONCLUSIONS	83
5.1	Discussion	83
5.2	Conclusions	84
6	FURTHER DEVELOPMENT AND FUTURE WORK	85
6.1	Further development	85
6.2	Future work	86
7	REFERENCES	87
	APPENDIX A: GANTT CHART	I
	APPENDIX B: CALCULATIONS OF LOAD CASES FOR THE THREE SELECTED SPREADER COMPONENTS	IV
	APPENDIX C: PUGH’S MATRIX	XII
	APPENDIX D: FEA OF MAIN PLATE FOR CONCEPT TESTING	XIII
	APPENDIX E: MATLAB CODE FOR THE INTITAL TESTING	XVI
	APPENDIX F: MATLAB CODE FOR LOAD BEARING I-BEAM FOR THE CENTER WEB PLATE SUBSTRUCTURE	XXI
	APPENDIX G: FEA OF MAIN LOAD BEARING BEAMS FOR THE CENTER WEB PLATE SUBSTRUCTURE	XXII
	APPENDIX H: FEA OF THE MAIN STEEL STRUCTURE OF THE FATIGUE TESTING RIG	XXIV

1 INTRODUCTION

The introduction chapter presents the background, purpose and delimitations of the master thesis, as well as the selected method for realizing it.

1.1 Background

As one of the world's technical leaders in crane spreaders, the company "Cargotec Sweden AB, Bromma Conquip" (hereafter only referred to as Bromma) has a high reputation when it comes to reliable, high performance crane spreaders. A vital part in their design work is the finite element analysis (FEA) which they use to dimension their spreaders and its crucial components to ensure a high fatigue life for their products. (Bromma, 2013) To be able to verify the FEA-models, fatigue tests have to be made on separate components on the spreaders and steel substructures that are most subjected to fatigue. While Bromma has their own test center with several fatigue testing rigs at their manufacturing facility in Ipoh, Malaysia, some fatigue testing have to be outsourced to another company within the Cargotec Group, HIAB in Hudiksvall, Sweden. This due to that Bromma hasn't got a suitable test rig for some of the components that need testing. The fatigue testing rig from HIAB, in which previous fatigue testing of Bromma's spreader components have been performed, is shown in Figure 1.1.



Figure 1.1. The fatigue testing rig at HIAB in Hudiksvall (Bergman, 2013)

Due to the limited space within the steel structure of the fatigue testing rig, as seen in Figure 1.1, new larger components couldn't be tested in this specific rig. Due to this issue Bromma wants to design their own fatigue testing rig that is more suitable for testing their components.

The new fatigue testing rig will allow Bromma to get better traceability of the tests, since they can be done in-house and testing can be closer linked to manufacturing. It will also reduce both cost and lead time by not having to outsource the testing.

1.2 Purpose

The purpose of this master thesis is to mechanically design a fatigue testing rig for testing three selected spreader components (Figure 1.2), each with its own defined load spectrum that will be given by Bromma. Fixation tools will also be designed for fixating these components correctly in the test rig, so that the desired load cases can be achieved.

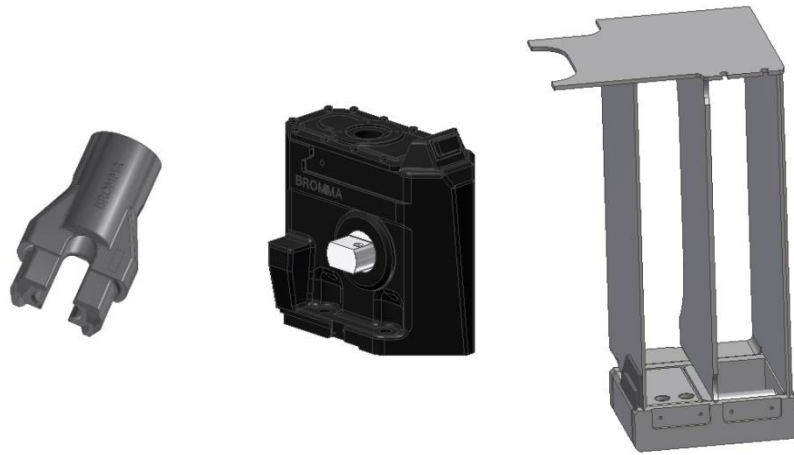


Figure 1.2. The three selected spreader components: Guide block, gearbox housing and center web plate substructure

The fatigue testing rig with its separate components such as the hydraulic cylinders, shafts, sensors, etc. as well as the fixation tools should be dimensioned to withstand fatigue for the load spectrums that are defined for the three selected spreader components. It's however beneficial if the design and functionality of the test rig is flexible enough so that other similar components can be tested in the future, with the help of other fixation tools.

1.3 Delimitations

Delimitations have to be made in order to scale the scope of the master thesis, in order to complete the thesis within the recommended time given by KTH.

The focus of the thesis will be on the design and dimensioning of the main steel structure that will form the basis of the fatigue testing rig, as well as the three fixation tools. CAD-models for the final design of the fatigue testing rig, as well as the fixation tools will be made, but no detailed drawings or manufacturing documentation will be presented in this thesis. The outcome from the thesis will form the basis for a fatigue testing rig that will be further developed and manufactured by Bromma. However no prototype of the final concept of the test rig will be made during the thesis.

The test rig will be dimensioned to withstand fatigue from the applied load spectrums given for the three selected spreader components, by using calculations from mechanics of solids and performing FEA to establish the stresses within the test rig.

Suitable hydraulic cylinders will be selected for the test rig, to fulfil the necessary load spectrums specified to test the three selected spreader components. The dimensioning of a complete hydraulic system for the fatigue testing rig will not be covered in this thesis.

Sensors will be incorporated into the final concept of the test rig, so that important data such as, applied force, deflection, etc. can be recorded during the tests. Recommendations for suitable sensors for the fatigue testing rig will be made, depending on the layout of the test rig and the preferred control system.

1.4 Method

A systematic approach to concept development is essential when developing any new product. To have the best chance of achieving a well thought out design for the fatigue testing rig, the main structure of a concept development process will be followed throughout the thesis according to Ulrich and Eppinger's (2012) the "Front-End Process" as seen in Figure 1.3.

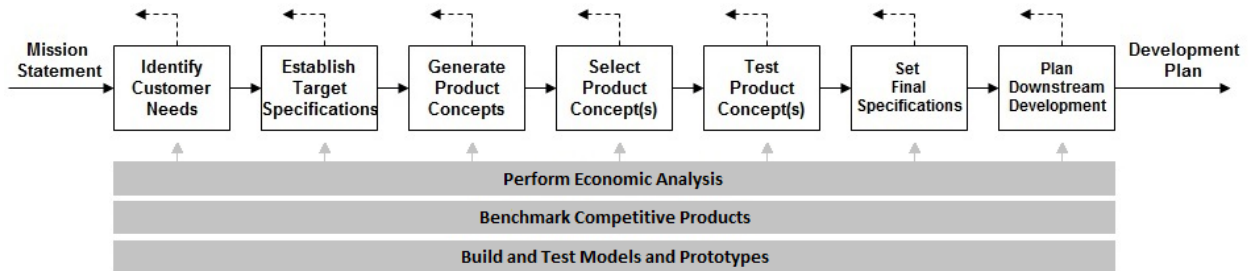


Figure 1.3. The Front-End Process (Ulrich & Eppinger, 2012)

When designing a new product it's common that some stages in the concept development have to be overlapped and iterations have to be made during the process (see dashed arrows in Figure 1.3). The following stages in this process is be defined below.

Identifying customer needs: Bromma Conquip has clarified that they are in need of a new fatigue testing rig, as presented in *1.1 Background* and *1.2 Purpose*.

A frame of reference will be made to get a deeper knowledge of the relevant areas that the project will cover, such as spreaders in general, how to design for fatigue life and how different types of fatigue testing machines function. A study visit to HIAB and other bigger Swedish manufacturing companies is made to study their fatigue testing rigs and gather information about how they perform their testing.

Establishing target specifications: A requirement specification is made to establish the essential features that the fatigue testing rig needs to fulfill. Other desirable features to the rig are also taken into consideration to the requirement specification.

Concept generation: With the help of underlying knowledge from the frame of reference and the knowledge gained from study visits to the bigger Swedish manufacturing companies, simplified concepts of the fatigue testing rig are derived during a brainstorming session.

Concept selection: The generated concepts are evaluated and compared against each other, using Pugh's decision matrix (Frank Cervone, 2009). It's done by scoring how well each concept fulfills the different factors that are both derived from the requirement specification and in regard to manufacturing, assembly and usability.

Concept testing: The concept that has scored the highest result according to Pugh's matrix is designed to a full scale CAD-model. This is done in order to verify that all of the three specific components that are going be tested fits in the test rig and can be tested in the way that Bromma intends to. Initial calculations and FEA will be performed to dimension the fatigue testing rig. This is an iterative process that can lead to several redesigns of the first concept.

Setting final specifications: When the design for the main steel structure of the test rig is dimensioned, the fixation tools for the three selected components can be designed and incorporated into the test rig, as well as suitable hydraulic cylinders and sensors. Depending on the mountings of the fixations tools within the main steel frame, some modifications are made to the test rig. Final dimensioning of the test rig, for the three different setups with the fixation tools for each selected spreader component, is made in order to verify that it can withstand the fatigue of the subjecting loads.

All the gathered information and results from each task of the concept process development is continuously included to the final report of the thesis.

2 FRAME OF REFERENCE

The frame of reference chapter presents information concerning different aspects that should be taken into consideration when designing a fatigue testing rig for spreader components. Information about how spreaders function, fatigue in general, established fatigue testing machines and existing fatigue testing rigs for component testing is studied.

2.1 Spreaders

A spreader is a device that's used for lifting intermodal containers and unitized cargo (Figure 2.1). They are mainly used in ports, so called maritime container terminals, for loading and unloading containers from container ships, as well as handling and stacking containers in the ports' yards. Spreaders are also used at inland container terminals, where containers are loaded and unloaded from trains onto trucks. (Steenken, et al., 2004)



Figure 2.1. Example of a Bromma spreader lifting a container (Credit1Coach, 2012)

Spreaders enable containers to be moved more rapidly, due to its design of how it attaches and detaches to containers. This means that containers can be loaded and unloaded faster to and from the transport vessels, which leads to higher efficiency and reduced cost per moved goods for the container terminal. (SORT+STORE, 2004/2005)

The working principal of a spreader is as follows: The spreader is lowered down from a crane onto a container. To simplify the task of lining up the spreader correctly onto the container, guide arms are lowered from the corners of the spreader to roughly steer the spreader into the right position over the container, as seen in Figure 2.2. The next stage is then to line up the twistlocks into the corner casts of the container. The twistlocks have an arrow-style tip so that they can slide into the corner casts if the position of the spreader is not fully aligned during the descent. (Bromma, 2013)

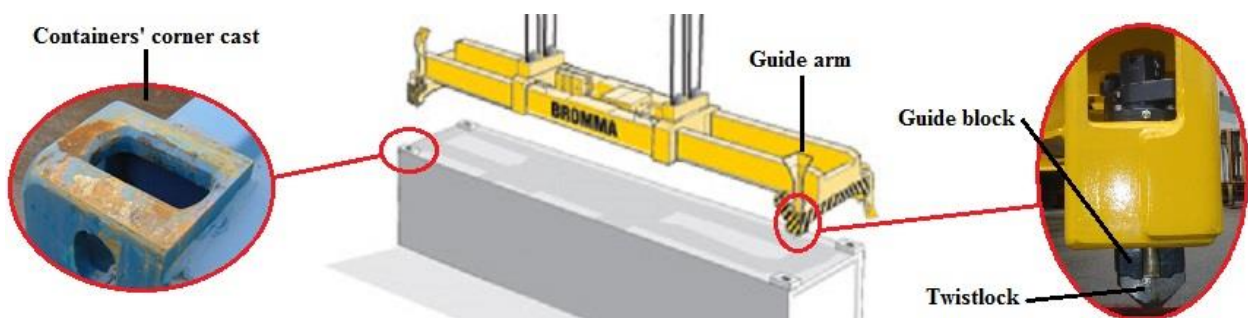


Figure 2.2. Attaching the spreader to a container

When the spreader lands on the container, the guide blocks secure the alignment of the spreader so that it doesn't move after the tip of the twistlocks have passed through the upper flange of the corner casts. The twistlocks are then turned 90 degrees so that the spreader locks on the container. The container can now be lifted with the spreader. (Bromma, 2013)

Spreaders are designed to handle the most common intermodal container sizes, which are the ISO-standard 20' and 40' containers as well as the U.S.-standard 45' containers. Depending on the needs of the container terminal, different types of spreaders with different functions can be used. Most types of spreaders used today have a telescopic function, allowing the operators to lift to lift both 20' and 40' or 45' with the same spreader. A high proportion of these spreaders also have a twin-lift function, enabling them to lift two 20' containers in one lift. An example of such a spreader can be seen in Figure 2.1. (Bromma, 2013)

The most common type of crane spreaders are: ship-to-shore, mobile harbor and yard spreaders, as seen in Figure 2.3. The ship-to-shore spreaders are used by quay cranes to move containers from the ships to the shore, either placing them directly on the quay or on a vehicle. The mobile harbor spreaders are used by mobile harbor cranes to load and unload containers from smaller container ships to the shore. This type of crane is most commonly used in smaller ports, but is also utilized along the smaller quays in bigger ports. The yard spreader is used by gantry cranes as well as the straddles and shuttle carriers. (Steenken, et al., 2004) These three types of spreaders are designed and dimensioned slightly different from each other, even though they can perform the same functions. The ship-to-shore spreader is generally the most robust designed out of the three, because it's subjected to higher loads during landing and lifting due to greater lifting speed by the quay cranes.

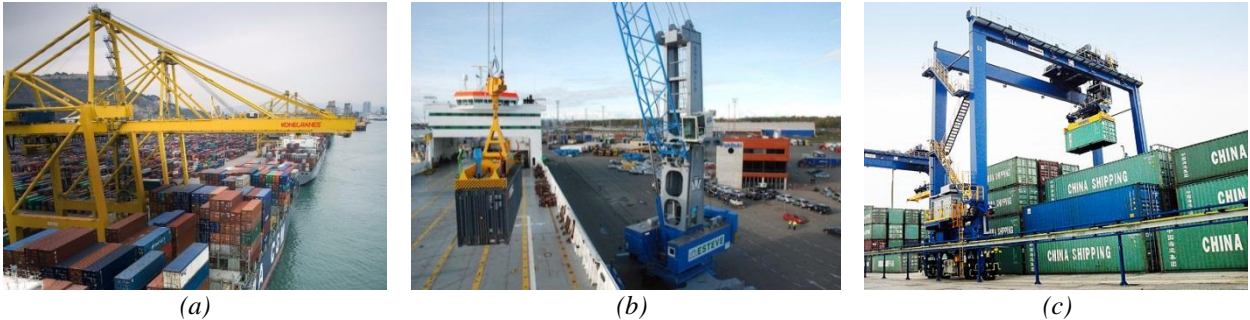


Figure 2.3. Cranes that uses spreaders: a) Quay crane (Konecranes, 2013), b) Mobile harbor crane (Esteve, 2012), c) Yard crane, in this case a rubber tired gantry crane (Terex, 2013)

Crane spreaders are one of the most highly stressed components within the container handling process (Geis, 2013). Due to container terminals constant effort to achieve a higher efficiency in their operation, more moves per hour have to be achieved. This results in that the crane driver is forced to operate the crane faster, thus subjecting the spreader and its components to higher shock loads during landing and lifting. It also increases the risk of damaging the spreader from it colliding into other containers, ship structures or due to misalignment when landing on a container.

2.1.1 Selected spreader components for testing

In order to get a better understanding of where the selected spreader components are situated on a Bromma spreader, all three components are highlighted in red in Figure 2.4. The CAD-model of the spreader has been slightly altered in the way that some parts have been removed from the complete spreader, in order to get a better view of the position of the three selected components. The function of each selected spreader component is further explained in the following paragraph.

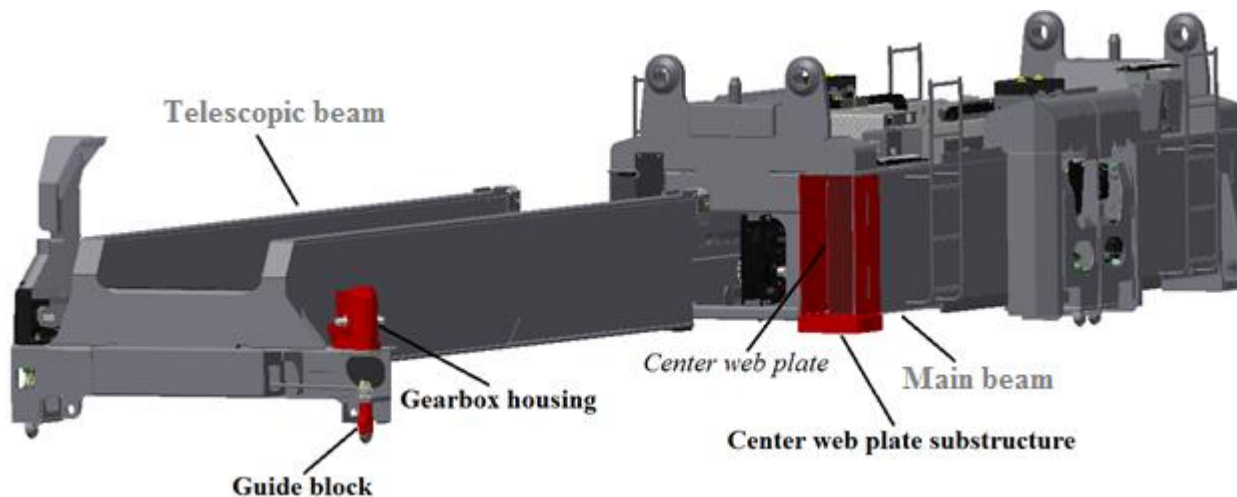


Figure 2.4. A simplified CAD-model of a full-electric Bromma ship-to-shore spreader, with the three selected spreader components highlighted in red

The guide blocks help to align the spreader during the final stage of the landing onto a container, so that the twistlocks can be turned without getting snagged in the container's corner casts due to misalignment. The guide blocks are subjected to high shock loads if the spreader misses the holes of the container's corner casts so that the twistlocks bang into the top of the container. The load from the impact is transferred from the twistlock, through the guide block, to the steel frame of the spreader.

The gearbox with its top-mounted electric or hydraulic motor lowers and raises the guide arms on the spreader. If the spreader hits a container with one of its guide arms in a lowered position during the descent to a container, the force from the impact will be transferred from the guide arm to the gearbox housing.

The center web plate is an extra strengthening plate within each end of the two main beams on the mainframe. The main beams form a type of box sections where the telescopic beams slide within, when telescoping between 20' mode to 40' or 45' mode (see Figure 2.1). When in 40' or 45' mode, the telescopic beams act as levers when a container is lifted, amplifying the load force from the container to the flanges on the main beam. The center web plate reduces the deflection of the flanges, as well as lowering the overall stresses in the ends of the main beams.

2.2 Fatigue

Fatigue is when a material is subjected to repeated or fluctuating strain at nominal stresses that have a maximum value less than the ultimate tensile strength or even more often less than the yield strength of the material. Fatigue may lead to cracks in the structure and cause fracture after a sufficient number of fluctuations. The shape of the structure will significantly affect the fatigue life; square holes or sharp corners will lead to increased local stresses where fatigue cracks can initiate. It's been estimated that fatigue contributes to approximately 80 to 90 percent of all mechanical service failures (Campbell, 2008). (Boardman, 1990)

The fracture features of a fatigue failure are divided into three different stages: *crack initiation*, *crack propagation* and *final fracture* as seen in Figure 2.5. Micro-cracks a_o are initiated due to cyclic plastic deformation, typically where there is a discontinuity in the material. These cracks are generally not discernible to the naked eye. A stress concentration will form around the micro-crack and it will locally plasticize, which in turn leads to the crack propagation. When looking at the surface of a fatigue failure (Figure 2.5), the propagation of the crack can clearly be seen as wavy dark and light bands that can be referred to as *beach marks*. The crack propagates exponentially until it has reached a critical size a_{cr} , as seen in Figure 2.6 (Bakhitiari, 2013). The final, sudden fracture then occurs during the final stress cycle when the remaining material in the cross section can't support the loads any more. (Shigley, et al., 2003)

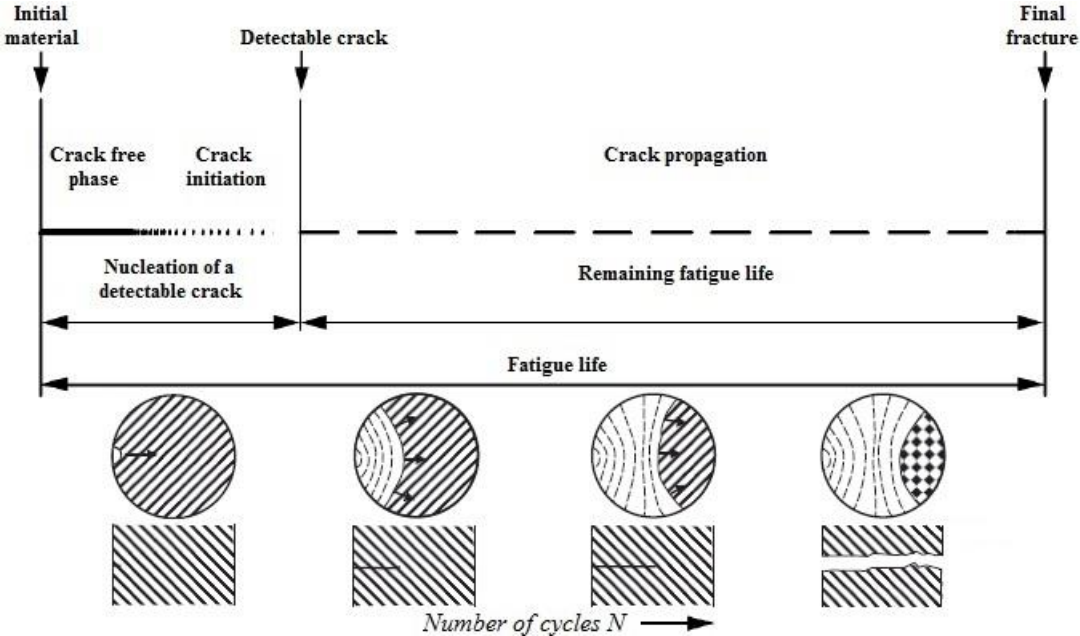


Figure 2.5. The different phases of fatigue life (Bakhitiari, 2013), (Campbell, 2008)

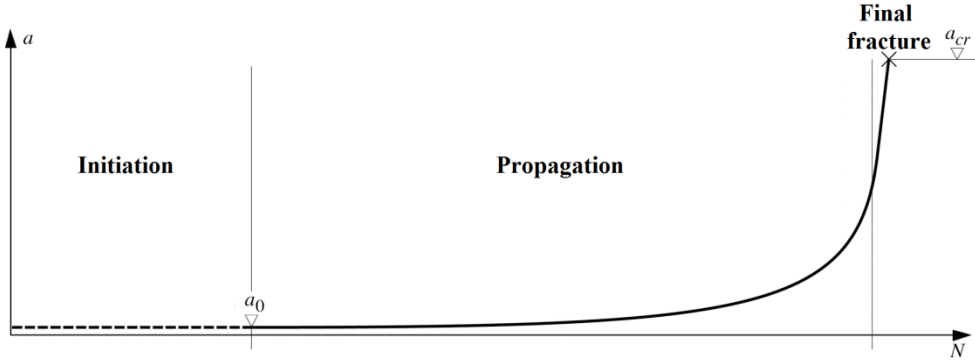


Figure 2.6. Crack propagation until a fatigue failure during constant amplitude loading (Bakhitiari, 2013)

where a is the crack size, a_o is the size of the initial crack, a_{cr} is the critical size of the crack and N is the number of cycles.

Fatigue failures can be considerably reduced by taking more consideration to design details and manufacturing processes. The first and most fundamental approach is to reduce stress concentrations by streamlining the parts, such as increasing the radius in sharp corners. Improvements in the fabrication of the parts as well as the fastening procedures should be made and sharp surface tears from punching, stamping or shearing should be avoided. Tensile residual stresses caused by manufacturing due to heat treatment or welding should also be reduced or fully eliminated if possible. (Boardman, 1990)

2.2.1 Cyclic loading

There are three rudimentary factors needed to cause fatigue: A maximum tensile stress of sufficiently high value, a large enough fluctuation in the applied stress and a sufficiently large number of cycles of the applied stress. Cyclic loading can be applied as cyclic axial stresses, cyclic bending stresses and cyclic torsional stresses (Fatemi, 2013). The cyclic stresses are often described as a sinusoidal pattern, which are determined by their different stress values, as shown in Figure 2.7a. Cyclic loading can be described in various types of stresses within the three categories of compressional stress, alternating stress and tensile stress. These different types of cyclic loading are described and illustrated in Figure 2.7b. (Shigley, et al., 2003).

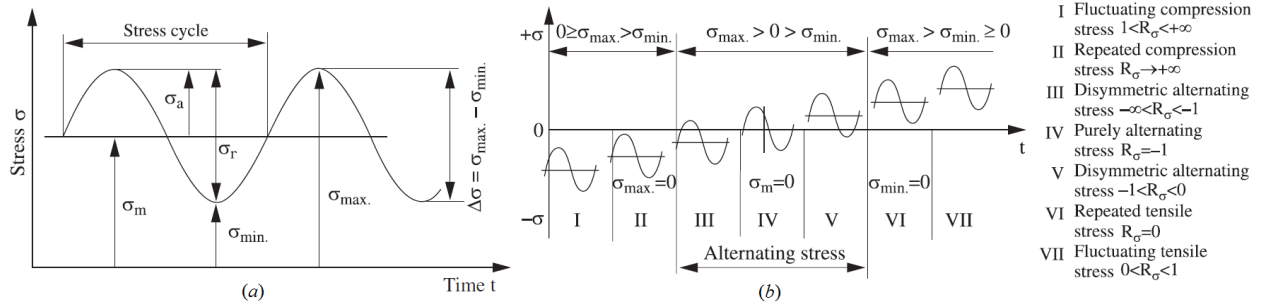


Figure 2.7. a) Different stress values for cyclic loading b) Repeated c) Fluctuating (François, 2008)

where σ_{max} is the maximum stress, σ_{min} is the minimum stress and $\Delta\sigma$ is the stress range.

The definitions of the different stresses are shown in equation (1)-(5).

$$\text{Mean stress} \quad \sigma_m = \frac{(\sigma_{max} + \sigma_{min})}{2} \quad (1)$$

$$\text{Stress amplitude} \quad \sigma_a = \frac{(\sigma_{max} - \sigma_{min})}{2} \quad (2)$$

$$\text{Stress range} \quad \sigma_r = 2\sigma_a = \sigma_{max} - \sigma_{min} \quad (3)$$

$$\text{Stress ratio} \quad R = \frac{\sigma_{min}}{\sigma_{max}} \quad (4)$$

$$\text{Amplitude ratio} \quad A = \frac{\sigma_a}{\sigma_m} = \frac{1-R}{1+R} \quad (5)$$

Load spectrums are commonly used when performing fatigue tests. They consist of several loads with different stress amplitude that occur in different quantities. The lower loads are usually in higher quantities within the spectrums compared to the higher loads. A load spectrum can be strictly systematical by repeating a periodic load cycles as seen in Figure 2.8, or it can be made up by a so called random load cycle. Combinations and intermediate forms of load spectrums are also common. (Sundström, 1999)

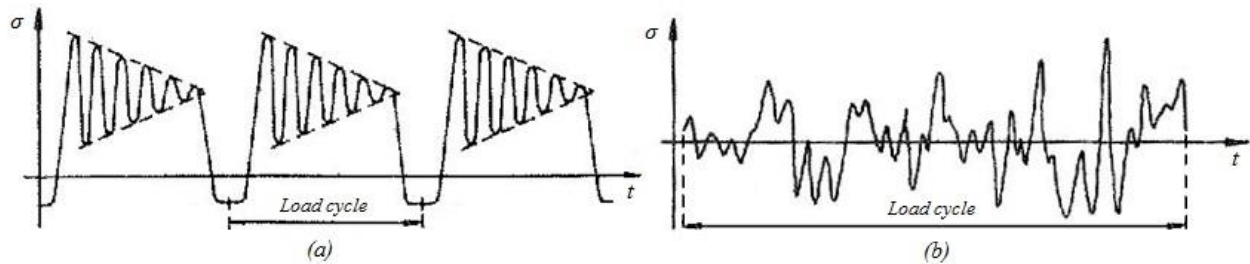


Figure 2.8. Load spectrums with a) periodic load cycle b) random load cycle (Sundström, 1999)

There are several different methods of calculating the fatigue stresses within a random load cycle spectrum, such as peak, range, level-crossing and rain-flow. Each of these methods (not covered in the report) leads to slightly different results, depending on what stresses are most interesting in the load spectrum. In general, these methods are used to find the global extreme values within the load spectrum, while small load variations are neglected. (Sundström, 1999)

Companies such as Volvo Construction Equipment and Scania regularly collect stress-data from their products when they are test driven under normal conditions. These data are adjusted to a specific load spectrum, often a periodical load spectrum, which can be used for fatigue testing. When performing the fatigue testing, it is not essential that the complete load spectrum is fully replicated. As long as the extreme values in the loads spectrum has been reached in the test. (Mrden, 2013)

2.2.2 S-N Diagram

S-N diagram (Stress range – Number of cycles diagram), also known as a Wöhler diagram, is used to illustrate the fatigue strength of a test specimen or an actual component against the number of load cycles to failure. The fatigue strength is the stress to which a component can be subjected to for a specified number of cycles (Boardman, 1990). To establish the fatigue strength of a component, a number of fatigue tests are required. The tests are done under constant amplitude loading, usually with a reversed stress cycle, where the first sample is subjected to a maximum stress slightly below the ultimate tensile stress σ_u of the component. The amount of load cycles the component can withstand before failure is counted and the result is registered in a log-log S-N diagram. This process is then repeated with gradually decreased fatigue stress. When a sufficient number of tests have been performed, a S-N curve can be plotted in the diagram as shown in Figure 2.9. (Shigley, et al., 2003)

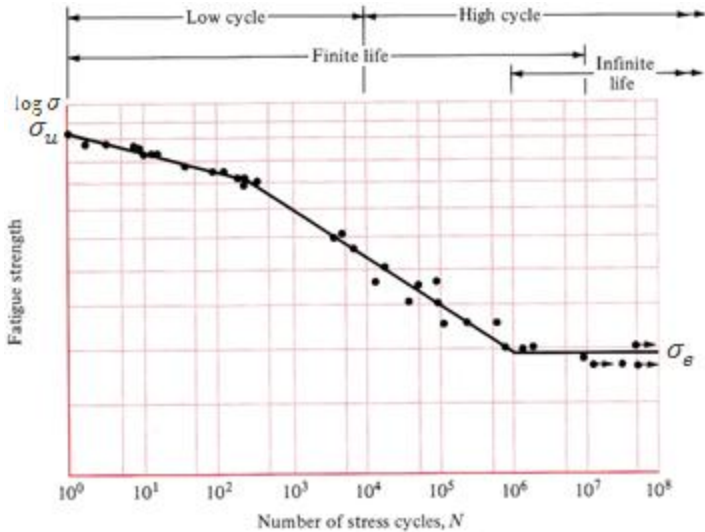


Figure 2.9. An S-N diagram plotted from the results of a reversed stress cycle fatigue test (Shigley, et al., 2003)

where the fatigue strength corresponds to the stress range σ_r used in each specific fatigue test and N is the number of load cycles.

The typical bends of the S-N curve can easily be distinguished when using the log-log diagram. The first bend is within the transition area between low and high cycle fatigue and the second bend shows the significant knee of the S-N curve. The fatigue strength corresponding to the knee is called the endurance limit σ_e or the fatigue limit. In the case of steel, the curve becomes horizontal at the knee as shown in Figure 2.9, which in turn means that fatigue failure will not occur during stresses below the fatigue limit and thereby enable an infinite life. For nonferrous

metals and alloys, the slope of the curve only decreases at this second bend but never becomes fully horizontal, hence these materials don't have a fatigue limit. The fatigue limit for e.g. aluminum is usually reported as the stress level it can survive at $N = 5 \cdot 10^8$ load cycles. (Shigley, et al., 2003)

Experimental data obtained from fatigue testing are scattered, which means that the results in the S-N curves have a failure probability of 50%, due to the adaptation of the curve to the results (see Figure 2.10a). When performing fatigue tests with spectrum loading, if the maximum stress range is higher in the spectrum than the endurance limit, the applied stress range below the fatigue limit will become important in the fatigue life of the component. The S-N curve after the knee should in this case be modified with a slight slope in the curve as seen in Figure 2.10b. (Sundström, 1999), (Bakhitiari, 2013)

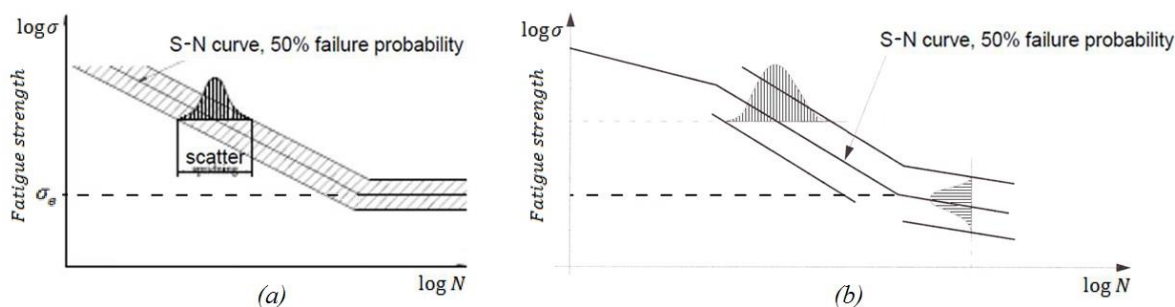


Figure 2.10. Failure probability when testing with a) Constant loading (Bakhitiari, 2013)
b) Spectrum loading (Sundström, 1999)

Failure probability

When dimensioning a structure against fatigue, predetermined S-N curves are provided for consideration of normal or shear stress ranges. These S-N curves have a certain failure probability, depending on which standard that is used. When dimensioning according to SSAB's "Design handbook" (SSAB, 2010) or according to "Boverkets handbok om stålkonstruktioner" (BSK07), the failure probability in the dimensioning S-N-curves are 2,3 %, while the IIW Fatigue recommendations have a 5% failure probability when dimensioning according to their document, "IIW document XIII-2151-07 / XV-1254-07" (Hobbacher, 2007). If a structure has to be dimensioned with a failure probability lower than the one given in the standard, a certain fracture risk factor can be added to the calculations. If the failure probability is lowered from 2,3 % to 1 ‰, it can be seen as lowering the S-N curve one standard deviation in the diagram. (Olsson, 2007)

Low cycle fatigue life and High cycle fatigue life

Low cycle fatigue (LCF) occurs generally at less than 10^4 cycles and is characterized by high stress amplitude that's greater than the yield strength of the material. Fatigue failure by LCF is propagation-dominated and controlled by the alternating strain amplitude, hence ductility of the material. A strain-life method is therefore used to calculate the fatigue life for these applications. (Shigley, et al., 2003)

High cycle fatigue (HCF) occurs generally at cycles greater than 10^4 and the stress amplitude is lower, or even much lower, than the yield strength of the material. Fatigue failure by HCF is dominated by the crack initiation stage and controlled by the maximum shear stress. A stress-life method is used to calculate the fatigue life for these applications. Even though this method is less accurate than the strain-life method (used in LCF), it's the most traditional method used due because it's the easiest to implement during testing and a lot of data published about it. (Shigley, et al., 2003)

Finite and Infinite life

If a component is designed within the *finite-life region*, it will be subjected to fatigue strength above the fatigue limit and the component will eventually fail after a sufficient amount of load cycles. If the component is designed within the *infinite-life region*, it will be subjected to fatigue strength under the fatigue limit and will therefore not fail. The boundary between these regions cannot be clearly defined, except for steel where it lies between the region of 10^6 - 10^7 cycles, as seen pervious in Figure 2.9. (Shigley, et al., 2003)

2.2.3 The effect of life in fluctuating cycle loading

To illustrate the effect of mean stress in fluctuating cycle loads, a Goodman diagram is most commonly used. In Figure 2.11 a modified Goodman diagram is illustrated, where the mean stress σ_m is plotted along the abscissa, and all other components of stress plotted on the ordinate, with tension in the positive direction. (Shigley, et al., 2003)

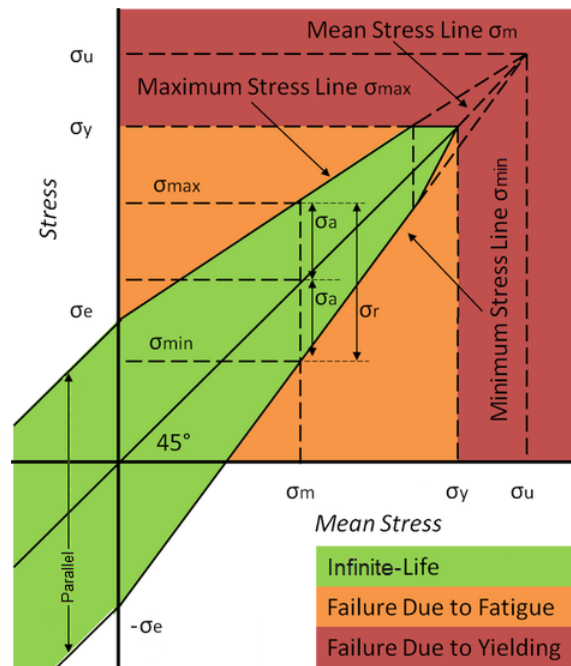


Figure 2.11. Modified Goodman diagram (Wimer, 2013)

The modified Goodman diagram is plotted by using the ultimate tensile stress σ_u , the yield stress σ_y and the materials fatigue limit σ_e from the ordinate, as well as the 45° mean stress line from the origin to the tensile strength of the material, as seen in Figure 2.11. Each modified Goodman diagram is different depending on the ultimate tensile stress and yield stress for the material and crucially deepening on its fatigue limit σ_e . If the material is steel, then the fatigue limit will be at the knee in the S-N curve and will therefore have an infinite-life if the mean stress σ_m and the stress range σ_r are within the boundaries as shown in green in Figure 2.11. If the stress range exceeds the boundaries in the modified Goodman diagram, the material will fail due to fatigue. (Shigley, et al., 2003)

The criterion equation for the modified Goodman relation is

$$\frac{\sigma_a}{\sigma_e} + \frac{\sigma_m}{\sigma_u} = 1 \quad (6)$$

If the material is subjected to a compressional cyclic load, the boundary lines for an infinite life will stay parallel with the mean stress line, as seen in Figure 2.11, until the maximum

compressional stress reaches the yield strength of the material, i.e. the sum of the mean stress and the amplitude stress σ_a are equal to the yield stress. This is due to the fact that tensile mean stresses propagate initial cracks and are therefore detrimental, while compressive mean stresses are beneficial (Fatemi, 2013). (Shigley, et al., 2003)

Constant fatigue life

The constant fatigue diagram is a unique way of displaying four of the stress components as well as the two of the stress ratios within the same diagram. A curve representing the fatigue limit for a specific material (in this case AISI 4340) for values of $R = -1$ to $R = 1$ begins at the fatigue limit σ_e on the alternative stress axis σ_a i.e. amplitude stress and ends at the ultimate tensile stress σ_u on the mean stress axis σ_m . Constant life curves for $N = 10^4, 10^5$ and $10^6 \& 10^7$ are shown in Figure 2.12, both for unnotched and notched materials. (Shigley, et al., 2003)

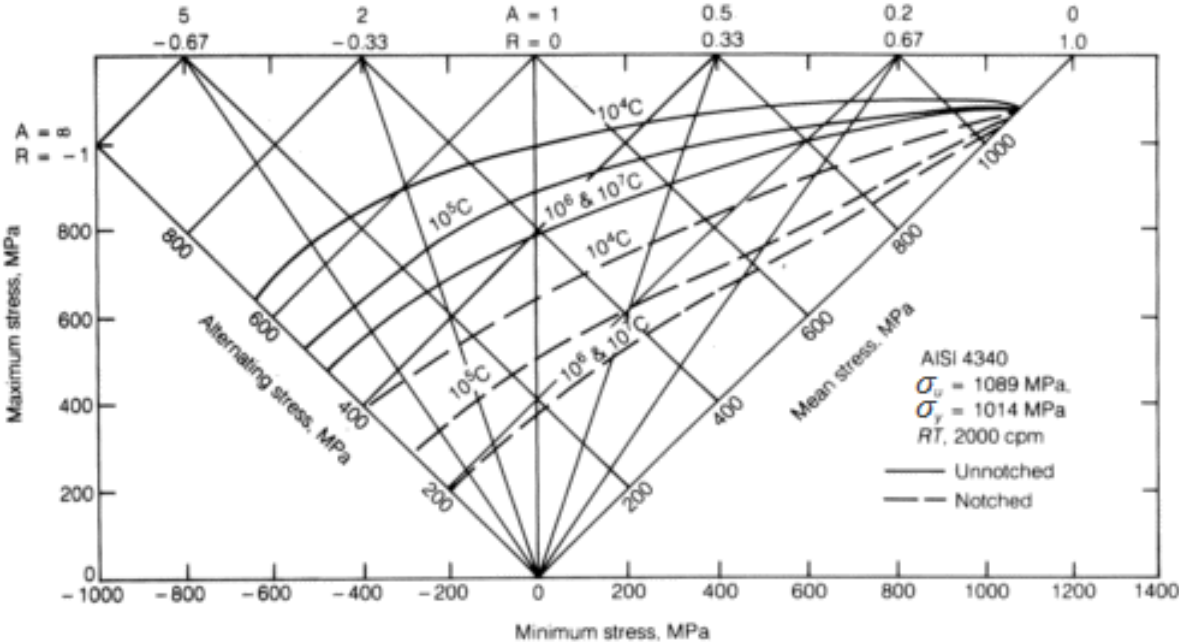


Figure 2.12 Constant fatigue life diagram of AISI 4340 steel (eFunda, 2014)

Any stress state can be described by the minimum and maximum components, which gives the stress ratio R or by the mean stress and amplitude stress which gives the amplitude ratio A . An infinite-life is achieved if the point described by its stress components lies below the constant-life line. (Shigley, et al., 2003)

2.2.4 Palmgren-Miner

Palmgren-Miner's rule is a method for calculating cumulative damage on structures subjected to spectrum loading. The rule implies that a structure is subjected to damage from each individual stress range cycle, independent of the other stress cycles in the stress spectrum. The damage from each individual stress range cycle is calculated and added together to obtain the accumulated damage D as seen in Figure 2.13 and in equation (7). The sequence of loading does not matter in this rule. (Bakhitiari, 2013)

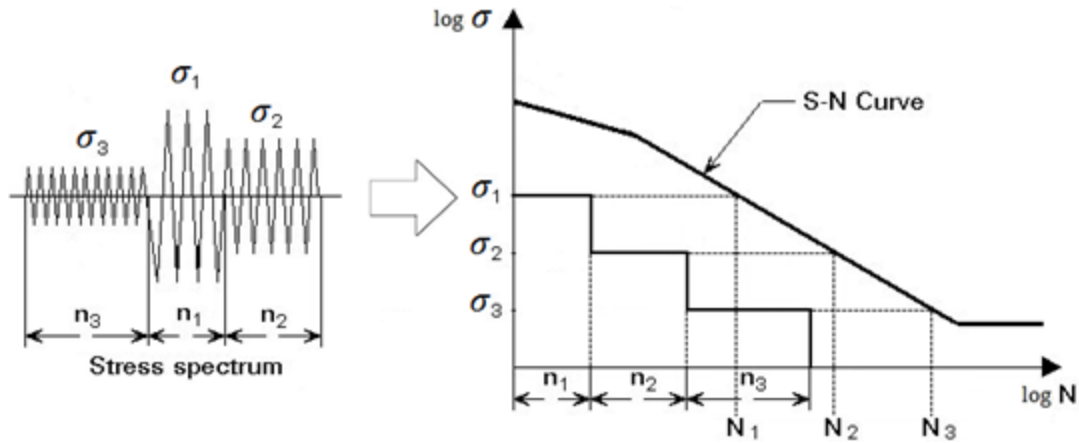


Figure 2.13. Schematic representation of the Palmgren-Miner rule (ESDEP, 2014)

The equation for Palmgren-Miner rule is

$$D = \sum_i \frac{n_i}{N_i} \quad (7)$$

where n_i is the number of cycles at stress level σ_i and N_i is the number of cycles to failure at stress level σ_i . When the accumulated damage is $D = 1$, failure ensues.

2.3 Fatigue testing machines

The first fatigue testing machine was developed by the German mining administrator Wilhelm Albert in the 1830's, after he in 1829 had observed, studied and reported the failure of iron mine-hoist chains arising from repeated small loadings, i.e. the first recorded account of metal fatigue. The machine he built was hydro dynamically driven with a paddle wheel that repeatedly applied load to a chain, as seen in Figure 2.14. (Rao, 2011) (Vervoort & Wurmman, 2014)

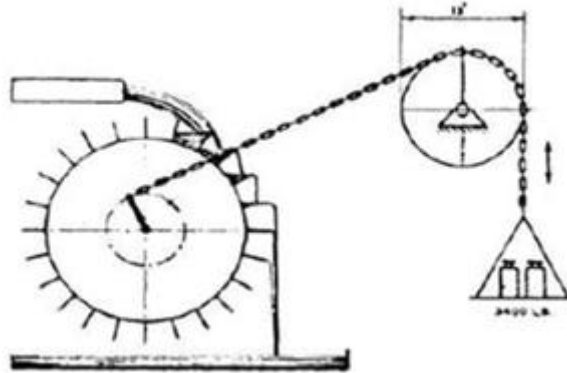


Figure 2.14. First fatigue testing machine for testing chains (Vervoort & Wurmman, 2014)

The first modern type of fatigue testing machine was developed by August Wöhler in the 1860's during his extensive work concerning fatigue failures of rail road axles. During his research, he developed the rotating bending fatigue testing machine, as seen in Figure 2.15b. With it, he initiated the development of design strategies for fatigue, identified the importance of cyclic and mean stresses, as well as introduced the S-N curve and with it the concept of fatigue limit. The machine was designed to simulate the rigors of a rail road axle, with a test specimen i.e. an axle suspended on two main bearings at each end and between these, two load bearings on which a weight is evenly suspended. A motor with a flexible coupling is then connected to one end of the axle. The weight hanging down from the load bearings will cause the axle to bend. When the axle starts to rotate, it will be subjected to both tensile and compressive stresses, i.e. be subjected to fully reversed loading. (Rao, 2011) and (Vervoort & Wurmman, 2014)

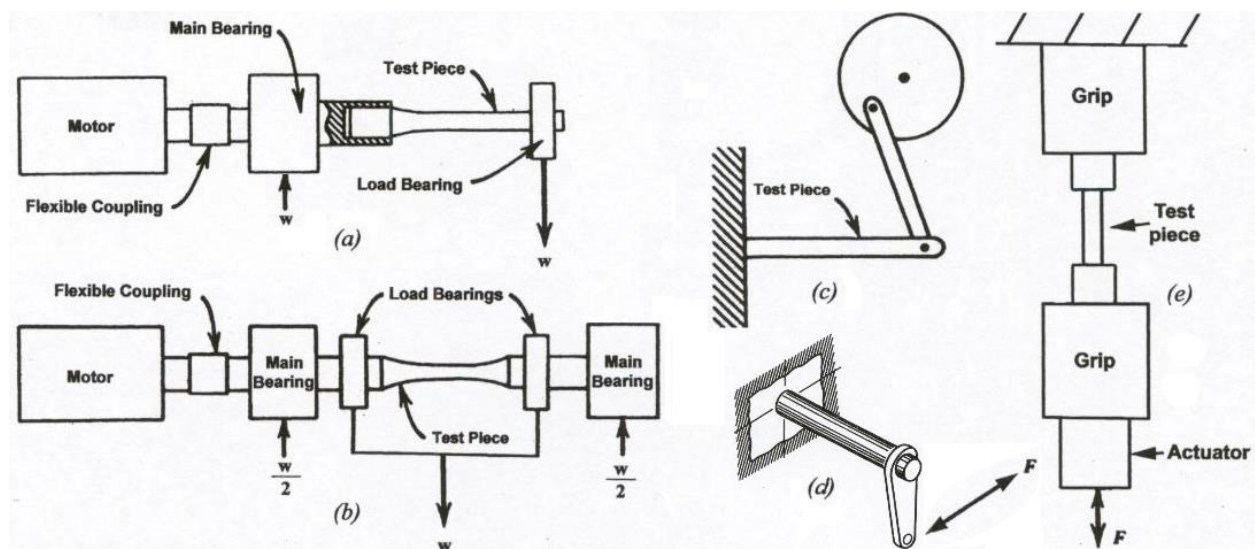


Figure 2.15. Fatigue test machines a) Rotating cantilever bending b) Rotating bending c) Constant deflection amplitude cantilever bending d) Combined in-phase torsion and bending e) Axial loaded (Fatemi, 2013)

Since the development of the first rotating bending fatigue testing machine, other fatigue testing machines have been developed. While Wöhler's fatigue testing machine subject the specimens to uniform bending, the rotating cantilever bending fatigue testing machine in Figure 2.15a subjects the specimen to non-uniform bending moment, due to the way it's suspended. For the constant

deflection amplitude cantilever bending fatigue testing machine in Figure 2.15c, the amplitude stress changes with the specimens' cyclic hardening or softening and decreases as cracks nucleate and grow. If this machine is fitted with an eccentric crank, it has the advantage over the rotating bending test machines in that the mean deflection, and hence the initial mean stress, can be varied. The combined in-phase torsion and bending in Figure 2.15d is similar to the rotating cantilever bending fatigue testing machine, but has the extra feature so that a specimen can be subjected to both uniform torque and a non-uniform bending in one motion. Unlike the previous fatigue testing machines the axial loaded fatigue testing machine (Figure 2.15e), the axial mean and amplitude stresses can be apply separately in both tension and compression as well as combined. (Fatemi, 2013)

The rotating bending fatigue testing machine was the first machine used to generate fatigue data in greater numbers. A lot of the earlier literature data for materials are therefore done for fully reversed bending. Since then, newer test machines such as the axial fatigue testing machine has made it possible to collect data from tension and compression loading in both the high- and low-cycle fatigue ranges. (Campbell, 2008)

Modern fatigue testing machines today are closed-loop servo-hydraulically controlled and can replicate practically any type of cyclic loading or be programmed with almost any desired fatigue spectrum. These types of machines can perform fatigue and durability tests for almost every conceivable situation, from small laboratory specimen to large scale complex structure (Fatemi, 2013). A typical modern axial loaded fatigue testing rig, with its modern sensors and alignment fixture, is shown in Figure 2.16. (Campbell, 2008)

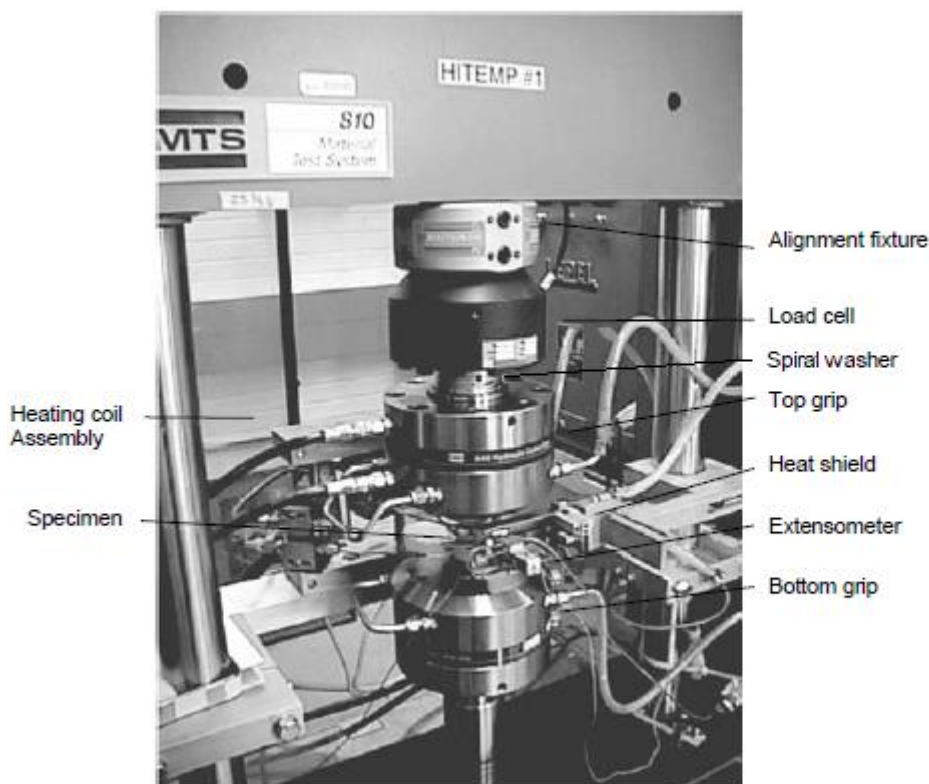


Figure 2.16. An Axial loaded fatigue testing machine by MTS (Campbell, 2008)

When performing an axial loaded fatigue test, as seen in Figure 2.16, a specimen is placed between the bottom and top grip. An extensometer can then be placed directly on the specimen in order to obtain strain data during the test. If a fatigue test has to be performed on specimen above room temperature, a heating coil assembly including a heat shield can be mounted to the fatigue testing machine to keep the specimen at a certain elevated temperature during the fatigue test. One of the key items in a modern fatigue testing machine is the load cell, that's positioned in line with the load direction, to measure the true force that the hydraulic cylinder subjects the

specimen with. To minimize the risk of applying a bending moment to the specimen, while performing axial loaded fatigue tests, a very precise alignment fixture is used to finely adjust the alignment so that the specimen stays perfectly in line with the applied loads. (Campbell, 2008)

The general principle of operations for a modern servo-hydraulic fatigue testing rig is as follows: An input signal of load, strain, or displacement is generated using a function generator. The input is applied through a hydraulic actuator on the specimen. The response on the specimen is measured via a load cell, clip gage, or a linear variable differential transformer (LVDT). The measured output is then compared with the sent input. If the desired force, strain, or displacement hasn't been reached in the output, the input value is adjusted and another cycle performed. This iterative process is made during every cycle throughout the whole fatigue test to ensure that the right test values are achieved. A multi-axial fatigue test can be set up with several hydraulic cylinders, according to the same principles as mentioned earlier. Depending on the force or displacement that is required, the test can be run at frequencies ranging from mHz to kHz. (Fatemi, 2013)

2.3.1 Previous fatigue testing performed by HIAB

Bromma has previously sent some spreader components for testing to HIAB's development laboratory in Hudiksvall to test them for fatigue. These tests have mainly been performed as comparison tests, where one spreader component from two or more manufacturers is tested. The test objects varied both in material and in the quality of manufacturing. Some of the previous tests are shown in Figure 2.17.

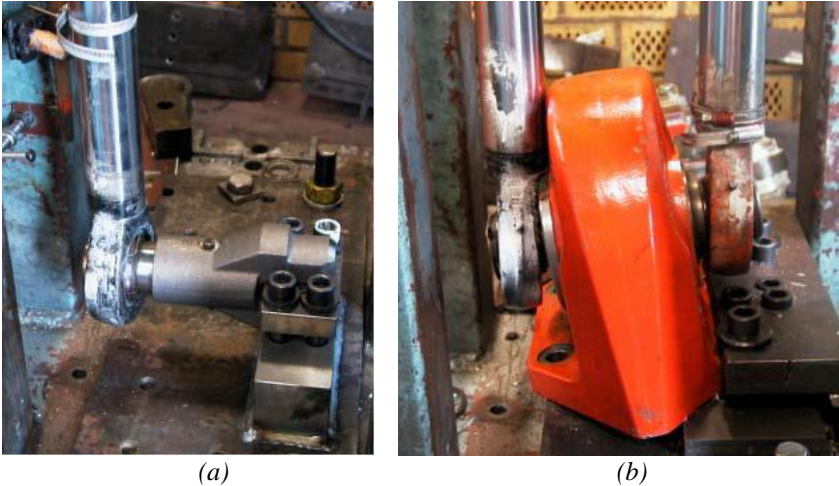


Figure 2.17. Spreader components tested at HIAB's Development laboratory a) Guide block (Bergman, 2013)
b) Gearbox housing (Bergman, 2007)

Because these tests were only made as comparison tests with one type of spreader component, produced by several manufacturers, these were made with a self-constructed fatigue testing rig (developed by HIAB in the 80's), with a less advanced control and monitoring system. One item from each manufacture batch was subjected to a static strength test, determining at what hydraulic pressure the component fractured. A "trial-and-error" approach was then taken, where the maximum hydraulic pressure was slightly lowered from the value where the component fractured. The hydraulic pressure was then adjusted down so that the components would reach a fatigue life of approximately 20 000 cycles. This level was chosen mainly to reduce the testing time for each component. The load, with which the components were tested with, was obtained from calculations with the hydraulic pressure and the cylinder diameter. (Bergman, 2007)

These tests have later been questioned due to the low amount of cycles each component was tested with. The boundary between low and high cycle fatigue can be anywhere in the span of

10^4 cycles up to $5 \cdot 10^4$ cycles according to some literature (Bakhitiari, 2013). This would mean that these spreader components were subjected to low cycle fatigue, instead of high cycle fatigue like it would under real circumstances. This in turn could mean that the components failed due to yielding instead of fatigue.

2.3.2 Recommendations for design of a fatigue testing rig

During the start of the thesis, study visits were made to different fatigue testing laboratories at some of Sweden's bigger manufacturing companies. Their types of axial loaded fatigue testing rigs have been studied and information concerning their way of performing these types of tests has been gathered. Some of these test rigs are fully welded with fixed mounting points while others are based on a modular design with bolted joints that can be disassembled and rebuilt to fit a new type of component. In general, a fatigue testing rig is only designed to test one specific type of component at a certain load case. In Figure 2.18 some of the different types of axial loaded fatigue testing rigs studied are shown.

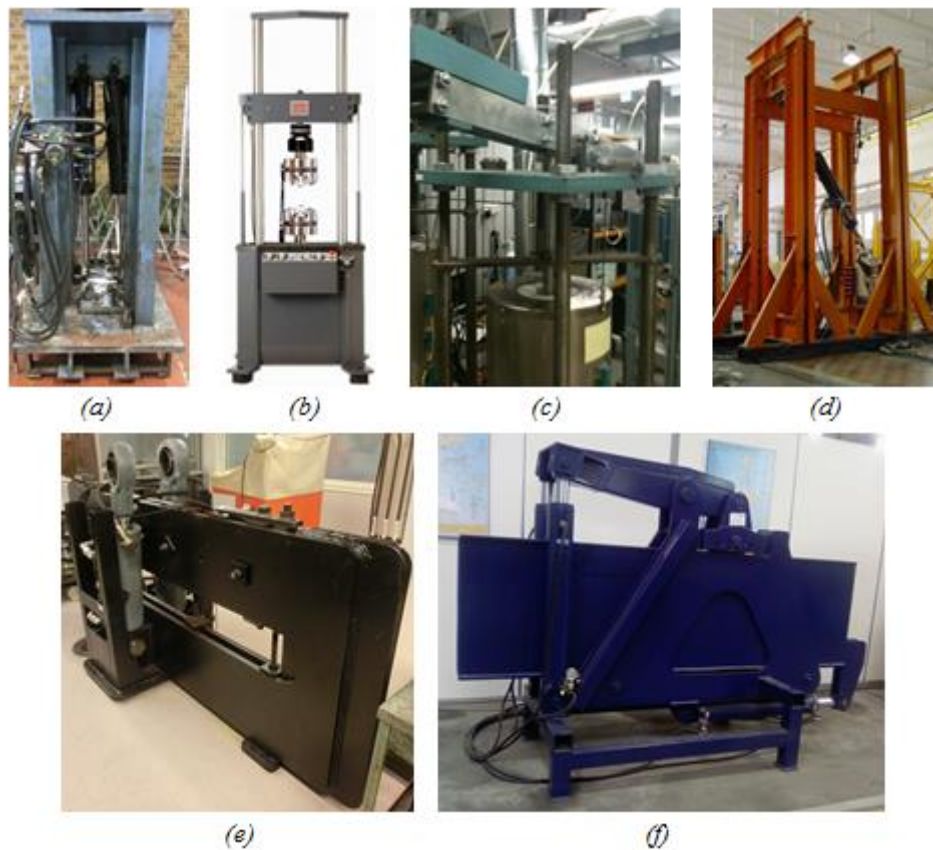


Figure 2.18. Several types of axial loaded fatigue testing rigs a) HIAB's fully welded test rig (Bergman, 2013) b) A typical MTS laboratory test rig c) A creep-rig designed with threaded rods and nuts (Hedegård & Östling, 2013) d) Floor-mounted, bolted joints modular test rig (Galín, 2010) e) Fully welded 3-point bending test rig with adjustable mounting points (Bergman, 2013) f) Fully welded test rig with a lever arm solution (Lindström, 2010)

HIAB's design with a fully welded test rig (Figure 2.18a) with fixed mounting points for both the components and the hydraulic cylinders have a big disadvantage in that the physical space for testing components is restricted to within the steel structure of the test rig. The position of the hydraulic cylinders, also mounted inside the steel structure on the upper part of the frame, restricts the space, as well as the stroke of the cylinder, even further. The fillet welds in each end of the four vertical main beams, which holds the test rig together, are heavily subjected to fatigue during the tests, and have had to be repaired several times during the test rigs lifetime. The test rig has further been strengthened by running threaded rods through the cavity of the four main beams and tensioning them with a nut from each end of the test rig. (Bergman, 2013)

The typical MTS fatigue testing rig for laboratory use (Figure 2.18b), has its hydraulic cylinder built in to the lower part of the test rig, enabling more space for a test specimen in the rig. The upper part of the test rig is held up by two polished steel shafts with inner threads, to which big bolts are fastened to secure the shafts to the lower part of the test rig. When performing fatigue tests with this type of test rig, it's crucial that the two polished shafts are pre-tensioned to approximately 10% more than the maximum tensile load subjected to the specimen in the fatigue test. This is done by mounting the specimen in to the test rig, statically loading it to the maximum tensile stress, thus subjecting the shafts to an equal amount of compressional load, at which point the bolts that fixates the shafts can be tightened to a certain torque. This type of test rig is optimal for laboratory testing of small specimens but not suitable for component testing, mainly due to its two pillar design could lead to linearity problems during testing which in turn could lead to large bending stresses that in the lower end of the polished shafts. (Hedegård & Östling, 2013)

The design of a creep rig at swerea|KIMAB is shown in Figure 2.18c. Even though the function of the rig is purely for static testing, the design of the steel frame structure is worth taking a closer look at. Compared to the MTS laboratory test rig, the creep rig got four main pillars, constituting of four partly threaded rods, with nuts holding the upper and lower part of the rig. Depending on the load case for the spreader components this concept could be a viable option for the test rig, especially if a pre-tensioning of the test rig is needed before carrying out the tests. (Hedegård & Östling, 2013)

Bigger manufacturing companies, such as Volvo Construction Equipment and Scania, use a modular design to their test rigs so that they can be modified when a new type of test needs to be performed (Figure 2.18d). These test rigs are generally built with standard types of beam units that are assembled with bolted joints with high strength bolts. These rigs are fixated to a rigid floor, as seen in Figure 2.18d, which gives the rig most of its rigidity. (Mrden, 2013) (Berg, 2014)

A fully welded test rig with adjustable mounting points for performing 3-point bending is shown in Figure 2.18e. This specific test rig is used to perform fatigue tests on crane beams. Similar to the MTS laboratory test rig, this test rig has its hydraulic cylinders mounted low down on the rig, generating an upwards stroke. This type of design makes it possible to test larger specimens in the rig due to the fact that there's no upper steel frame restricting the available free space. (Bergman, 2013)

If greater loads are needed when performing a fatigue test on a certain test object, the test rig itself can either be made bigger with bigger hydraulic cylinders or it can be constructed with a lever arm that can amplify the loads generated by the hydraulic cylinders, as seen in Figure 2.18f. The test rig in Figure 2.18f is designed with a lever arm that's operated by two hydraulic cylinders and has a load ratio of around 1:4. If for example one set of hydraulic cylinders are going to be used to test several different components, with some components requiring loads well above the rate that the cylinders can achieve, a lever arm solutions could be an option. (Lindström, 2010)

Steel, rig assembly and guidelines for dimensioning

When selecting steel for components that have to be designed to withstand fatigue, low and medium strength steels are preferred due to their clear fatigue limit. Even though high alloy, high strength steels have good strength properties, its fatigue limit isn't significantly higher compared to low and medium strength steels. Depending on which type of material that is used and of course depending on the fatigue loading, the fatigue limit for a component can vary from about 1 to 70 percent of the ultimate tensile strength. (Fatemi, 2013)

Other features that should be taken into consideration, when designing a structure for an infinite life is e.g. the used of cleaner metals, and generally smaller grain size for ambient temperature, that have better fatigue resistance. Frequency effects from testing are generally small or virtually none, when no other environmental effects such as corrosion and temperature change are present. When performing fatigue testing it is most beneficial if actual fatigue data, collected from real working conditions, can be used in order to get dependable results. If it's not possible, approximation of median fatigue behavior can be made. (Fatemi, 2013)

According to Hedegård at swerea|KIMAB (2013), whose research is within steels and welded structures, he concurred to previous mention literature that the most suitable choice of steel for a fatigue testing rig would be a cleaner metal with fewer discontinuities, preferably a 355 MPa steel with a slightly higher tensile strength compared to a low alloys steel, but still with a high fatigue limit. While both Volvo Construction Equipment and Scania use this type of steel for their main structures of their rigs, this further confirms the literature.

Both Volvo Construction Equipment and Scania use their modular design test rigs that are mounted to a rigid floor in their fatigue testing laboratories. This type of floor is made out of thick concrete with immersed steel rails running along the length of the room that creates a slot where high strength steel mounts can be slid in, as seen in Figure 2.19a. These mounts can be slid along the whole rail, which enables the rig to be fixated anywhere along one of the axis along the room. (Mrden, 2013) (Berg, 2014)

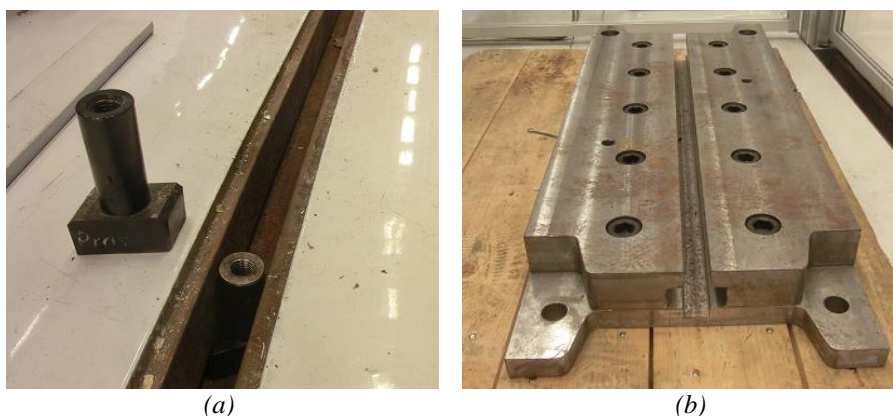


Figure 2.19. Mounting rails a) Concrete floor with steel rails b) Substructure rail system, assembled with bolts steel plates (Berg, 2014)

At Scania they have manufactured their own type of substructure rail system out of steel plates that are joined together with bolts, as seen in Figure 2.19b. The design is very similar to the one of the concrete floor, but can be manufactured as a stand-alone unit that can be moved around. This substructure concept is less rigid than the concrete floor, but might be applicable to bigger structures if designed with larger steel plate. (Berg, 2014)

When dimensioning a fatigue testing rig for a certain component, there are some guide values that should be followed according to Bergman (2013), Mrden (2013) and Berg (2014). The test rig should be dimensioned so that the maximum stress in the steel structure should not exceed 100 MPa, during the fatigue testing. In the case of having a bolt jointed test rig, as for Volvo Construction Equipment and Scania, the stress in the bolts should not exceed 50 MPa during the fatigue testing according to Mrden (2013) and Berg (2014).

Hydraulic cylinders and mounting

The hydraulic cylinder is mainly chosen depending on what load and stroke is needed for the fatigue testing. For example, when performing fatigue testing at Scania, the stroke of a hydraulic cylinder rarely exceeds 50 mm. Depending on what maximum load is needed for the fatigue testing, a hydraulic cylinder with a force rating just above the maximum load is selected. This is

done in order to retain a high hydraulic pressure, which in turn gives quicker response in the hydraulic cylinder (Bergman, 2013).

If a too powerful hydraulic cylinder is selected, it would require a higher oil flow due to the bigger cylinder area, as well as a lower hydraulic pressure to achieve the desired force. This would result in a less responsive cylinder that would slow down the testing. (Berg, 2014)

Another aspect that should be considered is at what frequency the fatigue testing should be performed at. The lower the frequency, the longer each test will take to perform. If the test is run at a too high frequency, the stress value in the peak of the load cycle may not be fulfilled in the component, due to dynamic losses. Should it be the case, the true stress can be measured in the specific area, by using strain gauges and the frequency of the test can be adjusted. According to Mrden (2013), if a component is tested with a specific load spectrum, it's not so important that the test rig simulates the exact load spectrum as long as the peak values within the spectrum are achieved in the test. (Berg, 2014)

The fatigue testing rig at HIAB uses conventional hydraulic cylinders with a proportional valve, as a matter of fact the same type of cylinders that are used on their cranes. These types of double acting hydraulic cylinders can direct the flow of the oil between the two sides of the piston, making the cylinder either extend or retract (Figure 2.20a). When one side of the piston is pressurized, the other side will depressurize and oil will flow back to the reservoir. When the control valve is switched, the same process will happen, but switched between the two sides of the piston. (Hyco, 2013) During the fatigue testing of the spreader components, HIAB performed the tests a 1/3 Hz, which can be seen as fairly low for fatigue testing. This may partly be to the length of the stroke of the cylinder which affects the amount of oil flow that have to be filled and emptied on either side of the piston and partly due to that the hydraulic block with the proportional valve is located three meters away from cylinder and connected with hydraulic hoses. (Bergman, 2013)

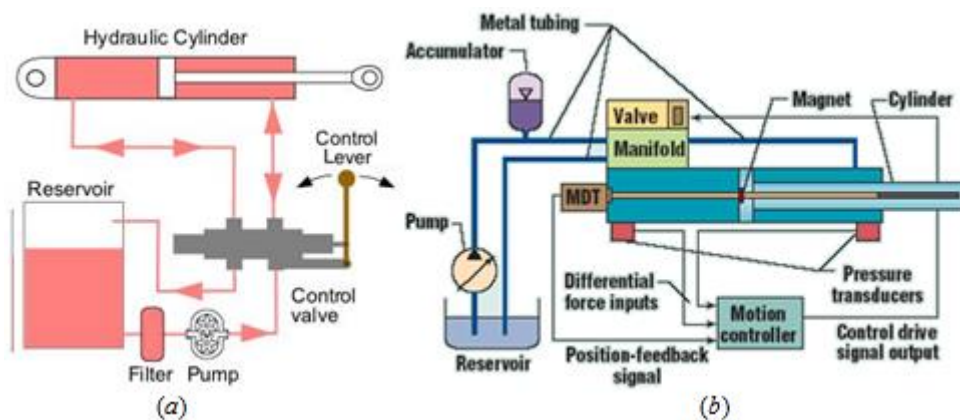


Figure 2.20. Hydraulic cylinder controlled by a) proportional valve (Hyco, 2013) b) servohydraulic valve (Nachtwey, 2006)

Both Volvo Construction Equipment and Scania use fatigue-rated servohydraulic cylinders (Figure 2.20b) for performing fatigue testing, mainly with components from MTS and Moog. These hydraulic cylinders have built in displacement sensor (LVDT) and load cells. There are two pressure transducers on either side of the piston in the cylinder that sends pressure data to the motion controller that calculates the set load from the cylinder. Due to the choice of cylinders, these tests can be performed up to 3-4 Hz before the dynamic losses in the testing become too great. (Berg, 2014)

For a servohydraulic system the hydraulic block with the servohydraulic valve is mounted directly on the cylinder to eliminate pressure losses between the block and the cylinder. The main difference between the proportional valve and the servo hydraulic valve lies in how the spools control the valve (Figure 2.21a 2.21b). Proportional valves move the spool either

manually with the help of a lever or with an electric coil and magnet, while the servohydraulic valve use a small torque motor to control hydraulic pilot pressure that then moves the spool. (Nachtwey, 2006)

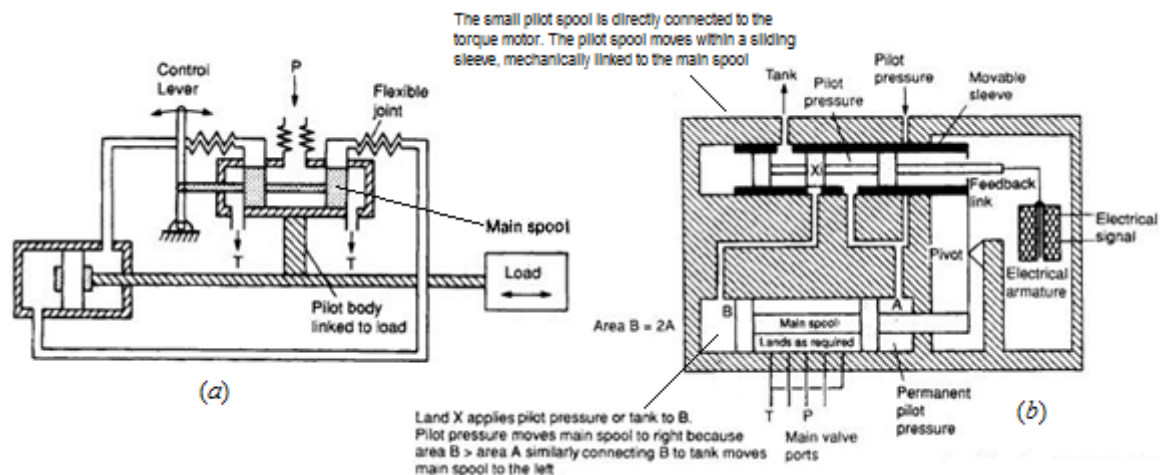


Figure 2.21. Schematic design of a) Proportional valve b) Servohydraulic valve (And, 2010)

When using proportional valves for fatigue testing, an amplifier is needed to convert the motion controller's output voltage to a high-current signal that drives the spool. With a servo-proportional valve, the amplifier compares the error between the control or reference signal and spool-position feedback from the LVDT. Depending on the generated force to shift the spool, the valve response differs between these two valves. Servohydraulic valves generally shifts faster because of a higher ratio of hydraulic force to spool mass, although some proportional valves have nearly the response of servohydraulic valves. Proportional valves must generate enough force to move the spool, in-line LVDT, and solenoid core, as well as overcome spring-centering forces. Due to this servohydraulic valves often work better in high-flow applications. (Nachtwey, 2006)

One of the most critical features within fatigue testing, according to Östling (2013), is the axial alignment of the hydraulic cylinder, between the test rig and the specimen. This is crucial when performing fatigue testing on materials in a scientific purpose. A typical alignment fixture from MTS that are often used in laboratory fatigue testing machines is shown in Figure 2.22a (MTS, 2014).

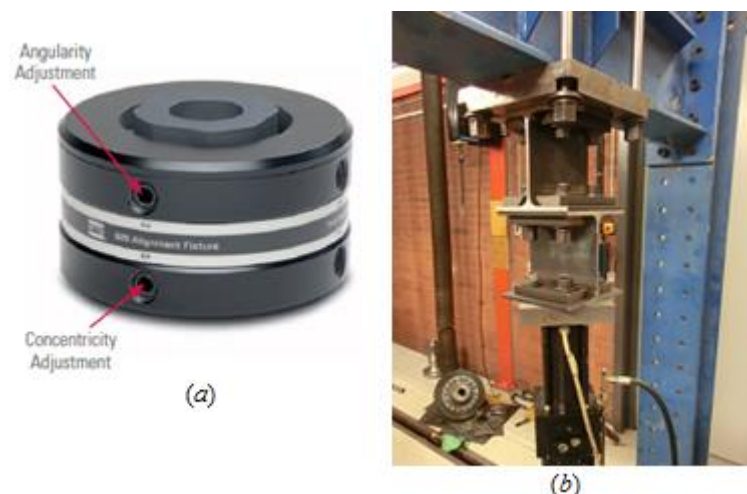


Figure 2.22. Alignment fixture a) A typical alignment fixture from MTS (MTS, 2014) b) Volvo Construction Equipment's H-beam concept to compensate for unwanted lateral loads (Mrden, 2013)

When performing fatigue testing on components, it's of great importance that the applied load to the component is correct. This can easily be verified by the load cell situated close to the component. Although lateral loads are not desired when performing fatigue testing, these forces

can be compensated for in other way, then just using an alignment fixture. Volvo Construction Equipment has developed their own solution of how to compensate for the lateral forces by absorbing the load using pieces of H-beams. Two square pieces of the H-beam, seen from the flange side, are bolted on top of one another with the web set 90 degrees to each other (Figure 2.22b). This assembly is then mounted between the test rig and the hydraulic cylinder, absorbing the lateral loads that are generated during fatigue testing.

Scania uses swivel mountings from MTS in the ends of the cylinders when mounting them in the test rig (Figure 2.23). This is done in order to reduce potential bending that might occur in the cylinders due to misalignment in the setup as well as to compensate for any greater angle changes at the hydraulic cylinders base during the fatigue tests due to large deflections. The swivel mountings allows the hydraulic cylinders to pivot freely at the base and can adjust for any backlash, thus removing as much relative movement in the setup as possible while allowing it to rotate during tension-compression loading (MTS, 2014). (Berg, 2014)



Figure 2.23. Swivel mounting from MTS (MTS, 2014)

When setting up a specimen in a fatigue testing rig, it's important that the hydraulic cylinder and the auxiliary components mounted to it, in the line of force, are tighten to each other with a specified torque so that there's no play between the components during the fatigue testing. If this happens, the sensors would receive incorrect data and in worse case subject the auxiliary components to fatigue instead of the specimen.

After the hydraulic cylinder and the auxiliary components are assembled and tightened correctly, the last step is to tighten the whole assembly to the specimen. If there's still some play in the setup, additional tightening can be made with the spiral washer (Figure 2.24). This auxiliary component has two flanges with interfacing planes that are slightly angled. When these two flanges are tightened in opposite direction of each other, it gives rise to an additional tensioning in the whole setup. (Hedegård & Östling, 2013)



Figure 2.24. A typical spiral washer for a laboratory fatigue testing machines

Sensors, control system, detection methods and safety

A vital part of the fatigue testing rig is its sensors that register the fatigue data as well as serving the control system with information for controlling the rig so that it can detect when a component has reached its fatigue life and safely stop the rig. Depending on the design of the test rig, different types of sensors can be used.

The most important sensor, when performing fatigue testing, is the sensor for measuring load. Without it, the loads that the fatigue testing has been performed with can't be verified. The most common type of load sensor used is a load cell, (Figure 2.25a). It's positioned directly in the point of where the hydraulic cylinder applies the load. This is to measure the true load that's actually applied to the specimen. Another typical load sensor that can be used is a load measuring pin (Figure 2.25b) that's placed as the mounting pin in the bottom mounting point of the hydraulic cylinder. (Mrden, 2013) (Bergman, 2013)

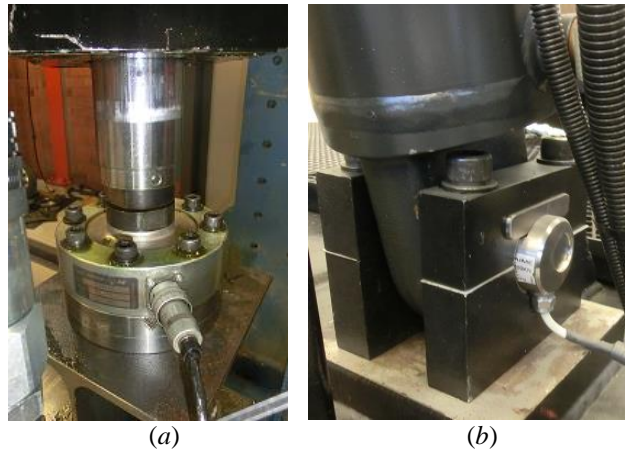


Figure 2.25. Sensors for measuring applied load a) Load cell (Mrden, 2013) b) Load measuring pin (Bergman, 2013)

One other important aspect in fatigue testing is to measure the displacement, i.e. the stroke of the hydraulic cylinder. This data gives a good indication of the deflection of the component during the fatigue testing. The most common sensor used for measuring displacement is a LVDT (Figure 2.26a), which is a type of electrical transformer. It converts a position or linear displacement from a mechanical reference into a proportional electrical signal containing phase (for direction) and amplitude (for distance). Another way of setting the limits of displacement is by the use of proximity sensor (Figure 2.26b), as used in HIAB's test rig. These sensors are able to detect the presence of nearby objects without any physical contact, in this case two hose clamps that are attached to the shaft of the hydraulic cylinder. When the component that's being tested starts to deflect more and more due to fatigue, the stroke of the cylinder will increase and the protruding screw on the hose clamp will eventually reach the position in front of the proximity sensor, at which point the test stops. (Mrden, 2013) (Bergman, 2013)

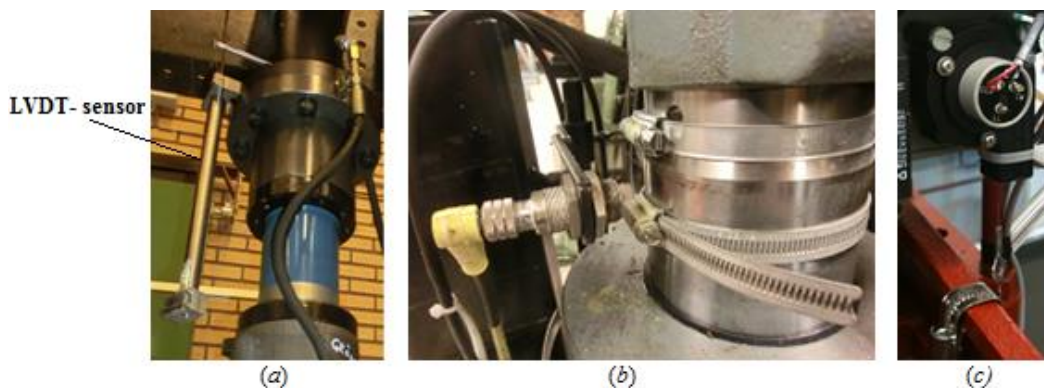


Figure 2.26 Sensors for measuring displacement a) LVDT-sensor (Berg, 2014) b) Proximity sensor (Bergman, 2013) c) Angle measuring sensor (Hedegård & Östling, 2013)

At swerea|KIMAB (2013) they use an angle measuring sensor that's got a thin self-retracting wire mounted on the axle of the sensor (Figure 2.26c). This setup is used for their creep rig, because of the high sensitivity in the angle sensor of detecting variations. Although it's a fairly accurate way of measuring displacement, it's unknown how well it performs during fatigue testing. Another possible way of measuring displacement is by the use of laser diodes and position sensitive detectors. This way of measuring displacement is done when conventional sensor can't be used. (Hedegård & Östling, 2013)

Another useful data that can be measured is the strain within the component. When performing laboratory fatigue testing on small test specimens, an extensometer can be placed directly on the specimen to measure the strain. For component fatigue testing this is often not possible, due to the complex shapes of the components themselves. Instead, several small strain gauges are mounted at certain areas on the component (often where the stress concentration is assumed to be the highest). Strain gauges can also be used to measure the acting force on the component, when a load cell can't be fitted in the setup. The use of measuring the acting hydraulic pressure with a separate pressure sensor is generally not needed when using a control system that controls the fatigue testing by iterating between the set load and the actual load. (Mrden, 2013)

Depending on the setup of the fatigue testing rig, different types of control systems are used. When using purpose made fatigue rated hydraulic cylinders and auxiliary components from a specific manufacturer, it's recommended that the user uses the control system from the same manufacturer. It is however possible to run the system with a different, often cheaper control system. Companies that have developed their own types of fatigue testing rigs with, e.g. regular hydraulic cylinders and use separate sensors in their testing, also often uses their own developed control system, programmed in e.g. LabVIEW or similar software (Bergman, 2013). Other sensors that could be useful for some specific testing would be a temperature sensor to measure the ambient temperature during the fatigue testing. (Mrden, 2013)

When performing fatigue testing it's crucial to detect certain events during the test. One feature in particular is the onset of the first crack. It can be detected either visually by manually checking the component for cracks within regular intervals or by filming the whole test, which would be synchronized to a cycle counter, at the position where a crack is most likely to occur (Mrden, 2013). An alternative or complement to these methods is to mount thin, brittle wires straight across the areas where it's believed that cracks would propagate through. These wires are attached with special brittle glue. During the test, current is sent through these wires, sending a signal to the control system. When a crack has propagated far enough, the brittle wire and glue will break and the control system will detect that it's not receiving a signal through the wire. Other ways of programming the control system to indicate a possible first crack is to set the program to shut off the test when the cylinder has reached a certain displacement. The amount of displacement would represent a certain amount of deflection i.e. at a certain strain when it's believed that a crack would occur. This could be when the cylinder has reached a displacement value that's 5% (or more depending on component) greater than the initial displacement. When the test has stopped, the component will visually be checked for cracks and if no cracks have appeared, the displacement limit is raised a few percentage points, and the test is continued. (Berg, 2014)

The control systems used to perform the fatigue testing, are generally programmed with some safety features so that the test shuts down if something goes wrong during testing. Allowed limits for the displacement can be set so if the displacement of the cylinder gets to great, possibly due to a final fracture of the tested component or a fixation that has come loose. If the span between the set load and the actual load is too great, the system also shuts down. This could be an indication of loss of pressure in the hydraulic system. A level indicator can be placed in the hydraulic reservoir ensuring that the level of hydraulic fluid stays at a certain level. If the level drops, it could mean that there's a leak somewhere in the hydraulic system. If the generated cyclic loading is out of phase with the measured cyclic loading, the system also shuts down. As

an extra insurance, if the control system shuts down, it can also empty the hydraulic cylinder from fluid, locking the cylinders. Other external safety features to the fatigue testing rig can be such simple things as plexiglas around the rig to prevent people from getting too close to the test rig and protecting them from unexpected flying parts if something in the rig would break during testing. (Mrden, 2013) (Berg, 2014)

Something to keep in mind when it comes to fatigue testing is that there is always a certain amount of scatter in the results from the fatigue testing due to different parameters. As an example there could be 10% scatter in the strength of the material for the tested component, 5% scatter in the testing itself, 5% scatter due to dynamic losses, etc.

3 DESIGN PROCESS

The design process chapter starts with presenting the dimensioning load cases as well as the requirements specification for the fatigue testing rig. The initial development of a concept for the fatigue testing rig is made in the concept generation where several concepts are created. These concepts are evaluated during the concept selection with the use of Pugh's decision matrix and the selected concept is initially tested in its design and dimensioned in the concept testing.

3.1 Fatigue loads for the three selected spreader components

Before designing the fatigue testing rig for the three selected spreader components, it's crucial that each load case is defined correctly for each component. The aim is to get each load case as similar as possible to what the component would be subjected to under normal running conditions. For some components it's not possible to replicate the actual load case when just testing the component separately. These components therefore need to be tested with a substructure that resembles a part of a real spreader, to achieve a comparable load case. From the start of the thesis it was predetermined that the center web plate needed to be tested within a substructure and during the course of the thesis it has further been determined that the guide block needs to be tested with the whole twistlock assembly, mounted in a substructure. The load cases for the three selected spreader components are illustrated in Figure 3.1.

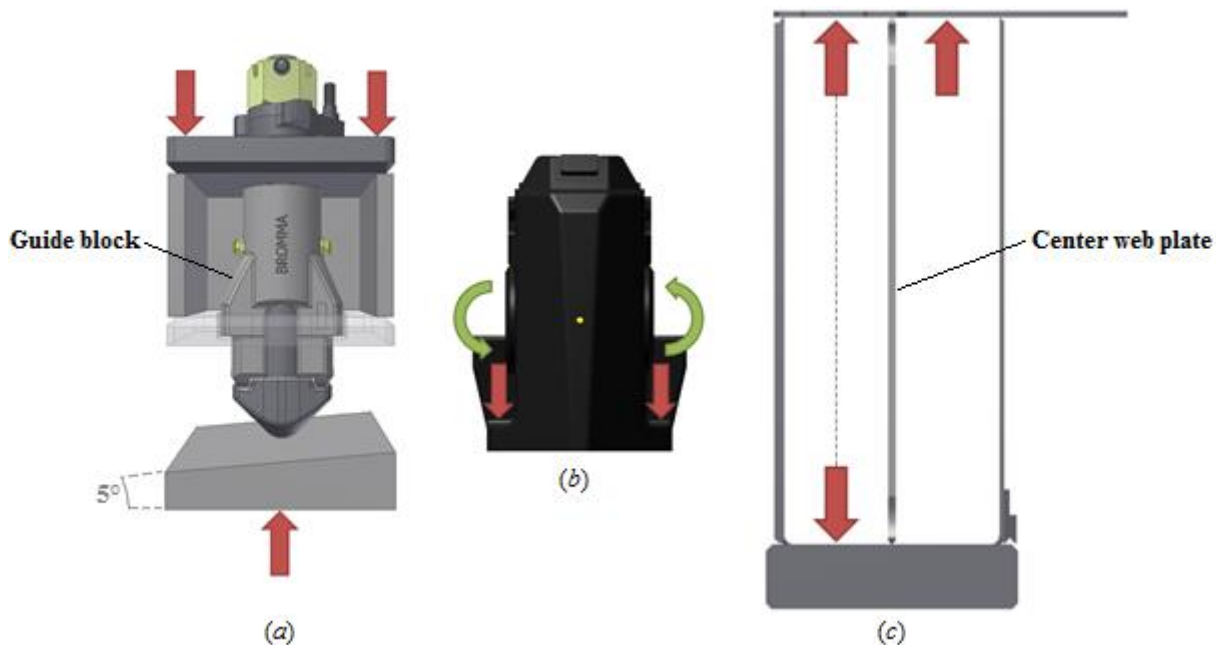


Figure 3.1. Load cases for the three selected spreader components a) Twistlock assembly substructure b) Gearbox housing c) Center web plate substructure

The guide block will be tested by subjecting the whole twistlock assembly, mounted within its substructure, to an axial load that's applied to the tip of the twistlock, via a 5 degree angled plane. The substructure of the twistlock assembly will be fully fixated in order to take both the main vertical force but also the reacting lateral force that will occur due to the slope of the angulated plane. When the angled plane applies the load the tip of the twistlock, the twistlock will bend and transfer the applied load unevenly through the guide block up to the substructure.

The gearbox housing will be tested in a similar way to how the old gearbox housing was tested at HIAB, as previously shown in Figure 2.17b. The gearbox housing will be subjected to a torque at its center point, in the middle of where the axle for the guide arm is usually situated. The bottom of the gearbox housing is placed flat on the base of the fatigue testing rig and fixated with bolts



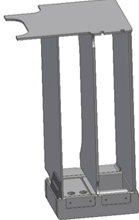
in both of its mounting flanges. A solid shaft is positioned through the gearbox housing and an axial up- and downward load is applied to the shaft at an equal distance from the center point, replicating the desired torque.

The center web plate substructure will be tested by fixating one end of the substructure to the base of the fatigue testing rig while the force is applied to the other end. Because the center web plate substructure will be unevenly loaded (as shown in Figure 3.1c), it's crucial that the substructure is fixated in a way so that it can take the load from the reacting torque that will occur, without using any external support, in order to achieve the desired load case.

The tests should be performed with repeated loading, i.e. Stress ratio $R = 0$. When doing so, a cycle will take longer time to perform if the system needs to be unloaded completely before the next cycle can be performed and it could interfere with the displacement measuring during the test, due to excessive play that can occur between the test rig, the test component and the hydraulic cylinder assembly when unloading completely. Due to these factors, companies such as Volvo Construction Equipment chose a stress ratio just above zero, i.e. $R > 0$, to keep the test rig under tension during the whole test (Mrden, 2013). For the tests of the three selected spreader components, Bromma has decided to use a minimum load that's 5% of the maximum load for each specific test, i.e. $R = 0,05$.

Each of the three selected spreader components will be tested in three to four different tests, depending on the component, with each test performed at a specified load given by Bromma (Table 3.1.). Every test will be performed with a batch of 20 test objects. The loads, to which the three selected spreader components are going to be tested with, are derived from FEA of the components and the desired amount of cycles before failure. These calculations have been performed by Bromma, according to SSAB's method of calculating fatigue in steel components and shown in Appendix B. (SSAB, 2010)

Table 3.1. Loads and estimated amount of cycles before failure for the three selected spreader components

Component	Twistlock assembly substructure	Gearbox housing	Center web plate substructure
<i>Picture</i>			
1st test			
Number of test objects	20	20	20
Estimated cycles before failure		50000 cycles	30494 cycles
Maximum load/torque	250 kN	46 kNm	1130 kN
Minimum load/torque	12,5 kN	2,3 kNm	56,5 kN
Stress ratio, R	0,05	0,05	0,05

2nd test			
Number of test objects	20	20	20
Estimated cycles before failure		150000 cycles	60988 cycles
Maximum load/torque	*	37 kNm	897 kN
Minimum load/torque		1,85 kNm	44,85 kN
Stress ratio, R	0,05	0,05	0,05

3rd test			
Number of test objects	20	20	20
Estimated cycles before failure		300000 cycles	121976 cycles
Maximum load/torque	**	32 kNm	712 kN
Minimum load/torque		1,6 kNm	35,6 kN
Stress ratio, R	0,05	0,05	0,05

4th test			
Number of test objects			20
Estimated cycles before failure			243952 cycles
Maximum load			565 kN
Minimum load			28,25 kN
Stress ratio, R			0,05

* The maximum load is adjusted depending on the outcome of the 1st test

** The maximum load is again adjusted depending on the outcome of the 2nd test

The summarized information from Table 3.1, is that the fatigue testing rig must be capable of testing components with a load varying between 245-1030 kN and perform an estimated amount of cycles between 30000-300000 cycles, per fatigue test.

3.2 Requirements specification

A requirements specification for the main steel structure of the fatigue testing rig has been defined together with Bromma, in order to establish the essential and desirable requirements that the test rig needs to fulfill. The requirements have been divided into external and internal requirements, as shown in Table 3.2.

Table 3.2. Requirements specification

Internal requirements	Essential	Desirable	Verification method
The test rig should be geometrically designed to fit the three selected spreader components.	x		CAD
The test rig should be dimensioned for an infinite life, relative to the loads cases given for the three selected spreader components.	x		MATLAB/FEA
At least two cylinders should be fitted in the test rig, in parallel to each other.	x		CAD
The hydraulic cylinders should be fitted so that one of the cylinders can easily be disabled, in order to only run one cylinders when performing tests.	x		CAD
The hydraulic cylinders should be dimensioned to fulfill all the required loads that are required for the testing of the three specific components	x		Product sheet/ Hand calculations
The test rig should be designed so that the hydraulic cylinders can easily be changed if other cylinders needs to be fitted		x	CAD
External requirements			
External requirements	Essential	Desirable	Verification method
Maximum geometrical size of 3m x 3m wide, 4m high	x		CAD
The test rig should be able to be moved with a fork lift, able to lift 7,5 tones.	x		CAD
The test rig should be design in a way so that sensors, such as force sensors, displacement sensors, etc. can be incorporated in the rig.		x	CAD
Design the rig to be modular, so that it can be re-assembled to fit testing for other components then only the three specific ones		x	CAD

3.3 Concept generation

In order to generate a sufficient amount of conceivable concepts to the concept selection face, a brainstorming session was held at Bromma's headquarters, where all the mechanical engineers at the R&D department were invited to sketch some concepts of the fatigue testing rig. During the brainstorming session, the participants were first presented with only the load cases for the three selected spreader components and the requirements specification and where then asked to sketch a suitable concept for the test rig. During the brainstorming session they were successively presented with more information concerning other fatigue testing machines, and additional information gathered from previous study visits to fatigue testing laboratories at bigger Swedish manufacturing companies. Meanwhile, they were asked to further complement or change their concept when been presented with the additional information.

The brainstorming session resulted in several sketched concepts that were collected for further evaluation. Notable was that even though the engineers at Bromma have a strong connection of working with fully welded structures, most of the sketched concept used some form of bolted design. Another detail that should be pointed out is that a lot of the sketched concepts referred to a ridged “foundation” that the test rig was mounted to, which would take up most of the load when performing fatigue testing. However none of these concepts specified how this “foundation” would be constructed. Some of the sketched concepts only referred to complementary components for a test rig. These concepts will only be generally looked at during the concept generation, but not further evaluated in the concept selection.

3.3.1 Main steel structure

After evaluating all the sketched concepts over the main steel structure, a lot of them could be categorized into smaller groups, due to their similar design features. Ultimately, five different concept designs could be extracted from the gathered material. The basics of these concepts are described and illustrated with a simplified model.

Concept 1

The first concept of the main steel structure for the test rig consists of two hydraulic cylinders that are permanently fixated in the two ends of a ridged bottom plate or foundation. A sturdy beam is mounted on top of the piston of each hydraulic cylinder and the components that are going to be tested are mounted in the middle of the test rig, as shown in Figure 3.2. The two hydraulic cylinders will apply an equal load to achieve an axial load from the middle of the beam.

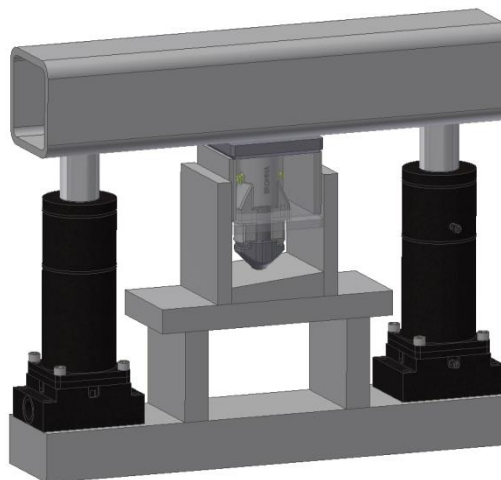


Figure 3.2. Concept 1 of the main steel structure for the test rig

Advantages

- Easy to manufacture and assemble
- No extra external steel structure is needed

Disadvantages

- Dependent on always using two hydraulic cylinders
- Not modular enough
- Highly restricted space for testing

Concept 2

The second concept consists of a base or foundation made out of welded square section beams, as shown in Figure 3.3. Square section beams with pre-drilled mounting holes are welded perpendicular to the base at each connection point, to form a sleeve for the upper structure to slide in to. A wide U-shaped upper structure is welded together with slightly smaller square section beams that have similar pre-drilled mounting holes on each end, as to the sleeve. The height of the upper structure can be adjusted depending on which holes the mounting bolt is positioned in. The underside of the upper structure and the top surface of the transverse beam are fitted with adaptor plates, where both the hydraulic cylinders and the fixation tools for the three selected spreader components can be fitted. This makes it possible to mount the hydraulic cylinders so that they either hang down from the test rig, as in Figure 3.3, or are mounted on the base in an upright position.

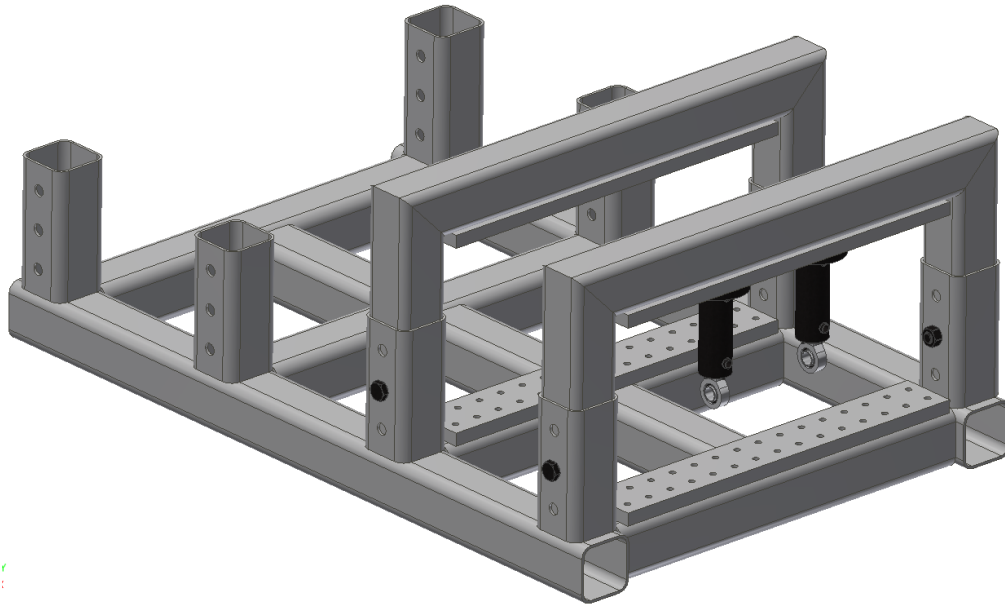


Figure 3.3. Concept 2 of the main steel structure for the test rig

Advantages

- Semi-modular design

Disadvantages

- Welded in several load bearing components, where stress concentration will occur
- Risk for unwanted play at the main mounting pins
- The mounting points inside the test rig are predetermined and unequally spread apart

Concept 3

The third concept consists of two or more squared O-shaped main plates that form the main structure of the test rig. Each main plate is cut from one single plate, i.e. no welds in the main structure. The inside of the main structure is lined with interchangeable mounting plates, which holds together the complete test rig (Figure 3.4). This design allows the hydraulic cylinders and the fixation tools to be mounted both to the top, bottom and on the sides, which in turn makes it possible to perform multi axial fatigue testing. If taller components need to be tested in a vertical position, the whole test rig can be turned 90° (Figure 3.4b). The test rig can be made both stiffer and longer by adding more main plates and/or replacing the mounting plates for longer ones.

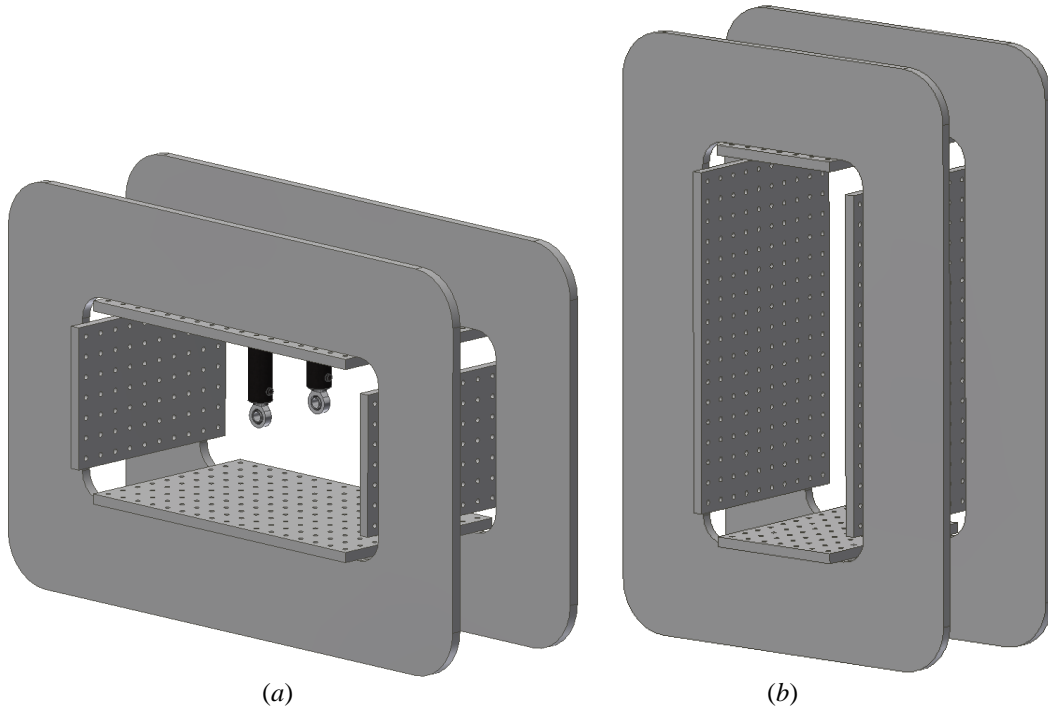


Figure 3.4. Concept 3 of main steel structure for the test rig a) normal mode b) upright mode of higher test objects

Advantages

- Modular design, with mounting points equally spread apart
- Mounting points on the sides
- No welding required, i.e no heat-affected joining areas with

Disadvantages

- Restricted space for testing

Concept 4

The fourth concept is based on a modular design, where standard beams are used. These beams have pre-drilled holes, set at an equal distance, making it possible to assemble the rig to fit each spreader component, as seen in Figure 3.5. The test rig is joined together by high strength bolts and nuts, making it easy to re-assemble. This concept relies on a ridged foundation or floor with rails, as mentioned in 2.3.2 *Recommendations for design of a fatigue testing rig*, where the main uprights can be mounted to the floor and its position can be adjusted along the rail.

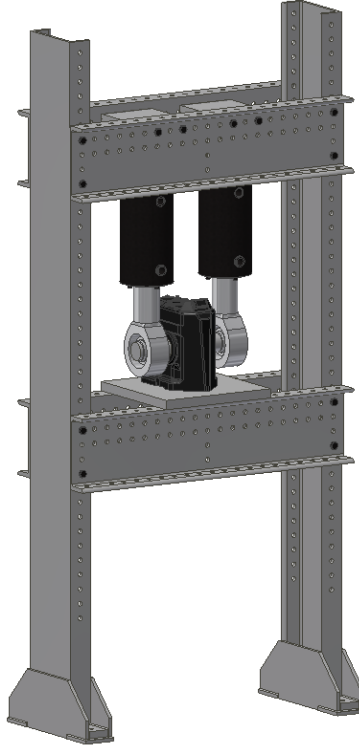


Figure 3.5. Concept 4 of main steel structure for the test rig

Advantages

- Highly modular design, which can be made smaller or bigger by repositioning the beams
- Easy to manufacture while only standard beams are used

Disadvantages

- Dependent on a foundation to which the test rig is mounted to

Concept 5

The fifth concept consists of four threaded rods, with two main plates mounted on the rods with a nut on each side (Figure 3.6). This design makes it possible to variably adjust the height on the test rig, as well as making it possible to pre-tension the test rig before starting fatigue testing. This concept is fairly similar to the creep rig at swerea|KIMAB. Compared to a MTS laboratory rig, this concept uses regular threaded rods instead of polished rods, in order to simplify the design of the test rig. Depending on the fatigue characteristics of the threaded rod, this component may have to be altered.



Figure 3.6. Concept 5 of the main steel structure for the test rig

Advantages

- Easy to manufacture and assemble

Disadvantages

- Poor fatigue properties in long threaded rods that aren't pre-tensioned
- Very large threaded rods are needed to manage the high loads

3.3.2 Complementary components

During the brainstorming session, concepts for complementary components to the earlier presented concepts of the main steel frame were also sketched. The complementary components form an essential part in these concepts, in order for the test rig to be able to perform fatigue testing on all the three selected spreader components.

Lever arm

After examining the different load cases in Table 3.1, it can be distinguished that two out of the three selected spreader components will be tested with a maximum load that's less than 250 kN. The twistlock assembly with the guide block will be tested with a maximum load of 245 kN. If the gearbox housing is tested with the line of force from the two hydraulic cylinders one decimeter from the center of rotation, it will be tested with a maximum load of $F_{gearbox} = 230$ kN (Equation 8).

$$2 \cdot F_{gearbox} = \frac{46 \text{ kNm}}{0,1 \text{ m}} \rightarrow F_{gearbox} = 230 \text{ kN} \quad (8)$$

The maximum load for the center web plate substructure, F_{web} , when divided into two equal forces, is

$$2 \cdot F_{web} = 1040 \text{ kN} \rightarrow F_{web} = 520 \text{ kN} \quad (9)$$

In order to achieve the necessary load for the center web plate substructure, F_{web} , without having to over dimension the hydraulic cylinders for the two other selected spreader components, a lever arm solution can be used to mechanically increasing the load. Two different solutions for the lever arm were proposed during the brainstorming session. One where the lever arm support is in between the two forces (Figure 3.7a) and one with the support in one end of the lever arm (Figure 3.7b).

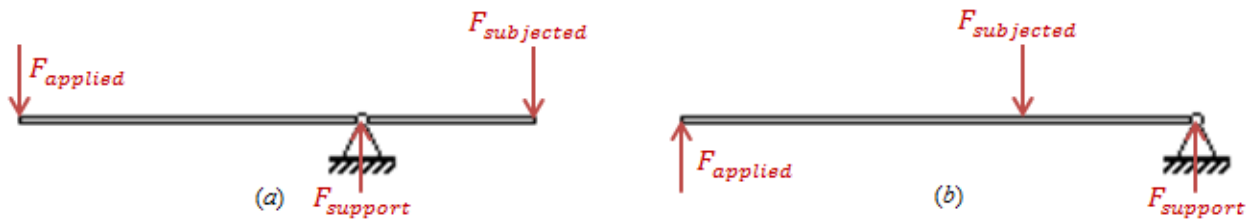


Figure 3.7. Lever arm with the support a) in between the two forces b) in one end of the lever arm

where $F_{applied}$ is the applied load from the hydraulic cylinders, $F_{support}$ is the load on the support for the lever arm and $F_{subjected}$ is the subjecting load on the test object.

The example in Figure 3.7a can be seen as the typical lever arm solutions where the support is placed in between the applied and the subjecting force. This solution results in the highest load over the support, as shown in Equation (10-11). When performing fatigue testing, it's more preferable if the resulting forces can be kept as low as possible throughout the whole test rig. Because the subjecting load, $F_{subjected}$, is a fixed value that must be met during testing for both solutions it's more beneficial, in a fatigue point of view, if the highest load is the subjecting load as in Figure 3.7b and shown in Equation (12-13).

$$\text{Figure 3.7a} \quad \uparrow: F_{support} - F_{applied} - F_{subjected} = 0 \quad (10)$$

$$F_{subjected} = F_{support} - F_{applied} \quad (11)$$

$$\text{Figure 3.7b} \quad \uparrow: F_{applied} + F_{support} - F_{subjected} = 0 \quad (12)$$

$$F_{subjected} = F_{applied} + F_{support} \quad (13)$$

Freestanding rail mounting system

Due to the requirement of having a mobile test rig, concepts relying on a rigid foundation must instead be mounted to a stiff base-construction that can be moved in accordance with the set requirements in the requirements specification. The freestanding rail mounting system in Figure 3.8 is a solution primarily intended for concept 4, but could most likely be implemented in other concept as well. The design for the concept comes from Scania’s substructure rail system, previously shown in Figure 2.19b. The base-construction is made out of one main plate (situated on top of the H-beams), and several narrower plates where the edges on the long-side have been milled out half way through the plates thickness on one side of the plate. These narrower plates have countersunk bolt holes so that bolts don’t protrude above the flat surface of the plates, making it possible to variably move the test rig along the rails. The complete base-construction is assembled with bolts that go straight through the narrow plate, the main plate, the upper flange of the H-beam and tightened with a nut on the underside of the flange. High strength steel mounts like in Figure 2.19a are slid into the created cavity and the test rig is bolted down to these mounts, which in turn clamps the test rig in place on the freestanding rail mounting system.

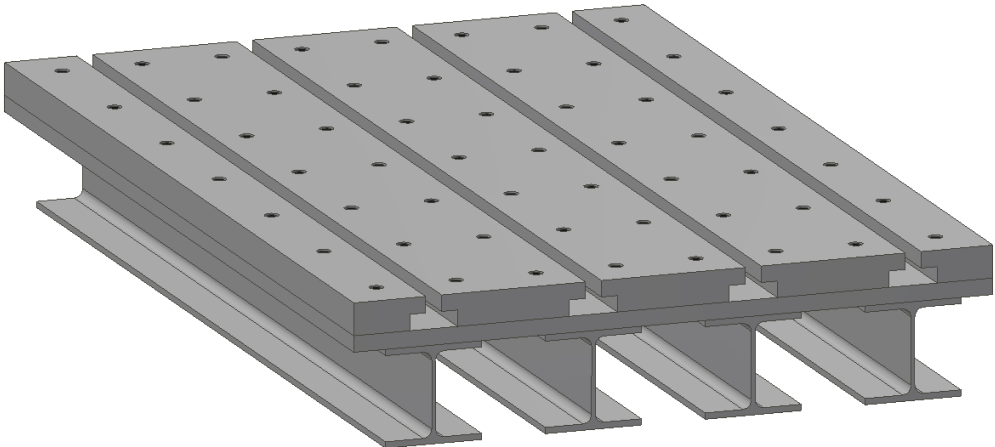


Figure 3.8. Freestanding rail mounting system

When combining e.g concept 4 of the main steel structure with the lever arm solution and the freestanding rail mounting system, it could form a complete system for testing all the three selected spreader components, without having to change the main setup of the test rig. A schematic sketch of how this system could look like is shown in Figure 3.9.

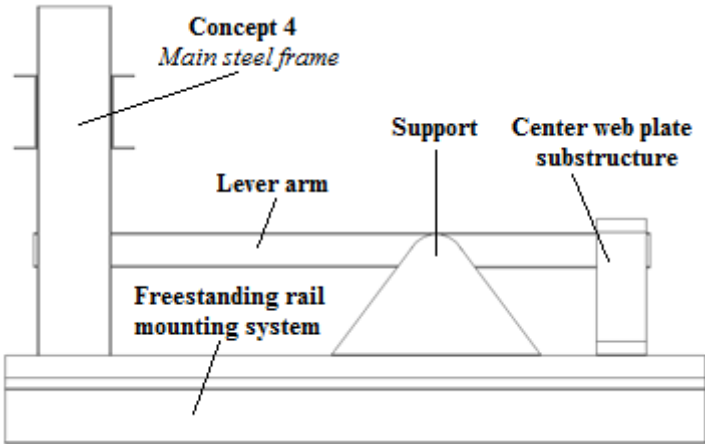


Figure 3.9. Concept 4 of the main steel frame, with the freestanding rail mounting system and lever arm solution

3.4 Concept selection

To determine which concept of the main steel structure that should be further developed, all of the concepts will be evaluated in a selection stage. No evaluation or selection concerning the complementary components or the fixation tools for the three selected spreader components will be done in this stage. This is due to the high influence of the design aspects of the test rig, depending on which concept is selected.

3.4.1 Selection of concept for main steel structure

A final concept of the main steel structure will be determined by the use of Pugh's decision matrix (Frank Cervone, 2009), where the concepts will be compared to each other and evaluated against a so called "baseline" or reference, in this case HIAB's test rig. All the concepts will be assessed on different criteria, from which a selection of factors are determined and compared for each concept to the baseline according to the rating scale in Table 3.3.

Table 3.3. Rating scale for Pugh's matrix

Points	Compared to baseline
3	Much better
2	Better
1	Slightly better
0	Same
-1	Slightly worse
-2	Worse
-3	Much worse

Because each selected factor not will have the same, each factor is assigned a "weight" in regard to its relative importance to the fatigue testing rig. The number of points each factor has been assessed with is multiplied with its weight i.e. its importance, giving a weighted result. The scale for determining the weight of a factor is shown in Table 3.4.

Table 3.4. The scale for determining the weight of a factor

Weight	Importance
5	Crucial
4	Important
3	Relevant
2	Minor
1	Insignificant

The results from the Pugh's matrix will be displayed as four different scores: the number of plus scores, the number of minus scores, the overall total scores and the weighted total scores. The overall total scores are calculated by summing the total plus scores and the total minus scores and the weighted total scores are the sum of the points for all the factors times its respective weighting factor. Note that the concept with the highest score is not necessarily the most important, but the relative scores (plus, minus, total) also provides useful information regarding the selection of the final concept. (Frank Cervone, 2009)

The selected factors, from the criteria for comparison, are partially derived from the requirement specification and partially formulated with regard to the processes of manufacturability, assembly and usability of the fatigue testing rig. The selected factors that are shown below have been developed and weighted in consultation with Bromma.

Selected factors derived from requirements specification

- **Geometrically dimensioned to fit the three selected spreader component**
It's crucial that the test rig is able to fit the three selected spreader components.
- **Modular mounting solution for hydraulic cylinders**
Make it possible to change the hydraulic cylinders in the test rig, to either bigger or smaller cylinders depending on the need for the fatigue testing.
- **Easily disable one hydraulic cylinder under normal setup**
During some fatigue testing, both hydraulic cylinders may not be need. It's therefore beneficial if one hydraulic cylinder can be disabled from the test rig.

Selected factors with regard to manufacturability

- **Ability to manufacture the test rig at Bromma's own manufacturing facility**
To reduce the cost of manufacturing, Bromma has a desire to be able to manufacture as much parts and components as possible in their own manufacturing facility.
- **Use of readily available material and components at Bromma's manufacturing facility**
It reduces the need for outsourcing and gives Bromma the opportunity to more easily make corrections or adapt changes to the main steel frame of the test rig.
- **Use of standard parts and components to reduce complexity**
If more standard parts and components can be used, the complexity of the test rig can be reduced and it can simplify the manufacturing and reduce both cost and lead-time.

Selected factors with regard to assembly

- **Reduce the amount of welds**
Due to the poor fatigue properties of welds with their tensile residual stresses, compared to none heat affected steel, the amount of welds on the test rig should be reduced as much as possible or in best case avoided completely.
- **Reduce the amount of subcomponents**
In order to simplify the assembly of the steel structure, the amount of subcomponents needed for the test rig should be kept at a minimum. This will in the end affect the overall robustness of the test rig.
- **Modular design**
There's a desire from Bromma to make the test rig as modular as possible, in order to later be able to perform fatigue testing on other components then just the three selected spreader components. One key aspect is to implement a modular mounting solution for the test objects to the design.

Selected factors with regard to usability

- **Accessibility and general ease of mounting and dismounting test objects**
When performing fatigue testing with the test rig, especially with larger batches of the same test objects, it's beneficial if the procedure for mounting and dismounting can be done as simple and quickly as possible, in order to reduce downtime on the test rig.
- **Ability to move the test rig**
The test rig should be constructed as a freestanding unit, which can be move with a heavy lifting forklift or more powerful overhead crane. This is an important aspect, due to the high likeliness that Bromma has to move their testing laboratory to a different facility within the near future.
- **Ease of maintenance, service and repair**
In order to simplify maintenance and make preventive repairs to the test rig, the concepts should be well thought out and designed with these aspects in mind.
- **Ability to perform multi-axial fatigue testing**
If hydraulic cylinders can be installed perpendicular to the sides of the test rig, it would enable the opportunity to perform multi-axial fatigue testing.
- **General safety aspects concerning user safety during fatigue testing**
The concept should be planned and designed in a way that the general safety for the user during fatigue testing is acceptable.
- **Long life time on subcomponents that are effected to wear**
The use of wearing parts in the test rig is justifiable if they can simplify the design of the test rig and they can easily be replaced before their expected life have been consumed. The wearing parts should be able to cope with at least five fatigue tests before they have to be replaced. If these parts were to fail during a fatigue test, it would generate some uncertainty in the evaluation of the test.

External selected factors

- **Cost of operation**
The cost of operation must be taken into consideration in relation to how fast each test can be performed. Investing in more expensive fatigue-rated hydraulic cylinders and a better control system that can speed up the fatigue testing, may well be worth the extra costs in return for shorter testing time for each test.
- **Manufacturing cost**
The aspect of cost is always a concern when developing new equipment. For the test rig, it's clearly beneficial if the cost of the manufacturing can be kept as low as possible.

The assessment of each concept in the Pugh’s matrix is made in respect to the explanation given to each selected factor and in comparison to the baseline. The summarized result of the scores for the different concepts is shown in Figure 3.10. The complete assessment of the Pugh’s matrix can be seen in Appendix C.

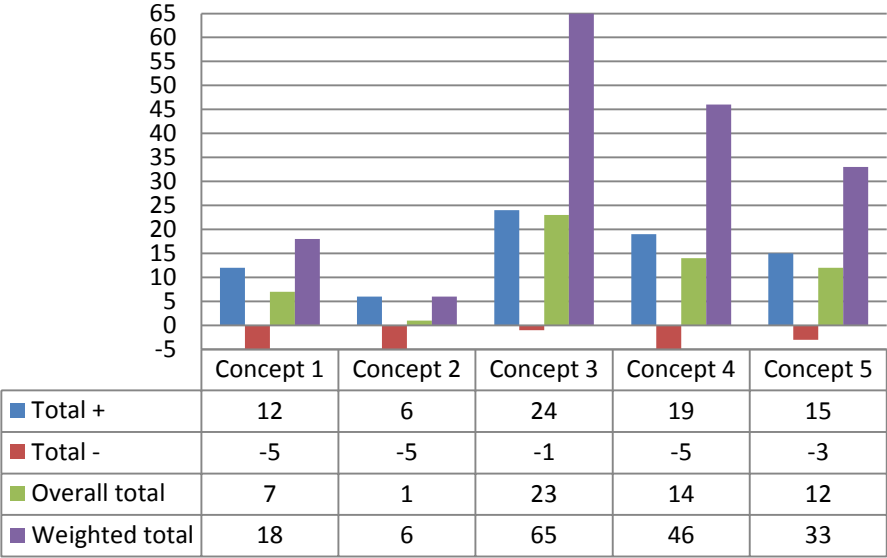


Figure 3.10. Summarized result of the scores from Pugh’s matrix

It can clearly be seen that Concept 3 has achieved the highest score in all the categories, including the least amount of minus. In comparison with the second highest scoring concept, Concept 3 have a better design when it comes to the use of readily available material and components at Bromma’s manufacturing facility, as well as a reduced amount of subcomponents. It’s however not as good as Concept 4 when it comes to the use of standard parts.

With the supporting data from the results of Pugh’s matrix (Appendix C), Concept 3 is selected as the most suitable concept for this application and should therefore continue to be developed.

3.5 Concept testing

Before the development of the final concept can be started, some initial testing on the selected concept as well as potential complementary components will be performed to determine whether the basis of their designs can be used for the fatigue testing rig.

3.5.1 Geometrical characteristics of the test rig

The main plates for the test rig must be cut from one single plate in order to avoid welding or bolting together several smaller pieces. This is a crucial aspect on which the whole concept is based on. The size of the main plate is therefore limited by the size of a standard of steel plate, 2000x6000mm (Bromma, 2014). This means that one of the outer dimensions of the main plate can't be more than 2 m in length.

For the initial design of the test rig, the proportion of the main plate is kept to the ones sketched during the concept generation. This gives an initial outer dimension of 2000x3000 mm, half the size of a standard size plate. In keeping with the ratios from the first sketch, the dimensions of the center cut out is set to 2000x1000 mm, giving the main plate a width of 500 mm along all the cross-sections of the O-shape. The inner and outer radiuses are also set to match the proportions of the sketched concept. The thickness of the main plates is set to 50 mm, in order to benefit from using evenly divisible sizes during the concept testing.

To check that the three selected spreader components fits within the confined space of the test rig, they are positioned within the main plate and checked for clearance, as seen in Figure 3.11.

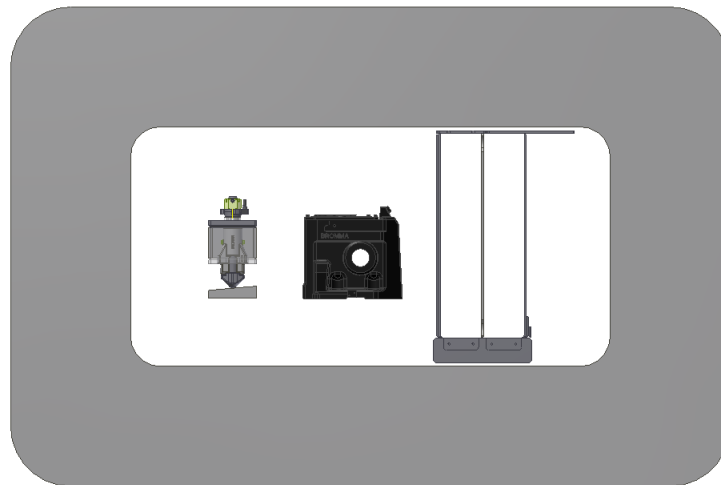


Figure 3.11 The three selected spreader components placed within the confined space of the main plate

All the three selected components fit within the confined space of the main plate, although the clearance for the center web plate substructure is considered to be too tight. Further changes will have to be made to the main plate in the final concept design.

3.5.2 Strength analysis of the main plate

The main plates form a key part in the test rig, where they act as an external skeleton to take up the loads that the test rig is subjected to during the fatigue testing. The advantage of using the main plates as the primary load bearing parts of the rig is that they haven't been welded together nor have any play in bolted joints where stress concentrations can occur, i.e there are no significant weak spots in the load bearing part.

In order to get a better understanding of how the design of main plate reacts to the loads, some initial strength calculations are performed on the initial dimensioned main plate where elementary load cases and equations from solid mechanics are used to calculate the maximum stresses σ_{max} and the deflection f . The results from these calculations are then compared to an

FEA of the main plate, in order to ensure that the two results are reasonably consistent. The material properties for the main plate are taken from regular structural steel. The maximum stresses and deflection are calculated in the marked cross-sections in Figure 3.12.

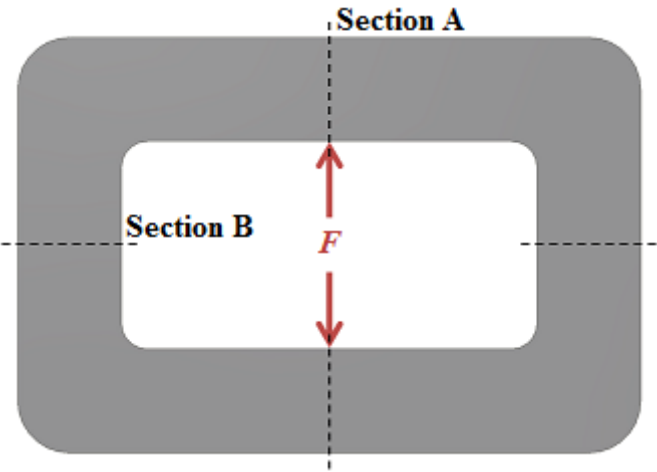


Figure 3.12. The main plate with highlighted cross sections

Figure 3.12 shows the worst possible load case for the main plate, where one hydraulic cylinder is placed directly above the center of one main plate, resulting in the subjecting force F .

Because the main plate has any constant width all along its O-shape in the initial dimensioning, the cross sections for both section A and section B are equal. The dimensions for the cross sections are shown in Figure 3.13.

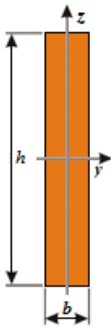


Figure 3.13 Dimensions for cross sections in section A and section B

where the height is $h = 500$ mm and the width $b = 50$ mm.

Initial calculations

The initial calculations are done with elementary load cases, which only apply for straight beams with constant cross sections, and equations from solid mechanics. The subjecting force F will be calculated as a variable for the results of the maximum stresses and the deflection.

Section A

The horizontal upper and lower part of the main plate can each be seen as a separate beam that will bend when load is applied on it. With the help of the elementary load case in Figure 3.14, the maximum stress and deflection can be determined for when the full load is applied in the test rig. (Björk, 2013)

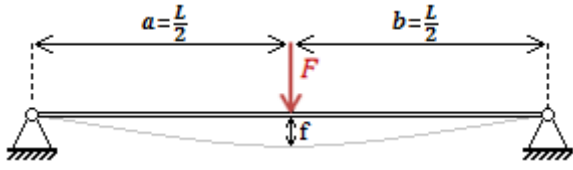


Figure 3.14. Elementary load case for a simply supported beam with constant cross section

The beam is simply supported at each end with a force applied in the center of the beam. In order to determine the maximum stress in the upper and lower part of the main plate, the maximum torque must first be calculated according to Equation (14). (Björk, 2013)

$$M_{max} = \frac{F}{2} \cdot \frac{L}{2} = \frac{FL}{4} \quad (14)$$

where F is the subjecting force and L is the length of the “beam”, in this case the length between the two horizontal parts of the main plate is $L_x = 2m$.

When the maximum bending moment is determined, the maximum stress can be calculated according to Equation (15) (Sundström, 1999)

$$|\sigma|_{max} = \frac{|M|_{max}}{I_y} \cdot |z|_{max} = \frac{F \cdot L_x}{4 \cdot I_y} \cdot \frac{h}{2} \quad (15)$$

where $|\sigma|_{max}$ is the absolute maximum stress, $|M|_{max}$ is the absolute maximum bending moment and $|z|_{max}$ is the distance from the central plane of the cross section of the beam to its outer surface, in this case half the height of the cross section of the beam and I_y is the area moment of inertia.

The area moment of inertia I_y for a solid beam is calculated according to Equation (16) (Sundström, 1999)

$$I_y = \frac{bh^3}{12} \quad (16)$$

The deflection f , in the center of the upper and lower part of the main plate, is calculated according to Equation (17). (Björk, 2013)

$$f = \frac{FL^3}{48EI} \quad (17)$$

where E is the Young’s modulus which is $E = 208 \cdot 10^3$ MPa for structural steel. (Sundström, 1999)

Section B

The two vertical parts of the main plate are each subjected to a tensile load that’s half the value of the subjecting force, due to that the force F is acting in the center of the upper and lower part of the main plate as seen in Figure 3.13. The maximum stress in each vertical part of the main plate is calculated according to Equation (18). (Björk, 2013)

$$\sigma = \frac{F}{2 \cdot A} = \frac{F}{2bh} \quad (18)$$

where σ is the stress and A is the cross section area of the vertical part of the main plate

The equation for calculating the elongation δ in the vertical part of the main plate is derived from Equation (19). (Björk, 2013) The length for this part is $L_y = 1m$.

$$\delta = \frac{FL}{2AE} = \frac{F \cdot L_y}{2bhE} \quad (19)$$

The influence of the bending moment in the ends of the vertical parts of the main plate, which is a reacting force from the bending of the upper and lower part of the main plate due to the subjecting force in section A, is disregarded in this calculation.

The maximum stress in both section A and section B can now be calculated as a function of the subjecting force F , as seen in Figure 3.15.

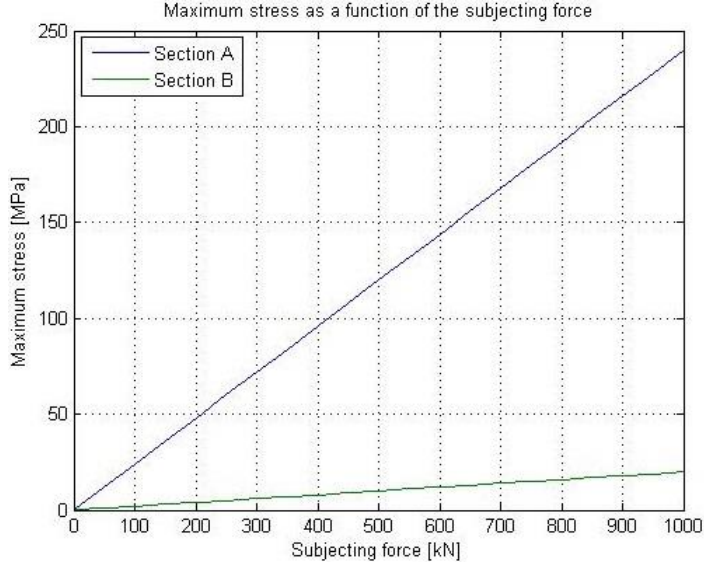


Figure 3.15. The maximum stress in section A and section B as a function of the subjecting force

The maximum stress in the upper and lower part of the main plate is substantially higher than in the vertical parts of the main plate.

The deflection of the upper and lower part of the main plate (section A) and the elongation of the vertical parts of the main plate (section B) can be calculated as a function of the subjecting force F , as seen in Figure 3.16.

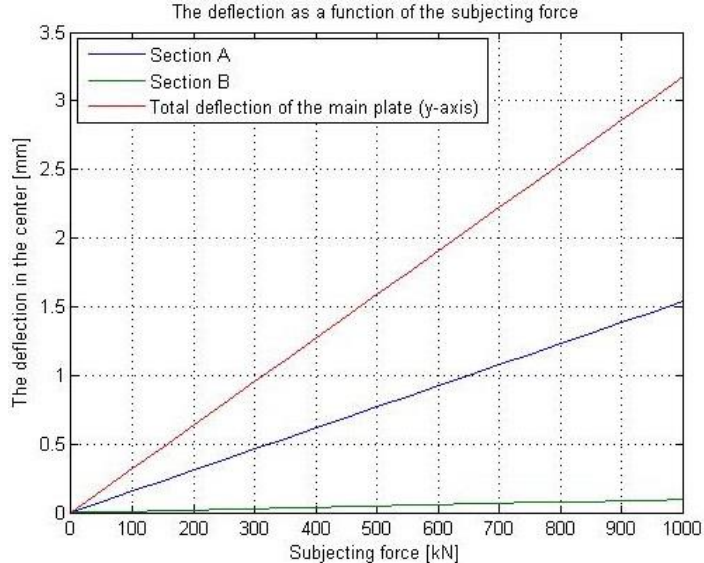


Figure 3.16. The deflection as a function of the subjecting force

The total deflection is calculated as the deflection from both the upper and lower part of the main plate, i.e. twice the deflection of section A, plus the elongation of the vertical parts of the main plate in section B.

The calculated maximum stress in Figure 3.15 is around 250 MPa at the highest load for the upper and lower part of the main plate. This is more than the recommended minimum stress of 100 MPa for fatigue testing applications, as earlier mentioned in 2.3.2 Recommendations for design of a fatigue testing rig. The calculations are however performed with only one main plate taking up the highest load for the worst possible load case. When the complete steel structure of the test rig is assembled the load will be distributed over several main plates, bringing down the maximum stress for the whole steel structure.

Buckling

When performing fatigue testing that has a reacting compressive stress on the main plate, there's a risk that the main plate could buckle. In order to assess that risk, Euler's column formula for a simply supported column is used to calculate stress at which the main plate risks to buckle (Figure 3.17).



Figure 3.17. Simply supported column

The equation for calculating the force at which a simply supported column risks to buckle is

$$P_k = \frac{\pi^2 EI}{l^2} \quad (20)$$

where l is the length of the column. In this case the length between the upper and lower part of the main plate ($l = 1$ m) due to that the load will be applied via the hydraulic cylinders that are mounted to the inner part of the test rig.

The area moment of inertia I_z of the cross section (Section B) is

$$I_z = \frac{hb^3}{12} = \frac{0,5 \cdot 0,05^3}{12} = 5,21 \cdot 10^6 \text{ mm}^4 \quad (21)$$

while the buckling will occur on the weakest side of the main plate.

When calculating the buckling force for the whole of the main plate, the area moment of inertia must be doubled due to that both the vertical parts of the main plate will be subjected to the force. The buckling force for the main plate is calculated in Equation (22)

$$P_k = \frac{\pi^2 E \cdot 2I_z}{l^2} = \frac{\pi^2 E}{l^2} \cdot 2 \cdot \frac{0,5 \cdot 0,05^3}{12} = 21,4 \cdot 10^3 \text{ kN} \quad (22)$$

The buckling force P_k is well under the highest load that the test rig will have to handle. The risk for buckling will further be reduced when the complete steel structure is assembled, because the load can then be distributed over several main plates, lowering the applied force on each main plate.

FEA of main plate

FEA is performed on the main plate, with the use of the software ANSYS 14.5, to establish the maximum stress and deflection. The values obtained from the FEA are then compared with the calculated values, to check the values credibility. If the deviation between the calculated value and the value obtained from the FEA is too great, it could be an indication that the FEA model could be set up incorrect or an error could have been made in the calculations.

In order to obtain an accurate enough value of the desired values, the model of the main plate is finely meshed. The meshed main plate in Figure 3.17a has an irregular fine mesh on the front of the main plate, which is not optimal, but it has a fine regular mesh along the edges which is the most important. The load case for the main plate is set up with a static force that's pushing upwards on the center of the upper part of the main plate and a fixed support in the center of the lower part of the main plate, as seen in Figure 3.18.

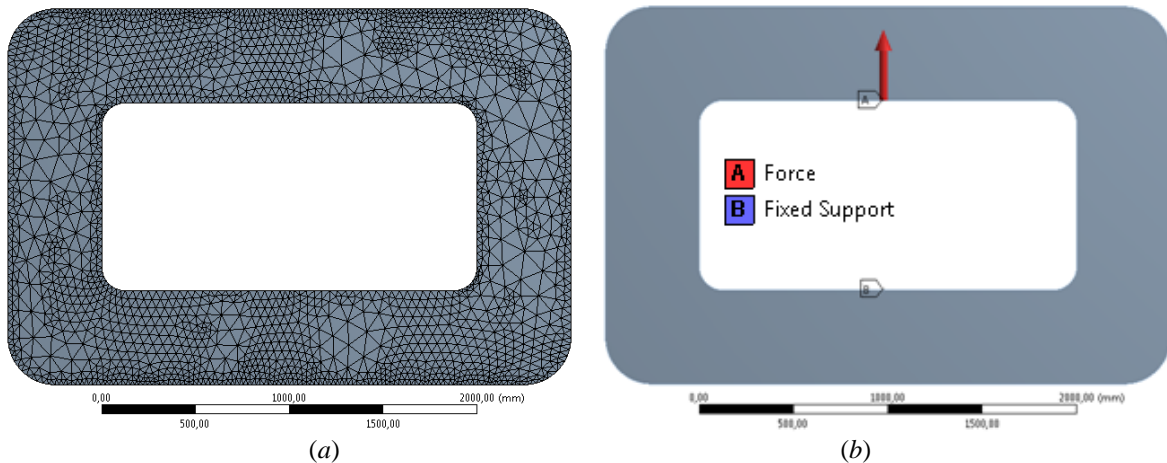


Figure 3.18. a) Finely meshed main plate b) Subjecting forces and fixations on the main plate

The FEA is performed for three different values of the subjecting force F : 250 kN, 500 kN and 1000 kN. The maximum principal stress in section A, section B and in the inner radius of the main plate are collected for all three subjecting forces. The results of the maximum stresses in the main plate, during a static force of 1000 kN, is shown in Figure 3.19.

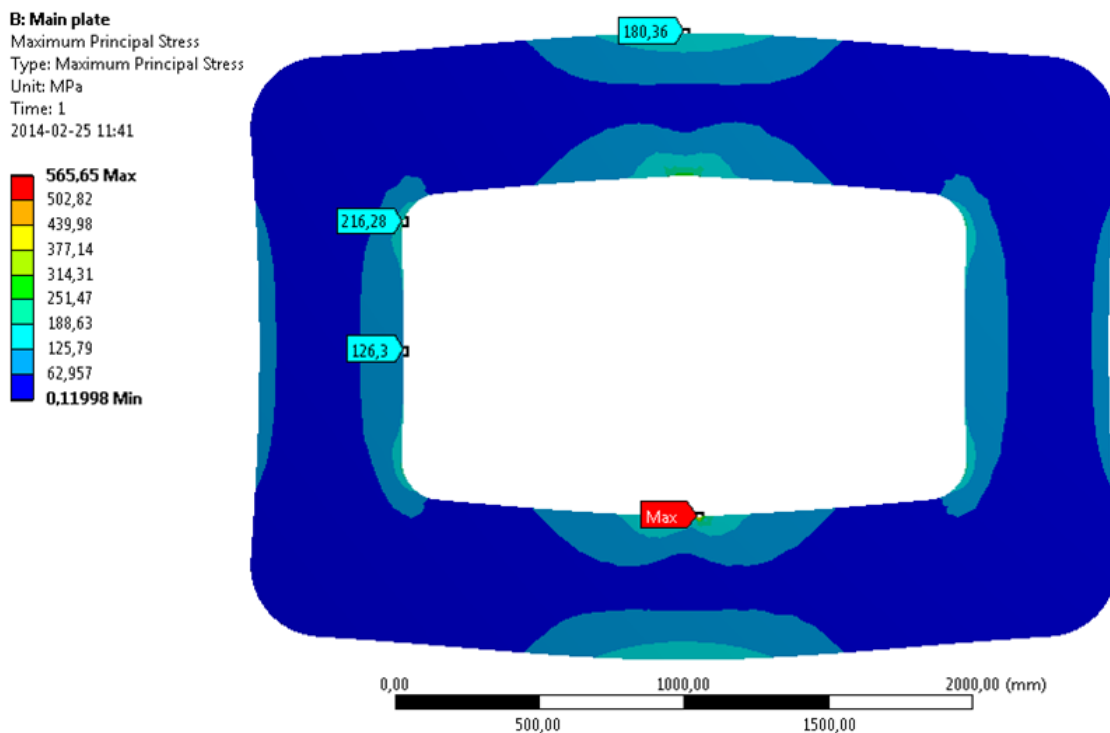


Figure 3.19. Maximum stresses during a static force of 1000 kN

The maximum stress for the main plate in Figure 3.19 is substantially higher than the stress in section B and in the radius. This is due to the singularities that occur around the area of where the fixed support is placed and where the force subjects the main plate. The stress in these areas are therefore disregarded.

The total deflection in the center of the main plate, during a static force of 1000 kN shown in Figure 3.20.

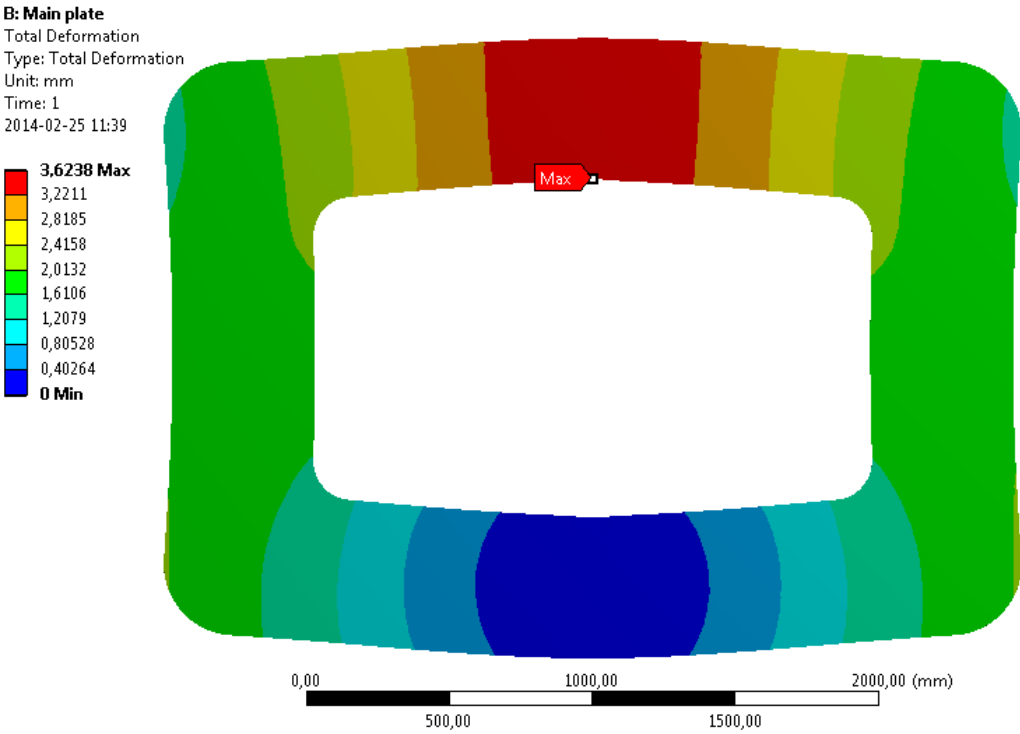


Figure 3.20. Total deflection in the center of the main plate

During closer inspection of the main plate in Figure 3.20, it’s clear that the vertical parts of the main plate are subjected to a bending moment, something that has been disregarded in previous calculations.

The results of both the calculated values and the obtained values from the FEA of the maximum stresses in section A, section B and in the inner radius, as well as the total deflection of the main plate, are shown in Figure 3.21 as a function of the subjecting force.

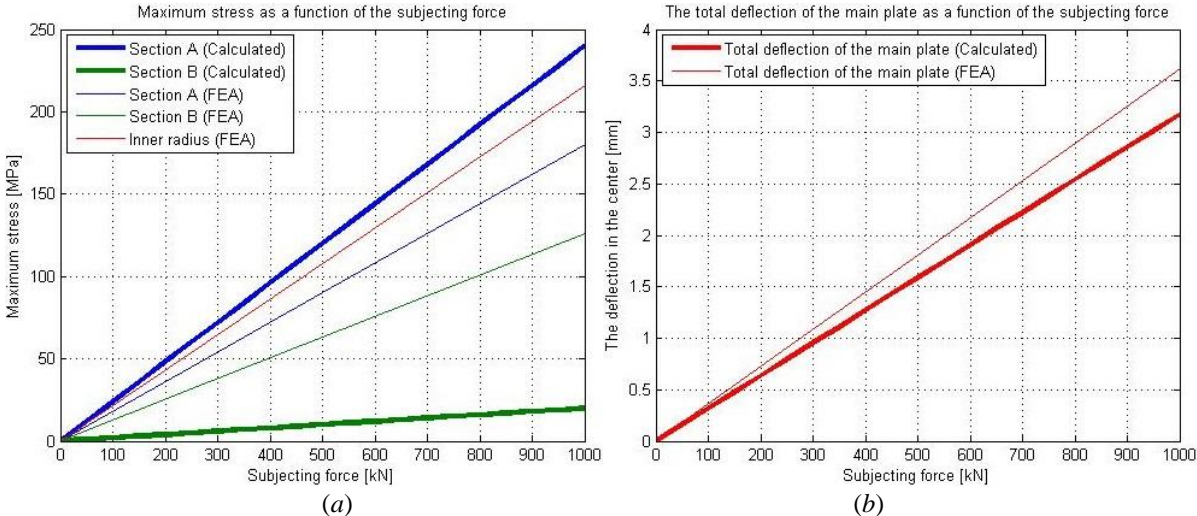


Figure 3.21. Comparison of a) Maximum stresses and b) Total deflection of the calculated values and values obtain from the FEA

The calculated values for the maximum stresses in section A are higher than the obtained value from the FEA. The deviation between these values is 33 %, which is more than what would be preferred. One explanation to this may be that the true maximum stress in section A lies within the area of the singularities where the force is subjecting the main plate, or there could be an error in the calculations.

The obtained values from the FEA for the maximum stresses in Section B are substantially lower than the calculated maximum stresses. The deviation between these values is more than 500 %, which indicates that an error must have been made in the calculations. The bending moment in the ends of the vertical parts of the main plate, that previously been disregarded, should be taken into consideration in the calculations!

It's noteworthy that the highest of the obtained stresses from the FEA lies in the radius of the main plate. This implies that the design of the main plate, especially the inner radiuses, must be modified so that the maximum stress in the radius doesn't exceed the maximum stress in section A.

The calculated values for the total deflection in the center of the main plate are less than the values obtained from the FEA. The deviation between these values is 14 %, which can be seen as satisfactory.

All the results from the FEA are presented in Appendix D.

Modifications to the initial calculations

The illustration of the deflection of the main plate (Figure 3.20) and the high deviation between the calculated values and the values obtained from the FEA of the maximum stresses in section B, clearly shows that an elementary load case with a bending moment in each end must be applied to the vertical parts of the main plate (Figure 3.22a). This in turn means that the elementary load case for the upper and lower part of the main plate must be change to one with a beam that is fixed supported, but still with a subjecting force in the center of the beam (Figure 3.22b). (Björk, 2013)

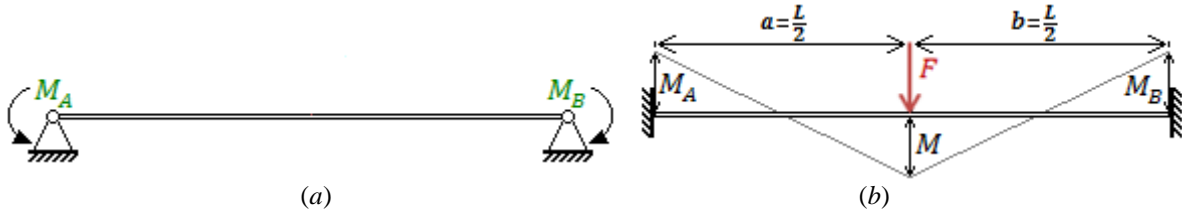


Figure 3.22. Elementary load cases for bending for a) simply supported beam with a bending moment in each end b) Fixed supported beam with a subjecting force in the center

The maximum bending moment M for the upper and lower part of the main plate is equal to each reacting bending moment i.e. $M = M_A = M_B$. These reacting bending moments are in turn subjecting the vertical parts of the main plate, affecting the maximum stress in section B. The bending moments are calculated according to Equation (23). (Björk, 2013)

$$M = -M_A = -M_B = \frac{F \cdot L_x}{8} \tag{23}$$

The length of the calculated beam for the upper and lower parts of the main plate is changed to $L_x = 2,5\text{m}$ so that it starts from the center plane of each vertical part of the main plate. The length of the calculated beam for the vertical parts of the main plate is also changed to $L_y = 1,5\text{m}$ so that it starts from the center plane from the upper to the lower part of the main plate. These changes are done in order to improve the calculation model.

The deflection f , in the center of the upper and lower part of the main plate, is calculated according to Equation (24). (Björk, 2013)

$$f = \frac{FL^3}{192EI} \tag{24}$$

Because the vertical parts of the main plate are subjected to equal bending moments in each end, the maximum bending moment over the vertical part of the main plate is constant i.e. $M_{max} = M_A$. The maximum stress in section B is calculated according to Equation (25).

$$|\sigma_{max}| = \frac{|M_{max}|}{I_y} \cdot |z|_{max} + \frac{F}{2 \cdot A} \tag{25}$$

The maximum stresses and total deflection of the main plate are calculated as a function of the subjecting force with the new elementary load cases, according to the same procedure as before. The results are shown in Figure 3.23, together with the obtained values from the FEA.

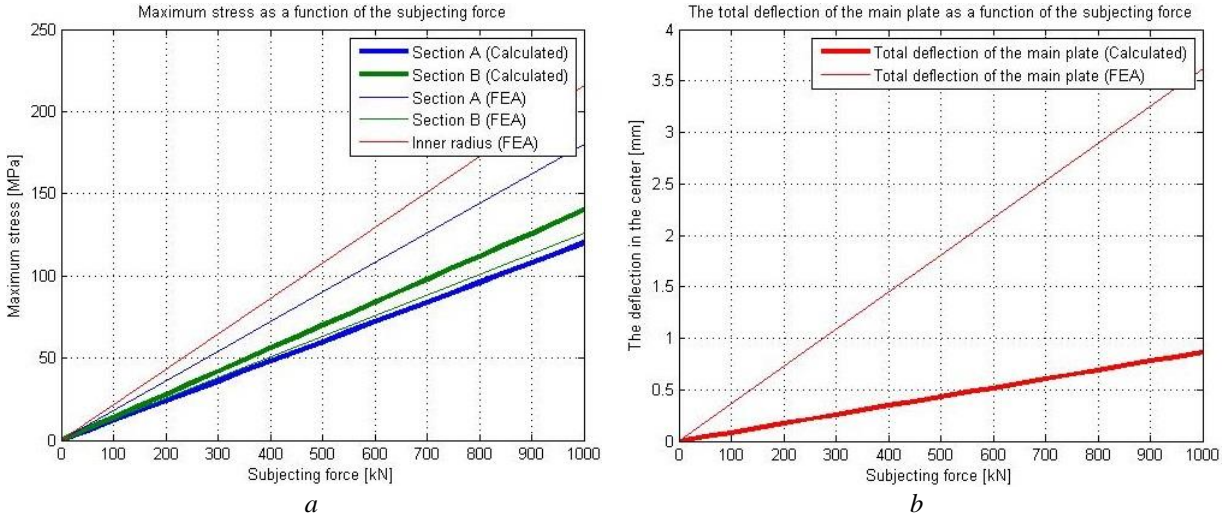


Figure 3.23. a) Maximum stress; b) Total deformation as a function of the subjecting force

The calculated values of the maximum stresses in section B are now greater than the calculated values of section A, which is highly contradictory compared the values obtained from the FEA. The calculated deviation of the total deflection is now more than 300 %, which again indicates that an error must have been made in the calculations

When these new elementary load cases are used, the calculated values of the maximum stresses in section A are reduced and the maximum stresses in section B are significantly increased in comparison to the original initial calculations. When comparing the results of the maximum stresses from the original initial calculations (Figure 3.20) and the modified initial calculation (Figure 3.23), it's notable that a combination of the original and the modified initial calculations would better simulate the maximum stresses in the specific cross sections in the main plate.

Different ratios between the results from the original and the modified initial calculations are therefore tested. After some iteration, it could be established that a ratio of 25% of the original initial calculations and 75 % of the modified initial calculations gave a low deviation between the calculated values and the values obtained from the FEA for the maximum stresses in section A and section B, as well as an equal balance of the deviations between section A and section B (Figure 3.24).

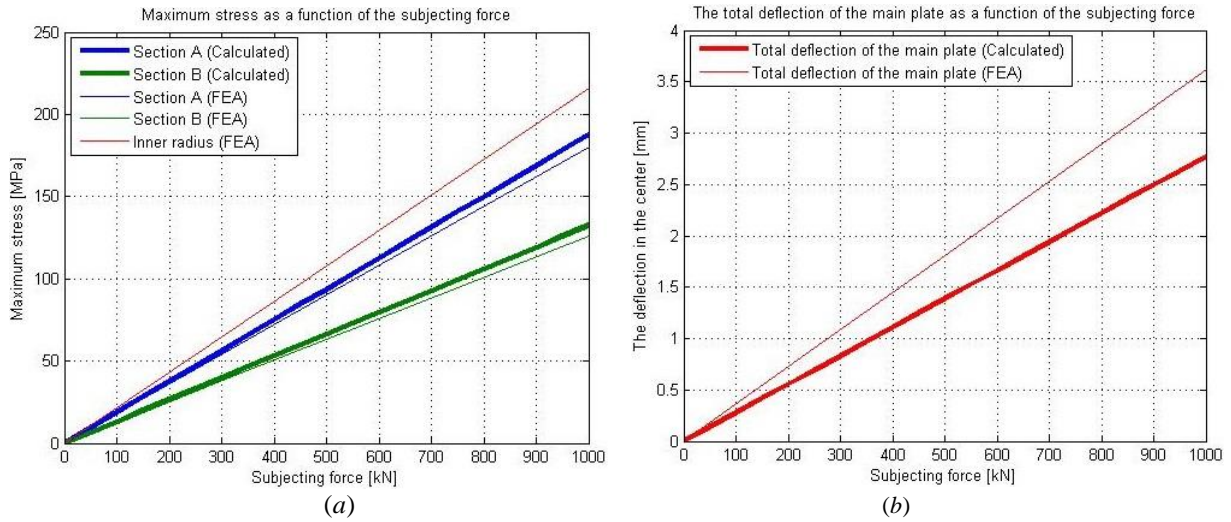


Figure 3.24. a) Maximum stress b) Total deflection

The calculated values of the maximum stresses in section A and B are both greater than the obtained values from the FEA. The deviation between the calculated values and the values obtained from the FEA are 4 % for section A and 5% for section B, which can be seen as a good result. The deviation between the calculated value and the value obtained from the FEA for the total deflection is 30 %, which is more than twice the deviation of the original initial calculations (Figure 3.21). Despite this, the 25:75 ratio of the original and the modified initial calculations is a good combination for calculating the maximum stresses in section A and B, while they are the most essential factors to calculate.

If the external dimensions were to change, the ratio between the original and the modified initial calculation may have to be changed. An FEA of the new model would then have to be made in order to obtain new values to compare with.

3.5.3 Strength analysis of the lever arm solution

A lever arm solution could be used when testing the center web plate substructure, in order of only having to use one set of hydraulic cylinders, rated at 250kN, for testing all of the three selected spreader components. This rules out the operation of having to change the hydraulic cylinders when testing different spreader components.

Two lever arms will be used for testing the center web plate substructure, one in each slot. This setup is selected because it best replicates the preferred load case, as well as it reduces the stress in the whole lever arm. Each of the lever arms can either be controlled individually with one hydraulic cylinder, or in pair with both hydraulic cylinders connected to both lever arms.

In order to keep the design simple, standard I-beams are initially chosen for the lever arms due to their favourable stiffness properties and slim design. The dimension of the lever arms are limited to the amount of space within each slot of the center web plate substructure, i.e. the space between the center web plate and the side of its substructure (Figure 3.25). To prevent the lever arm from deflecting too much, the biggest standard I-beam that will fit within the slot is selected. In this case the IPE 330, according to DIN 1025. A solid beam with the same outer dimensions will also be tested, in order to compare the results for the two beams.

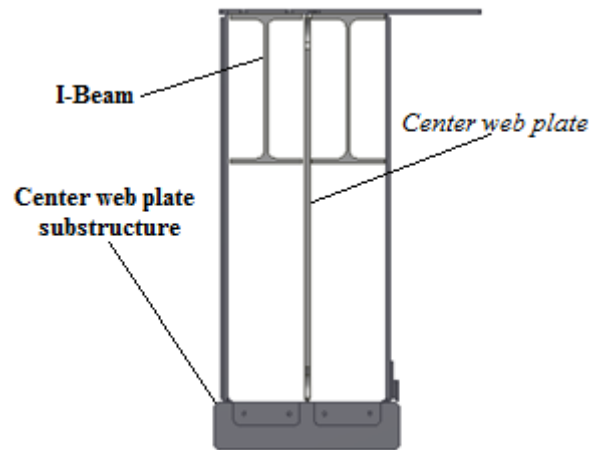


Figure 3.25. Center web plate substructure with inserted lever arms

To determine the maximum stress σ_{max} and the deflection f for the lever arm, an elementary load case that simulates the lever arms' function the best is used. In this elementary load case the beam is simply supported with one mounting support at one end, one non-fixating support at a set distance along the beam and an applied force at the other end (Figure 3.26).

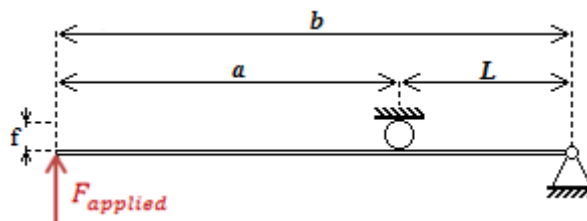


Figure 3.26. Elementary load case of one lever arm, when performing testing on center web plate substructure

The applied force $F_{applied}$, is derived from Equation (26), where the reacting force from the non-fixating support can be seen as the subjecting force $F_{subject}$. Since two lever arms are used the subjecting force from each lever arm will only be subjected to half of the maximum load with which the center web plate substructure will be tested with, i.e. $F_{subject} = 520$ kN.

$$F_{applied} \cdot b - F_{subject} \cdot L = 0 \rightarrow \frac{b}{L} \cdot F_{applied} = F_{subject} \quad (26)$$

In order to keep the maximum applied force $F_{applied}$ under 250 kN, the ratio $\frac{b}{L}$ of which the lever arms must be set at is derived from Equation (27).

$$\frac{b}{L} \cdot F_{applied} > F_{subject} \frac{F_{subject}}{F_{applied}} \rightarrow \frac{b}{L} > \frac{520}{250} \rightarrow \frac{b}{L} > 2,08 \quad (27)$$

In reference of the criteria from Equation (27) the ratio is set to $\frac{b}{L} = 2,2$ giving a maximum applied force for the center web plate of $F_{applied} \approx 236$ kN, which is in between the maximum load with which the twistlock assembly and the gearbox housing are going to be tested with.

In order to calculate the maximum stress in the lever arm, the maximum torque must first be calculated according to Equation (28). (Björk, 2013)

$$M_{max} = F_{applied} \cdot a \quad (28)$$

The maximum stress in the lever arm can now be calculated according to Equation (29) (Sundström, 1999)

$$|\sigma|_{max} = \frac{|M|_{max}}{I_y} \cdot |z|_{max} = \frac{F_{applied} \cdot a}{I_y} \cdot \frac{h}{2} \quad (29)$$

where $|\sigma|_{max}$ is the absolute maximum stress, $|M|_{max}$ is the absolute maximum torque and $|z|_{max}$ is the distance from the central plane of the beam to its outer surface in the z-axis.

The area moment of inertia I_y for an I-beam is calculated according to Equation (30) and for a solid beam according to Equation (31). (Sundström, 1999)

$$I_{y_{I-beam}} = \frac{t_l h^3}{12} + \frac{1}{2} t_f b h^2 \quad (30)$$

$$I_{y_{solid\ beam}} = \frac{b h^3}{12} \quad (31)$$

where all the variables in Equation (30) and (31) corresponds to a specific length according to DIN 1025 for an IPE 330 (Figure 3.12).

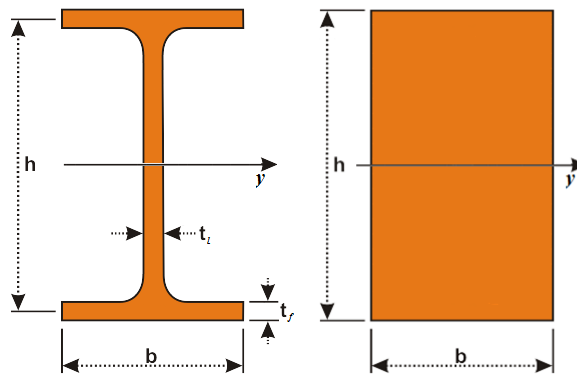


Figure 3.27. Dimensions of an I-beam and Solid beam

The deflection f in the end of the beam, where the force $F_{applied}$ is applied, is calculated according to Equation (32). (Björk, 2013)

$$f = \frac{F a^2 b}{3EI} \quad (32)$$

where F in this case is the applied force $F_{applied}$, a is the distance from the force to the non-fixating support, b is the full length of the beam, E is the Young's modulus and I is the area moment of inertia.

With the applied force $F_{applied}$ and the ratio $\frac{b}{L}$ determined and the geometrical relationships in Equation (33) and (34)

$$L = \frac{b}{(\text{ratio} + 1)} = \frac{b}{(\frac{b}{L} + 1)} \quad (33)$$

$$b = a + L \rightarrow a = b - L \quad (34)$$

the maximum stress and the deflection can be determined as a function of the total length b of the lever arm (Figure 3.28). The length b is varied between 1-2 m due to the geometrical restrictions within the confined space of the test rig where the lever arm could be placed.

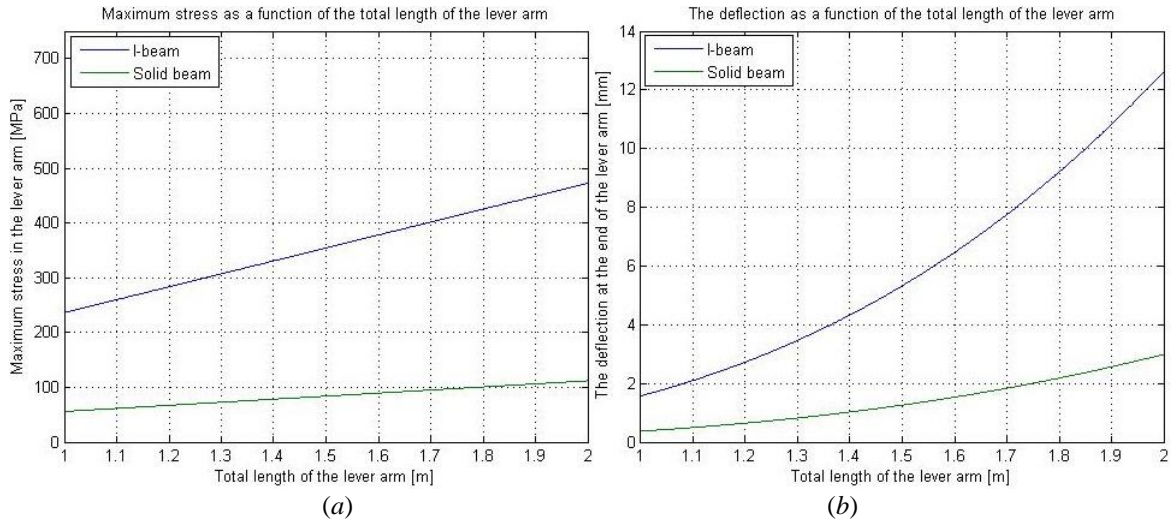


Figure 3.28. a) Maximum stress and b) Total deflection as a function of the total length of the lever arm

The maximum stress for the I-beam is between 250-500 MPa, which is more than the recommended value, while the solid beam essentially has a maximum stress of less than 100 MPa. It should however be noted that the maximum stress in the lever arm has a linear relation to the total length of the lever arm.

The calculated deflection in Figure 3.28b, gives an indication of how long the stroke of the hydraulic cylinders need to be. The elastic deformation of the center web plate substructure will however further increase the total displacement of the end of the lever arm.

In order to reduce the maximum stress, as well as the deflection in the end of the lever arm, with the current ratio setup, the area moment of inertia I_y needs to increase i.e. changing the beam to one with a larger cross-section area. Due to the limited space between the center web plate and its substructure, as seen in Figure 3.25, only the height of the beam can be changed.

The use of a solid beam for the lever arm can be questioned, while the sheer weight of the lever arm would make it difficult to handle when installing it in the test rig, as well as its greater inertia would affect the frequency of which the fatigue testing can be performed at. In order to reduce unnecessary weight and inertia is to use an I-beam type lever arm with a variable cross section. An example for this type of lever arm can be seen in Figure 3.29.



Figure 3.29. Lever arm with variable cross section

This lever arm would be designed with the highest web in the area of the pivot point where the maximum stress is the highest, and then linearly decreased to e.g. half of the maximum height in each end. The drawback with this design is that the lever arm would have to be custom made for one specific ratio, and it has to be welded together, unlike a standard I-beam that has a rolled profile.

Alternative solution

If more powerful hydraulic cylinders are used, i.e hydraulic cylinders that are rated above 250 kN, a solution that is similar to the one described in concept 1 can be used for testing the center web plate substructure. In this case, a shorter piece of IPE 330 can be used in each slot of the center web plate substructure, similar as in Figure 3.25. The static load case for each beam would be according to Figure 3.30, where the subjecting force $F_{subject} = 520$ kN and the applied force from the hydraulic cylinders are equal i.e. $F_{applied} = \frac{F_{subject}}{2} = 260$ kN.

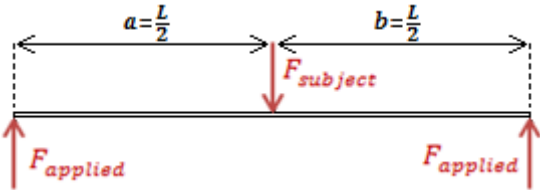


Figure 3.30. Load case for each beam

The maximum stress in the beam is calculated in the same way as for section A in the main plate, according to Equation (14)-(16). The maximum stress in the I-beam (IPE 330) is calculated as a function of the length of the beam (Figure 3.31). The relevant length of the beam is no more than between 0,5-1 m, so that it will both reach through the center web plate substructure as well as fit within the enclosed space of the test rig.

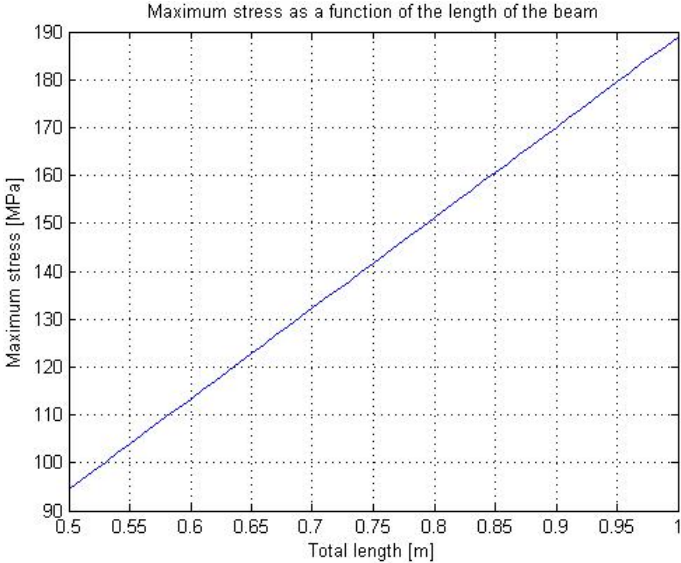


Figure 3.31. The maximum stress as a function of the length of the beam

The maximum stress in the beam is greater than 100 MPa, already when the beam is longer than half a meter. Another profile with a greater area moment of inertia should be selected if the beam needs to be longer than half a meter.

The two beams are either controlled separately with a total of four hydraulic cylinders, two for each beam with an applied force from the cylinders of 260 kN, or controlled in pair with only two hydraulic cylinders, one at each end, with an applied force from the cylinders of 520 kN.

All calculations for the diagrams in 3.5 Concept testing are performed in MATLAB and can be seen in Appendix E.

3.5.4 Conclusion of concept testing

After performing some initial calculations in the concept testing, the following conclusions can be made:

Geometry of the test rig

- The main plate is limited to 2 meters in one of the outer dimensions.
- The height of the cross section of the upper and lower parts of the main plates needs to be reduced in order to fit the center web plate substructure within the enclosed space of the test rig, without having to rotate the test rig 90 degrees for this test.

Main plate

- The maximum stress in the main plate is located as stress concentrations in the inner radiuses. The inner radiuses should therefore be increased in order to lower the stresses in this location.
- The width of the main plate could be decreased in order to reduce the bending moments, i.e. the maximum stresses, in the test rig.
- In order to calculate the maximum stresses and the total deflection, a combination of two different elementary load cases needs to be used.
- Be critical to the obtained values from the FEA, while some of them may be false due to e.g. singularities. Always control the obtained values from the FEA with calculated values to make sure that they roughly coincide.

Lever arm solution

- The lever arm solution is mainly used for testing the center web plate substructure
- There are two alternatives for testing the center web plate substructure.
 - Using the lever arm system, in order to mechanically increase the subjecting load while still using hydraulic cylinders that are only rated at 250 kN.
 - Having shorter beams straight through the center web plate and using more powerful hydraulic cylinders on each side of the beam.

4 FINAL CONCEPT

The final concept chapter starts with presenting the general design and dimensioning process that is followed and used throughout the chapter. The main steel structure of the test rig as well as the fixation tools for the three selected spreader components are thereafter thoroughly described. Final dimensioning of the complete test rig is at last performed in order to determine if the test rig can withstand the fatigue it will be subjected to.

4.1 General design and dimensioning process

The design of the fatigue testing rig and the fixation tools for the three selected spreader components is a highly iterative process where several changes have to be made during the design work, in order to establish an interface that works for all fixation tools. During the final design process, several components will have to be dimensioned and re-dimensioned due to design changes along the way. A systemic way for dimensioning components such as bolted joints, hydraulic cylinders, etc. will be established, in order to make quick dimensioning analyses during the design or re-design of a component. The system can be applied as a calculation program in MATLAB, where external parameters are input, from which the output can be obtained instantly. In that way no larger time-consuming calculations will have to be made during each design step or design change.

In order to keep the amount of dimensioning calculations at a suitable level for this thesis, only the most severely stressed components, mountings and joints will be thoroughly dimensioned in this report. Other components, such as subcomponents in the fixation tools, etc. that are not severely stressed by the dynamic load, will be designed so that they aren't liable to fatigue.

4.1.1 Initial design input

Before starting the design work, Bromma has specified a strong desire for an over dimensioning of the test rig, in relation to the fatigue strength needed for testing the three selected spreader components. The main reason for this is that Bromma wants to be able to continue using the test rig for further fatigue testing after the already determined tests are completed.

Since Bromma already have a well-established relationship with its suppliers for their spreader components, such as steel, hydraulic cylinders and sensors, they have a desire to primarily use components from these suppliers in the fatigue testing rig. This will allow Bromma to more easily source the required parts for the test rig as well as facilitate the assembly of the complete test rig, while having prior knowledge of working with similar components.

The main material that will be used for the test rig, if nothing else is specified for a specific component, will be S335J2 steel. This selection is made while the static strength of steel is virtually independent from its fatigue properties in its tensile strength and with support from previously mentioned literature in 2.3.2 *Recommendations for design of a fatigue testing rig.*

4.1.2 Fatigue dimensioning with several load cases

When dimensioning a structure against fatigue, a nominal stress method is most commonly used for classifying the fatigue assessment for structural details on the basis of the maximum principal stress range in the section where potential fatigue cracking is considered. Separate S-N curves are provided for consideration of normal stress ranges, where each fatigue strength curve is identified by the characteristic fatigue class (FAT) of the structural detail in MPa at 2 million cycles. (Hobbacher, 2007)

The fatigue testing rig will be dimensioned for three different load cases, at three to four different loads, that are estimated to run for a certain amount of cycles before fatigue failure of the spreader component. Each specific test will be repeated 20 times, as previously mentioned in Table 3.1. A method for calculating the fatigue life of the test rig, while taking into consideration the different amount of loads for the estimated amount of cycles, is needed.

A calculation model from SSAB (SSAB, 2010) is used for calculating the maximum allowed stress range, for a selected fatigue life, within a structure that is subjected to fatigue by a certain stress collective. This model calculates the maximum allowed stress range for a certain area in the structure, usually the most critical areas of the structure where the stresses are the highest. These areas have previously been determined in 3.5 *Concept testing* i.e. Section A, Section B and the inner radiuses of the main plate. The basis of this calculation model is based on Palmgren-Miner's method as presented in 2.2.4 *Palmgren-Miner*.

The first step in this calculation model is to calculate the allowable design stress intensity value, s_m , according to Equation (35).

$$s_m = \frac{N_t}{2 \cdot 10^6} \cdot k_m \quad (35)$$

where N_t is the dimensioning number of cycles before fatigue failure and k_m is the stress intensity factor, which is calculated according to Equation (36).

$$k_m = \sum_i \left(\frac{\Delta\sigma_i}{\Delta\sigma_{ref}} \right)^m \cdot \frac{n_i}{n_t} \quad (36)$$

where $\Delta\sigma_i$ is the principal stress range at the selected area of the test rig for one of the specific load cases tested at a specific load, $\Delta\sigma_{ref}$ is the reference value of the stress range i.e the maximum principal stress at the selected area for all of the load cases, m is the exponent of the S-N curve, n_i is the number of cycles for each load in each load case and n_t is the sum of all the number of cycle for all the load cases at all loads.

For the dimensioning of the test rig, the dimensioning number of cycles will be set to the sum of all the number of cycle for all the load cases at all loads, i.e. $N_t = n_t$. The stresses $\Delta\sigma_i$ and $\Delta\sigma_{ref}$ can be obtained from both calculations of mechanics of solids and by FEA.

The maximum allowed stress range, $\Delta\sigma_{Rd}$, is calculated according to Equation (37).

$$\Delta\sigma_{Rd} = \frac{FAT \cdot \varphi_t \cdot \varphi_m \cdot \varphi_e}{\gamma_m \cdot m \cdot \sqrt{s_m}} \quad (37)$$

where FAT is the fatigue class of the structural detail at the selected area, φ_t is the thickness factor for the material ($\varphi_t = 1$ for none-welded base material), φ_m is the material factor ($\varphi_m = 1$ while $\varphi_t = 1$), φ_e is the stress alternating factor ($\varphi_e = 1$ for $0 \leq R \leq 0,5$) and γ_m is the partial factor of safety. Depending on the consequence of failure, a suitable partial factor of safety is chosen from Table 4.1. $\gamma_m = 1,21$ is chosen for the fatigue testing rig.

Table 4.1 Partial factors of safety for allowable stress ranges and acceptable risk of failure (SSAB, 2010)

Consequence of failure	Partial factor of safety, γ_m	Approximated risk of failure
Insignificant	1,0	10^{-2}
Less serious	1,1	10^{-3}
Serious	1,21	10^{-4}
Very serious	1,32	10^{-5}

With the already determined values for Equation (37), the equation can be simplified to

$$\Delta\sigma_{Rd} = \frac{FAT}{\gamma_m \cdot m \sqrt{s_m}} \quad (38)$$

In order for the fatigue testing rig to withstand fatigue from all the tests, the highest stress subjected to the test rig, i.e. $\Delta\sigma_{ref}$ must be lower than the maximum allowed stress range, giving the dimensioning criteria.

$$\Delta\sigma_{Rd} > \Delta\sigma_{ref} \rightarrow [R = 0] \rightarrow \Delta\sigma_{Rd} > \sigma_{max} \quad (39)$$

4.1.3 Dimensioning of prestressed bolted joints

Because all of the fixation tools and selected spreader components must be easy to install and remove from the test rig, in order to change the setup for the test rig, they are mounted with bolted joints. In order for the bolts to withstand fatigue from tensile loading during fatigue testing, all bolts needs to be prestressed to 70 % of their yield strength, while that's the maximum stress that can be achieved by using normal torqueing of the bolts before the friction becomes too great (Nord-Lock, 2014). A properly prestressed bolt mounted on a flange can withstand far higher fatigue loads compared to a manually tightened bolt.

When a bolt is torqued on a flange the bolt will elongate, Δl_b , and the flange will compress Δl_f . Both the bolt and the flange will be prestressed to the same value, while they are each other's counterforce. In Figure 4.1 the stiffness of the bolt k_b is illustrated as the line from O to C and the stiffness of the flange k_f is illustrated as the line from A to B.

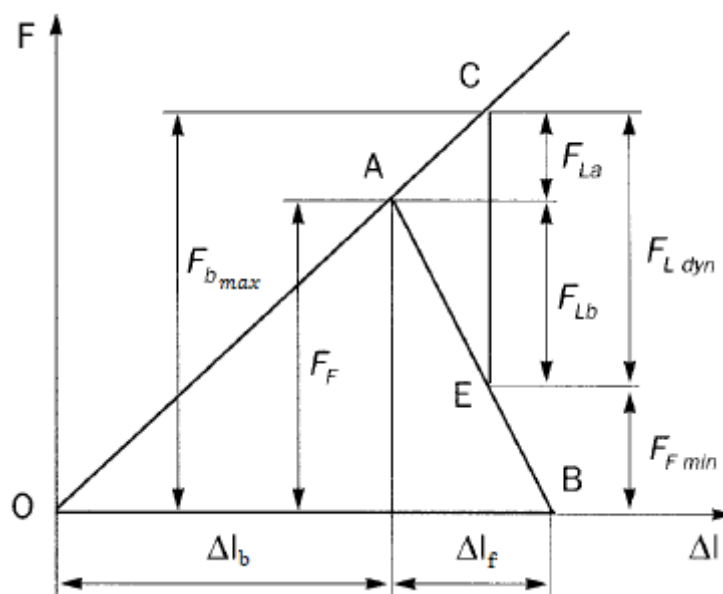


Figure 4.1. Diagram showing the force in the prestressed bolt and flange as a function of the elongation (Colly, 1995)

where F_F is the prestressing in both the bolt and the flange, $F_{F_{min}}$ is the residual prestressing of the flange, $F_{L_{dyn}}$ is the maximum internal tensile load in the bolt which is a quota of the external tensile load F_{tot} , F_{La} is the part of the internal tensile load that additionally loads the bolt and F_{Lb} is the part of the internal tensile load relieving the compressed flange.

A calculation model from Colly (Colly, 1995) is used for dimensioning the bolted joints against the fatigue tensile loads that they will be subjected to during fatigue testing. The first step in this calculation method is to establish the stiffness of both the bolt and the flange according to Equation (40) and (41).

$$k_b = \frac{A_b \cdot E_b}{L} \quad (40)$$

$$k_f = \frac{A_f \cdot E_f}{L} \quad (41)$$

where L is the clamping length of the bolted joint, E_b is the E-modulus for the bolt and E_f is the E-modulus for the flange. While both the bolt and the flange are made of steel, both E-modulus are set to $E = E_b = E_f = 210 \cdot 10^3$ MPa (Colly, 1995).

and where the bolts cross section area, A_b , is calculated according to Equation (42) and the flange effective cross section area, A_f , is calculated according to Equation (43) (KTH, 2008).

$$A_b = \frac{\pi}{4} \cdot d_p^2 \quad (42)$$

$$A_f = \frac{\pi}{4} \cdot ((H + 0,3 \cdot L)^2 - D_h^2) \quad (43)$$

where d_p is the pitch diameter of the threads on the bolt, H is the head size of a hexagonal bolt and D_h is the diameter of the clearance hole for the bolt.

The prestressing force F_F is obtained according to Equation (44)

$$F_F = (\sigma_{y_{bolt}} \cdot 0,7) \cdot A_b \quad (44)$$

where $\sigma_{y_{bolt}}$ is the yield strength of the bolt and “0,7” stands for the 70 % that the bolt is prestressed to.

The total external tensile load F_{tot} that subjects the fixation tools and the selected spreader components to fatigue in the test rig must be divided over N_s number of bolts, in order for the bolted joints to withstand the fatigue load.

$$F_{L_{dyn}} = \frac{F_{tot}}{N_s} \quad (45)$$

When dimensioning a bolted joint, it's essential not to over dimension the joint, while it could require unnecessary large bolts and increase the torque that the bolts must be prestressed with. It's therefore recommended by Colly that the residual prestressing of the flange, $F_{F_{min}}$, is set to around 10-20 % of the maximum internal tensile load in the bolt, $F_{L_{dyn}}$. A conservative dimensioning criterion in Equation (46) is established for dimensioning the bolted joints for the test rig.

$$F_{F_{min}} > 0,2 \cdot F_{L_{dyn}} \quad (46)$$

In order to establish the N_s number of bolts needed in the bolted joint with regard to the dimensioning criteria in Equation (46), two more equations are needed. (KTH, 2008)

$$F_{b_{max}} = F_F + F_{L_{dyn}} \cdot \frac{1}{1 + \frac{k_f}{k_b}} \quad (47)$$

$$F_{b_{max}} = F_{L_{dyn}} + F_{F_{min}} \quad (48)$$

where $F_{b_{max}}$ is the absolute maximum load the bolt will be subjected to.

When inserting Equation (45), (46) and (48) into Equation (47), the following dimensioning criteria can be established.

$$F_{L_{dyn}} > \frac{F_{tot}}{N_s} \cdot \frac{1}{\left(1,2 - \left(\frac{1}{1 + \frac{k_f}{k_b}}\right)\right)} \quad (49)$$

Both the maximum internal tensile load in the bolt, $F_{L_{dyn}}$, and the number of bolts needed, N_s , can be established by iteration of $N_s = 1, 2, 3, \dots$ until the dimensioning criteria in Equation (49) is fulfilled.

There are also further dimensioning criteria when dimensioning against fatigue. The stress amplitude, σ_a , ranges in the region of where the bolt is additionally loaded (F_{La} region). The stress, that's presented in Equation (50), must be less than the maximum allowed stress amplitude σ_{up} . If this criterion is fulfilled, the bolt will have a fatigue life of more than 10^7 load cycles.

$$\sigma_a = \pm \frac{F_{La}}{2 \cdot A_b} \quad (50)$$

where the additional loading on the bolt, F_{La} , is calculated according to Equation (51).

$$F_{La} = F_{b_{max}} - F_F \quad (51)$$

The maximum allowed stress amplitude, σ_{up} , depends on the grade of the bolt and its specification when manufactured, as shown in Table 4.2.

Table 4.2. Maximum allowed stress amplitude σ_{up} (Colly, 1995)

Grade	Specification	Allowed stress amplitude σ_{up} N/mm ²
8.8	Rolled thread, untreated + zink plated	50 - 60
	Rolled thread, galvanized	35
	Cut thread, untreated	35
10.9	Rolled thread, untreated + zink plated	45
12.9	Rolled thread, untreated	35

When looking back to the recommendations for the maximum stress in the bolts, in 2.3.2 *Recommendations for design of a fatigue testing rig*, Mrden and Berg recommended that the stress in the bolts shouldn't exceed 50 MPa during the fatigue testing. Their recommendation is supported relatively well with the better performing bolts in Table 4.2.

4.1.4 Dimensioning of hydraulic cylinders

The hydraulic cylinders for the fatigue testing rig must be double acting, i.e pressure can be applied on both sides of the cylinder, in order to achieve a force both when the cylinder extends and when it retracts (Figure 4.3). This feature is vital in order to be able to test the gearbox housing according to the predetermine load case. It also helps in potentially reducing the cycle time while the retracting force can reset the piston to its starting position, compared to letting the reacting force from the selected spreader component force it back, before starting a new load cycle. (Roymech, 2013)

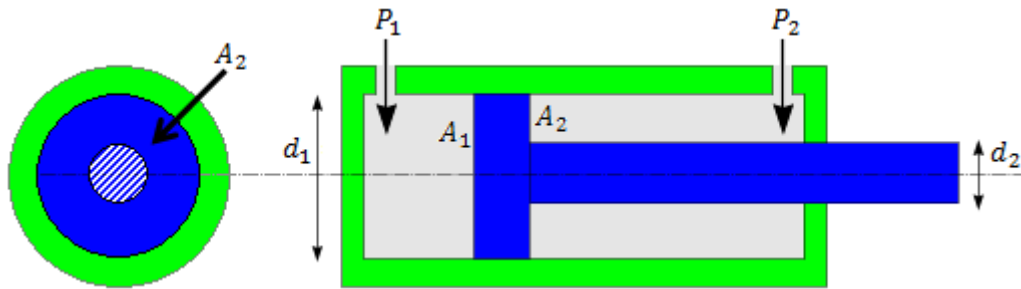


Figure 4.3. Schematic sketch of a double acting hydraulic cylinder (Roymech, 2013)

When selecting a cylinder that can apply both the right pushing force, F_{push} , as well as the right pulling force F_{pull} for a specific load case, these forces are calculated according to Equation (52) and (53).

$$F_{push} = P_1 \cdot A_1 = P_1 \cdot \frac{\pi}{4} d_1^2 \quad (52)$$

$$F_{pull} = P_2 \cdot A_2 = P_2 \cdot \frac{\pi}{4} (d_1^2 - d_2^2) \quad (53)$$

where P_1 is the pressure on the face of the piston, P_2 is the pressure on the rod side of the piston, A_1 is the area of the cylinder, A_2 is the effective area around the piston rod, d_1 is the diameter of the cylinder and d_2 is the diameter of the piston rod.

It should be noted that in order for Bromma to be able to use the hydraulic cylinders, without having to modify their existing hydraulic pumps that are used on their other fatigue testing rigs, the hydraulic pressure for the cylinders shouldn't exceed 300 bar, i.e. $P_1 < 300$ bar, $P_2 < 300$ bar. The hydraulic cylinders should however be dimensioned so that the hydraulic pressure is kept high in order to get a more responsive cylinder and reduce the cycle time, as previously mentioned in 2.3.2 *Recommendations for design of a fatigue testing rig*.

4.2 Main steel structure

The main steel structure of the test rig is divided into three different subcomponents: The main plate substructure, the main boxes and the side boxes (Figure 4.4). It's designed so that the fixation tools can easily be mounted into the test rig, by fixating it with bolts to the main and side boxes. The complete fatigue testing rig is a freestanding structure that doesn't need any extra support or fixation in terms of its fatigue strength.

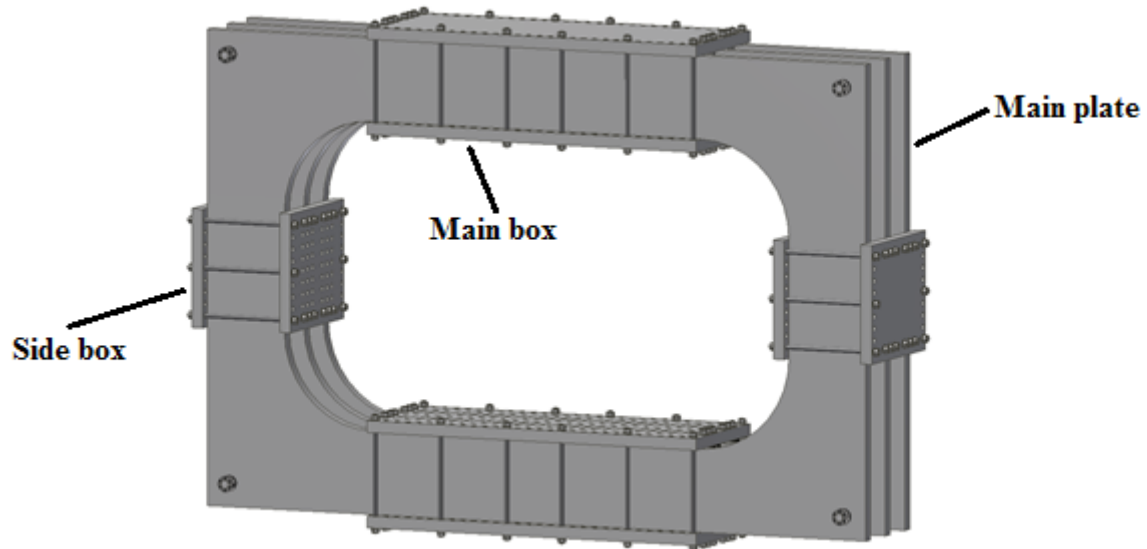


Figure 4.4. The main steel structure of the fatigue testing rig

4.2.1 Substructures of the main steel structure

All the steel plates for both the main plates as well as the main- and side box are gas cut from 50 mm S335J2 steel plate. This allows the plates for the main- and side box to be cut from the inner cutouts of the main plates, reducing the amount of waste material from the original steel plate from which the main plates are cut from.

Main plate

The main plates are designed to take up the main loads during the fatigue testing. The main principal with this design is that more main plates can be added to the test rig to further strengthen it.

The initial outer dimension of 2000x3000 mm are kept for the final design, but the center cut out is increased in order to fit the fixation tools needed for testing the three selected spreader components within the test rig. The height of the cross section in the O-shape of the main plate has been reduced to 350 mm, reducing the stiffness of the main plate. The inner radiuses of the main plates are increased in order to lower the stress concentrations that previously been identified from the FEA in 3.5.2 *Strength analysis of the main plate*.

The main plate substructure is assembled by placing the main plates at a distance next to each other and inserting threaded rods through each of the holes in the corners of the main plates, with spacers in between each main plate (Figure 4.5). The spacers insure that the main plates are positioned at an equal distance from each other. A nut, in form of a Multi-bolt tensioner nut (MJT-nut), is screwed on from each end of the threaded rods, tightening together the whole substructure.

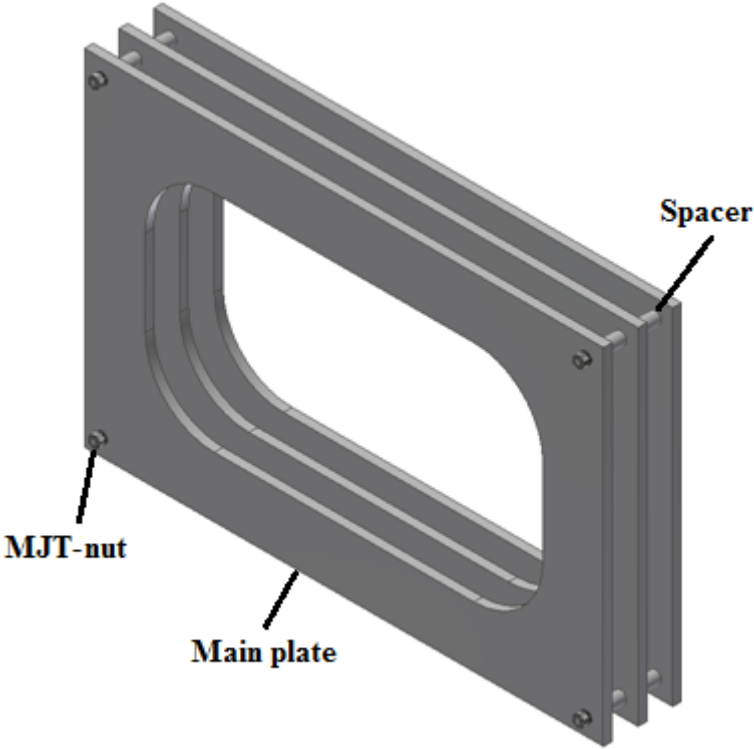


Figure 4.5. The main plate substructure

The threaded rods have a M36 thread and are of grade 8.8. These are selected because they are the largest standard threaded rods, with that high steel grade. Each threaded rod is 550 mm long.

The MJT-nuts are used for prestressing the threaded rods. The nut is made out of a main round nut that is hand screwed on. Several smaller bolts that are placed in a circular pattern around the round main nut are then each tightened against a stiff washer that is placed in front of the nut. Due to the system of tightening several small bolts, the MJT-nut requires less torque to tension the threaded rod to the desired prestress. (Nord-Lock, 2014)

The spacers are made out of structural steel tubing that have an outer diameter of 70 mm and an inner diameter of 38 mm. Each spacer is cut to 150 mm in length. These acts as the effective area for the flange to which the MJT-nuts can be prestressed against.

Main and side box

The main and side box substructures are made out of an outer and an inner mounting plate with a number of 22 mm in diameter holes (Figure 4.6). These are clamped over the main plate substructure with M20 threaded rods of grade 8.8, which are screwed tight with regular nuts and Nord-lock washers at each end of the threaded rod. The plates for the main box are 1500x550 mm while the plates for the side box are 500x550 mm. Fastening plates are mounted on the inside of the inner mounting plates.

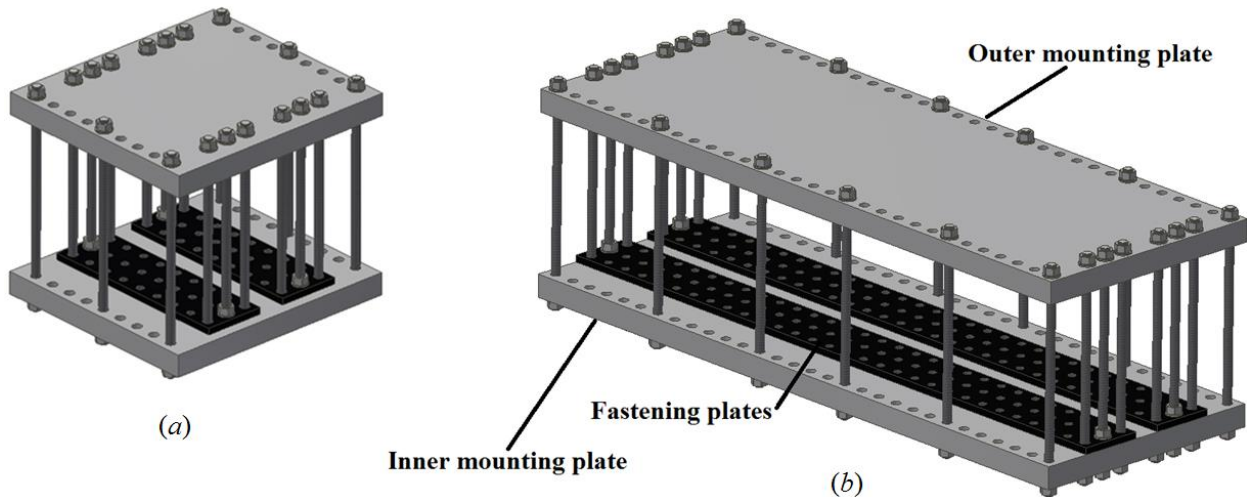


Figure 4.6. a) The side box substructure b)The main box substructure

The outer mounting plate have equally spaced holes at a distance of 50 mm along the outer edges of the plate, except for where the main plates interface. No holes are needed in the inner part of the plate, while no fixation tools are going to be mounted to the outside of the test rig.

The inner mounting plate have equally spaced holes at a distance of 50 mm over the whole plate, except for where the main plates interface.

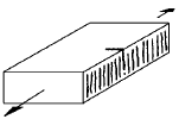
The fastening plate has M20 threaded holes in the same hole-pattern as the inner rows of the inner mounting plate, except for the short sides where it has 22 mm holes. This makes it possible to position the fastening plates correctly via the M20 threaded rods, as well as fixating them in place against the inner mounting plate by tightening it down with a nut on each side, as seen in Figure 4.6. The fastening plate acts as a matrix of nuts, enabling the fixation tools to be bolted directly to the test rig without having to tighten the mounting bolts with a nut from the inaccessible space within the main and side boxes (when they are mounted on the test rig). It also helps to distribute the tensile load from the mounting bolts over a wider area compared to a separate nut. The fastening plate is made of 30 mm Weldom900 steel plate that's 1500x140 mm. This steel is selected while it has a yield strength that is equal to a 10.9 graded bolt.

4.2.2 Initial dimensioning of the fatigue testing rig

The initial dimensioning of the fatigue testing rig is done for one main plate, with the help of the modified calculation model that was established in 3.5.2 *Strength analysis of the main plate*, according to the load case in Figure 3.2. The calculation model is slightly altered in order to calculate the maximum stress, for all the fatigue testing with each load in each load case, in Section A for a main plate with a cross section of 350x50 mm. The results from these calculations can only be seen as guidance in how the fixation tools for the three selected spreader components should be designed and positioned in order to reduce the reacting loads on the test rig.

The maximum allowed stress range, $\Delta\sigma_{Rd}$, for one main plate, when calculating with the initial loads and number of estimated cycles for each load case (as previously shown in Table 3.1), is calculated according to the calculation method in 4.1.2 *Fatigue dimensioning with several load cases*. Since the main plate will be gas cut from one single plate, the FAT-class, *FAT*, and the exponent of the S-N curve, *m*, are chosen for the structural detail described in Table 4.3.

Table 4.3. Dimensioning values for gas cut material (Hobbacher, 2007)

No.	Structural Detail	Description (St.= steel; Al.= aluminium)	FAT St.	FAT Al.	Requirements and Remarks
122		Machine thermally cut edges, corners removed, no cracks by inspection $m = 3$	125	40	Notch effects due to shape of edges have to be considered.

In order to get an adequate result from the two calculations mentioned above, the loads and the estimated amount of cycles for the twistlock assembly must be determined. A reasonable estimation for these calculations is therefore made. The twistlock assembly will be tested with the loads: $F = 250$ kN, 200 kN, 150 kN at an estimated amount of cycles N that are equal to the ones for the fatigue testing of the gearbox housing.

The maximum allowed stress range for one main plate is $\Delta\sigma_{Rd} \approx 97$ MPa. The maximum stress for each load in each load case in Section A is illustrated in Figure 4.7, as well as the maximum allowed stress range for the whole main plate.

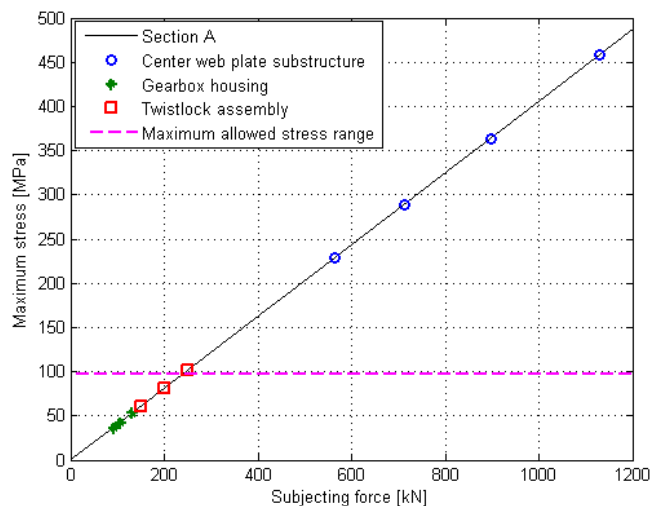


Figure 4.7. The maximum stress for each load in each load case as a function of the subjecting force

It should be noted that the result for the maximum allowed stress range corresponds well with the recommendations from Mrden and Berg in 2.3.2 *Recommendations for design of a fatigue testing rig*, that the maximum stress in the test rig shouldn't exceed 100 MPa. Although further dimensioning of the fatigue testing rig has to be made before any conclusions can be made.

The results in Figure 4.7 shows that the maximum stresses in Section A, when testing the center web plate substructure according to the load case in Figure 3.2, are well above the maximum allowed stress range. This result indicates that the center web plate substructure needs to be tested in a way so that all of the reacting forces from the fatigue testing don't subject the weakest point on the test rig. Since the center web plate substructure is going to be tested with loads that are significantly higher compared to the testing of the two other selected spreader components, it would be beneficial if the fixation tool itself could be the main load bearing part, thus reducing the stresses on the fatigue testing rig.

4.3 Fixation tools for the three selected spreader components

The fixation tools for the three selected spreader components are designed to mimic the load cases specified in 3.1 *Fatigue loads for the three selected spreader components*. Each fixation tool is unique to the selected spreader components that should be tested. During the design of the fixation tools, it was established that more than one type of hydraulic cylinder was needed in order to achieve the specified loads for the load cases.

M20 bolts of grade 10.9 are selected as the primary bolt used for mounting the fixation tools and spreader components to the test rig, while they are standard bolts that are easy to source and have a high maximum allowed stress amplitude, σ_{up} , as previously shown in Table 4.2. To achieve good fatigue strength in the bolted joints, the clamping length of each joint should be aimed to be as long as possible. A reference that's commonly used is that the clamping length L should be at least four times the diameter d of the bolt, i.e. ($L > 4 \cdot d$) (KTH, 2008).

4.3.1 Twistlock assembly

The fixation tool for the twistlock assembly is designed around a steel box into which the twistlock assembly is mounted. The steel box, here after referred to as the twistlock assembly box, is designed to replicate the design of the "corner box", where the twistlock is mounted in a real spreader, i.e. the same type of steel, cut outs, and plate thicknesses are used for the twistlock assembly box.

The fixation tool for the twistlock assembly is mounted into the test rig according to Figure 4.8.

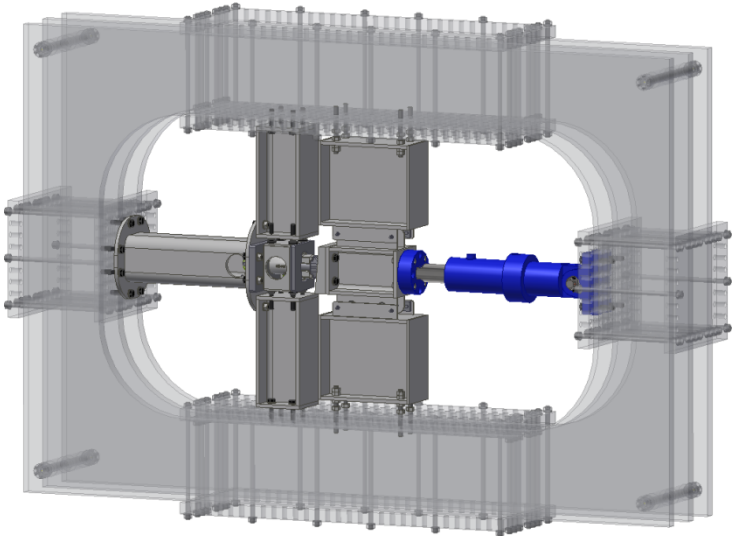


Figure 4.8. The fixation tool for the twistlock assembly mounted in the test rig

Due to the confined space within the test rig and the enabling of using the same hydraulic cylinder setup for two different fixation tools, the fixation tool for the twistlock assembly is mounted horizontally rather than vertically in the test rig.

The fixation tool for the twistlock assembly consists of four different substructures, excluding the twistlock assembly box and the hydraulic cylinder: The upper support, the upper side support for the twistlock assembly, the force distributor and the lower side support for the force distributor (Figure 4.9).

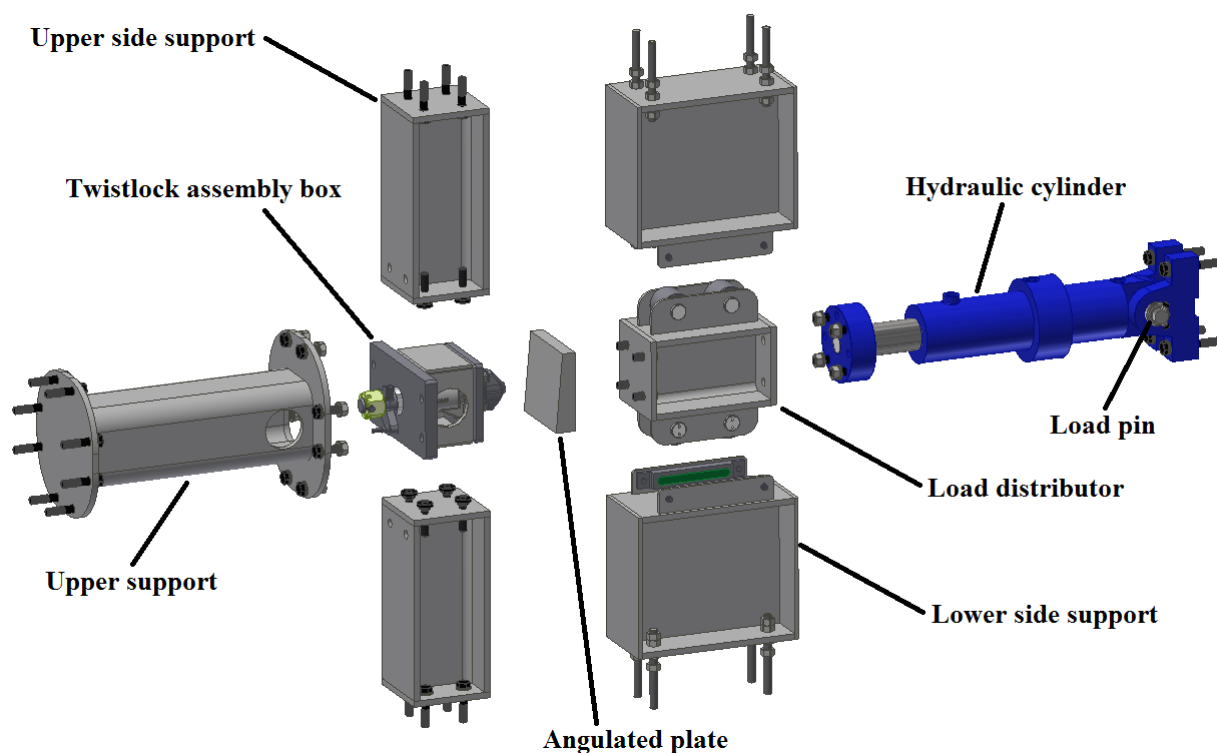


Figure 4.9. The substructures for the fixation tool for the twistlock assembly

The upper support is made out of a standard VKR 200x200x10 mm hollow square section with 10 mm thick plates welded to each end. The upper end mounts to the test rig, while the lower end mounts to the twistlock assembly box, as well as the two upper side supports, by bolted joints. The lower end plate has a central hole with the size of the inner area of the hollow square section, allowing free space for the protruding upper part of the twistlock assembly from the twistlock assembly box. The hollow square tube got a circular cut out from each side, towards the lower end of the beam, in order to visually inspect the protruding upper part of the twistlock assembly for cracks during the fatigue testing.

The upper side support is made out of standard H-beams, HEB200, with 10 mm thick plates welded to each end. One end mounts to the test rig, while the other end is supported by the upper support. The end plate that's closes to the twistlock assembly box got threaded holes where M20 pressure bolts are situated (Wiber, 2013). These bolts are used to fixate the twistlock assembly box, restricting it from rotating or moving laterally during the fatigue testing. The pressure bolts are selected, while they simplify the task of removing the twistlock assembly box when the twistlock assembly needs to be replaced after it has been tested to fatigue failure. It only requires the untightening of the pressure bolts (as well as undoing the bolted joints at the upper support), then the twistlock assembly box can be removed separately from the rest of the fixation tool. The twistlock assembly box can thereafter be taken to a work bench where the twistlock assembly can be changed.

The twistlock assembly box is designed to replicate the “corner box” of a real spreader. The top of the box is extended, with two holes at each end. These holes are for securing the box to the upper support via bolted joints. The box also got a circular cutout on each side, at the center force line, where the stresses are the lowest. This allows for visual inspections of the guide neck as well as the rest of the twistlock assembly, during the fatigue testing.

The force distributor is made out of standard H-beams, HEB200, with 10 mm thick plates welded to each end. It's fitted with rollers on the outside of each flange of the H-beam, in order to minimize the friction between the force distributor and the side support that will occur due to the lateral forces that will arise because of the angulated plate. The angulated plate is bolted to the upper end plate, with bolts from the back, while the lower end plate mounts to the rod end flange on the hydraulic cylinder.

The angulated plate is made out of Harddox400 steel, in order to better withstand the abrasive wear that it will encounter when pushing against the twistlock at an angle. The plate is 50 mm thick and has a dimension of 200x200 mm. The upper top of the plate has a machined 5 ° plane, and the bottom has four M20 threaded holes that goes half way through the plate, in order to have a continuous surface without any holes on the upper part.

The lower side support is necessary for taking up the lateral load that will occur, due to the angulated plate, as well as making sure that the force distributor stays perfectly aligned relative to the axial applied load from the hydraulic cylinder. The lower side support is a custom made I-beam with 15 mm thick flanges and 10 mm thick web and end plates. Small supports with plastic glide plates (In green in Figure 4.9) are mounted on the flanges closes to the force distributor. These form a slot for the rollers on the force distributor to roll in between, insuring that the force distributor is always in line with the applied load. The lower side support is designed so that a space of approximately 100 mm is left between the outer flange and the test rig. Within this space 200 mm M20 threaded rods are bolted with a number of nuts to the outer flange of the lower side support and screwed in to the test rig. By adjusting the system of nuts on the threaded rod, the position of the side support can be adjusted. This feature is essential for getting the right contact pressure with the rollers on the force distributor.

Hydraulic cylinder setup

The selected hydraulic cylinder is a double acting standard cylinder from PMC Cylinders, model “LHA 25” with spherical end attachment and a built in linear sensors (PMC_group, 2013). The cylinder has a cylinder diameter of $d_1 = 125$ mm, a piston rod diameter of $d_2 = 80$ mm and a stroke of 160 mm. The hydraulic cylinder is suspended from two mounting brackets where a custom made load pin from Brosa AG secures it in place (AG, 2013). This setup makes it possible to monitor both the actual applied load from the hydraulic cylinder, as well as the displacement of the cylinder during the fatigue testing. The selected hydraulic cylinder has a threaded rod end, which makes it possible to change the rod end setup of the cylinder depending on what type of testing it has to perform. This enables the possibility of using the same hydraulic cylinder for both testing the twistlock assembly as well as the gearbox housing, by just changing the rod end mounting tool. The hydraulic cylinder with its subcomponents is shown in Figure 4.10.

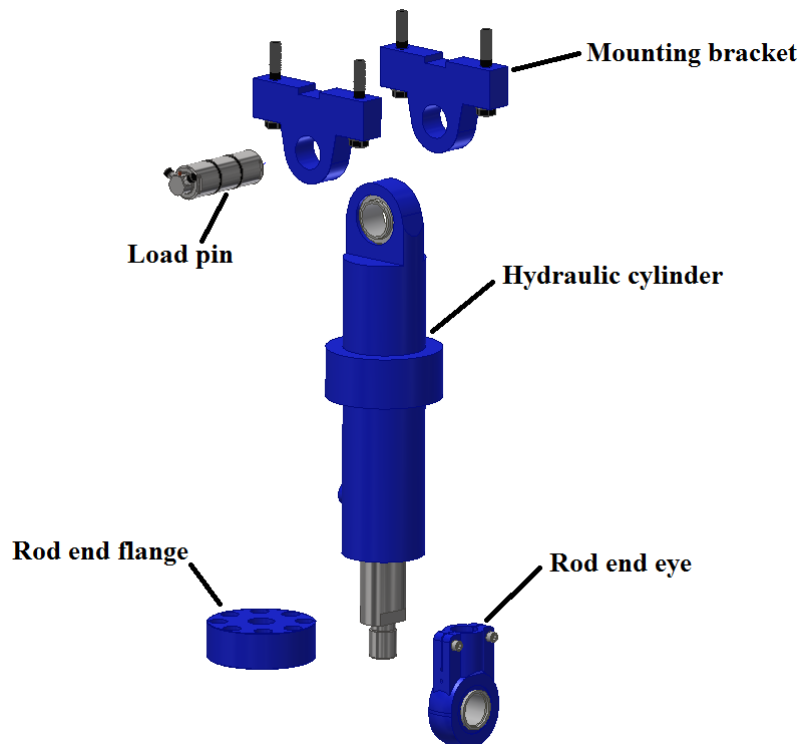


Figure 4.10. Hydraulic cylinder setup

When testing the twistlock assembly, the hydraulic cylinder is fitted with the ancillary rod end flange in order to bolt together with the force distributor for the fixation tool for the twistlock assembly. The hydraulic cylinder can deliver a pushing force of $F_{push} = 250$ kN at a pressure of $P_1 \approx 210$ bar, when calculated according to the calculation method in *4.1.4 Dimensioning of hydraulic cylinders*.

When testing the gearbox housing, two sets of hydraulic cylinders are needed to achieve desired load case on the gearbox housing. Both cylinders are mounted with the ancillary rod end eyes in order to attach to the shaft that's placed through the gearbox housing. The hydraulic cylinder can deliver a pushing force of $F_{push} = 130$ kN at a pressure of $P_1 \approx 110$ bar and a pulling force $F_{pull} = 130$ kN at a pressure of $P_2 \approx 185$ bar, when calculated according to the calculation method in *4.1.4 Dimensioning of hydraulic cylinders*.

Lateral forces due to angulated plate

Due to the design of the fixation tool with the angulated plate on the force distributor, lateral forces, F_{lat} , will occur during the fatigue testing. These forces will be distributed to the sides of the test rig, via the side supports. The lateral force can be calculated with the help of the geometrical relationship in Figure (4.11). The desired load that the fatigue tests are going to be performed with is the vertical force, F_{ver} . This is the force that the load pin will monitor during the fatigue testing.

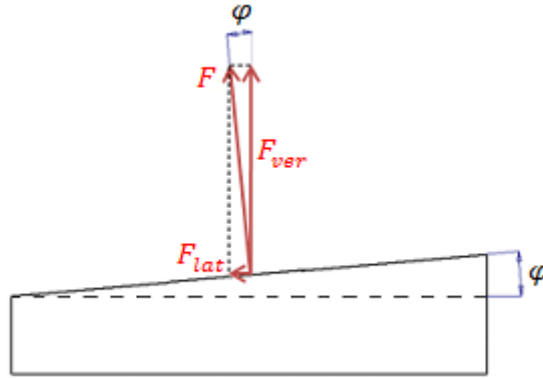


Figure 4.11. Angulated plate

where F is the normal force perpendicular from the angulated plane.

The lateral force, F_{lat} , is calculated according to Equation (54)

$$F_{lat} = \frac{F_{ver}}{\cos \varphi} \cdot \sin \varphi \rightarrow [\varphi = 5^\circ] \rightarrow F_{lat} \approx 0,087 \cdot F_{ver} \quad (54)$$

where φ is the angle of the angulated plane ($\varphi = 5^\circ$ for the predetermined load case)

The lateral forces that occur during the fatigue testing of the twistlock assembly will be taken into account during the final dimensioning of the fatigue testing rig. To be conservative, the lateral force is set to $F_{lat} = 0,1 \cdot F_{ver}$.

4.3.2 Gearbox housing

Since the gearbox housing will be tested with different torque loading, i.e both a pushing and a pulling force is applied to the gearbox housing, the fixation tool is highly dependent on the fatigue strength of the prestressed mounting bolts for fixating the gearbox housing to the test rig.

The fixation tool for the gearbox housing is mounted into the test rig according to Figure 4.12.

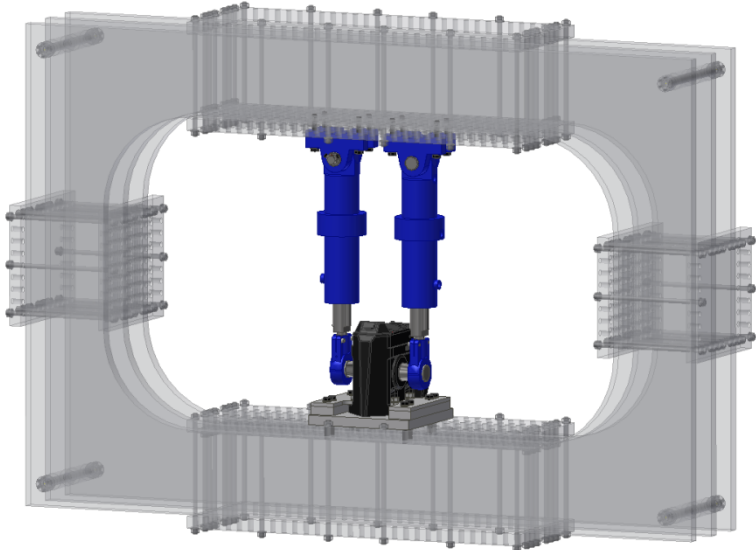


Figure 4.12. The fixation tool for the gearbox housing mounted in the test rig

The fixation tool for the gearbox housing consists of four different parts: The adaptor plate, the spacer plates, the holding plates, the machine shaft as well as the hydraulic cylinders (Figure 4.13). The plates will fixate the base of the gearbox housing to the test rig, while the machined shaft is positioned through the gearbox housing. The shaft helps to transfer the axial applied loads from the hydraulic cylinders, into the desired torque loading that the gearbox housing will be tested with.

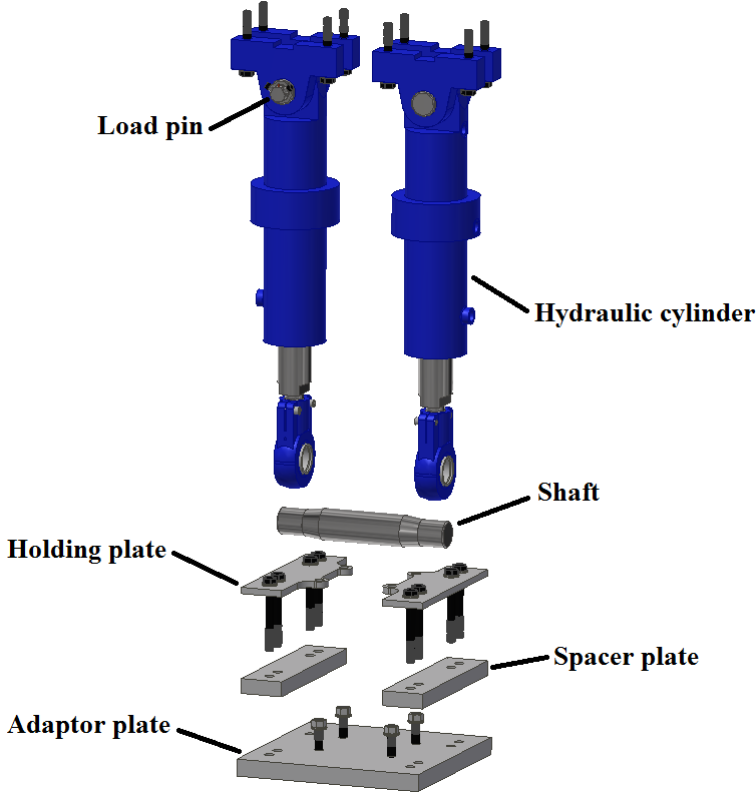


Figure 4.13. The fixation tool for the gearbox housing

The adaptor plate is needed since the mounting holes on the flanges of the gearbox housing don't match with the hole-pattern of the mounting plates on the test rig. The adaptor plate got a matching hole-pattern as the gearbox housing, positioned so that the center of the axle hole on the gearbox housing lines up with the center of the test rig. These holes are recessed 20 mm from the underside of the plate, in form of milled grooves that are the same width as the head size of a M20 hexagonal bolt. Bolts are fitted through these holes from the underside of the adaptor plates so that the threaded part of the bolts sticks up through the plate and the head of the bolts are locked from rotating in the recesses. The gearbox housing is placed over the protruding bolts. The adaptor plate also got holes according to the hole-pattern of the test rig, so it can be mounted to the test rig. The adaptor plate is made out of 40 mm plate that is 450x450 mm.

The spacer plate has the same thickness as the flange of the gearbox housing (30 mm), ensuring that the bottom surface of the holding plate is level with the upper surface of the flange. The spacer plate also acts as a part of the stiff flange that the bolts for mounting the adaptor plate to the test rig can be prestressed against.

The holding plate acts as an extra stiffening plate when fixating the gearbox housing. Each holding plate has an equal hole-pattern as the adaptor plate, and is designed to follow the outer shape of the gearbox housing. The gearbox housing is fixated by tightening nuts from the ends of the protruding bolts, with the holding plate and gearbox housing flange clamped in the bolted joint. This design is made to both increase the clamping length of the bolted joints that goes through the flanges of the gearbox housing as well as adding extra rigidity by having the extra clamping force from the outer bolts that mounts to the test rig. The holding plate is made out of 15 mm plate.

The shaft is machined from a 75 mm in diameter solid shaft, where the ends are milled down to 63 mm in order to fit the rod end eyes from the hydraulic cylinders to the shaft. The transition between the larger diameter in the middle of the shaft to the smaller diameters at each end is made with a smooth gradient, making sure that the ends of the gradient are finished with a smooth radius, in order reduce the stress concentrations in the shaft and increasing its fatigue properties.

Dimensioning of critical loaded bolts

Due to the load case for the gearbox housing, certain bolted joints will be subjected to high tensile loads during the fatigue testing. These are located at three specific mounting points: The mounting of the pulling hydraulic cylinder, the mounting of the adaptor plate to the test rig and the mounting of the gearbox housing to the adaptor plate with the protruding bolts. Each of these mountings has to be dimensioned in order to ensure that the bolted joints can withstand the fatigue loads. The subjecting loads for these mounting are illustrated in Figure 4.14.

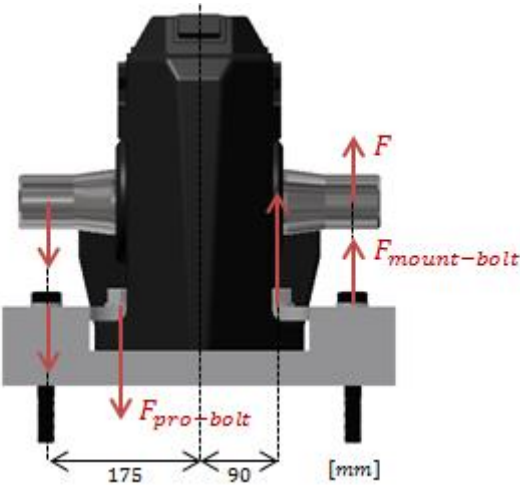


Figure 4.14. The subjecting loads on the specified bolted joints

The highest torque that the gearbox housing is tested with is $M_{GH} = 46$ kNm. With the rod end eyes for the two hydraulic cylinders, positioned 175 mm from the center of rotation for the gear box housing, the applied load F for each cylinder is calculated according to Equation (55).

$$M_{GH} = 2 \cdot 0,175 \cdot F \rightarrow F = \frac{M_{GH}}{2 \cdot 0,175} \approx 131 \text{ kN} \quad (55)$$

Since the subjecting load at the mounting of the adaptor plate to the test rig, $F_{mount-bolt}$, is in line with the applied load from the hydraulic cylinder, $F_{mount-bolt} = F$. The subjecting load at the mounting of the gearbox housing to the adaptor plate with the protruding bolts is calculated in Equation (56) according to the geometrical relationship in Figure (4.13).

$$0,175 \cdot F = 0,09 \cdot F_{pro-bolts} \rightarrow F_{pro-bolts} = 0,175 \cdot \frac{F}{0,09} \approx 256 \text{ kN} \quad (56)$$

Each mounting point is dimensioned according to *4.1.3 Dimensioning of prestressed bolted joints* to establish the least amount of bolts needed to achieve a effective bolted joint. If more bolts are used in the mounting point, compared to the dimensioned value, the designed mounting points will withstand the fatigue from the fatigue testing. In order to perform these calculations, the clamping length, l , and the subjecting force is needed for each mounting point.

The hydraulic cylinder is subjected to a load of 131 kN and is mounted with four M20x140 bolts, which have a clamping length of $l = 120$ mm. The least amount of bolts needed for this mounting point is one bolt, that has a stress amplitude of $\sigma_a \approx 20$ MPa (which is less than the allowed stress amplitude of $\sigma_{up} = 45$ MPa).

The adaptor plate is subjected to a load of 131 kN and is mounted with eight M20x90 bolts, of which four are subjected to tensile loading, that have a clamping length of $l = 140$ mm. The least amount of bolts needed for this mounting point is one bolt, that has a stress amplitude of $\sigma_a \approx 17$ MPa.

The protruding bolts that fixate the gearbox housing to the adaptor plate are four M20x160, which of two are subjected to tensile loading, that have a clamping length of $l = 70$ mm. The least amount of bolts needed for this mounting point is one bolt, that has a stress amplitude of $\sigma_a \approx 34$ MPa.

The results from the dimensioning show that the bolted joints in all the specified mounting points can withstand the fatigue from the fatigue testing. This dimensioning model does however presuppose that all the bolts are prestressed to 70% of their yield strength, which may not be case during the actual test. It's therefore reassuring that there's a sufficient safety margin for each bolted joint in the specified mounting points.

4.3.3 Center web plate substructure

In order to reduce the required load from the hydraulic cylinder, the alternative lever arm solution is used, as mentioned in *3.5.3 Strength analysis of the lever arm solution*, where one beam is placed through the slot of the center web plate substructure and two hydraulic cylinders apply half of the load each from each end of the beam.

The fixation tool for the center web plate substructure is mounted into the test rig according to Figure 4.15.

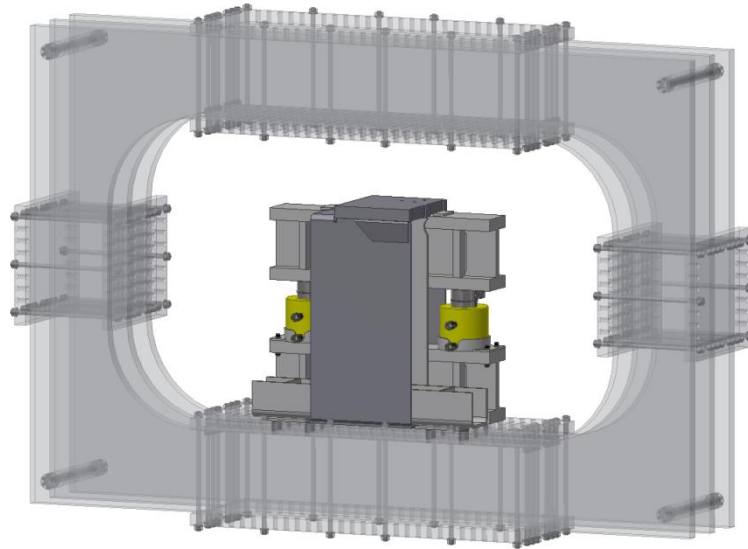


Figure 4.15. The fixation tool for the center web plate substructure mounted in the test rig

The center web plate substructure is significantly bigger than the other two selected spreader components, as well as requiring more powerful hydraulic cylinders. It was therefore established that two custom made load bearing I-beams could be used with the hydraulic cylinders placed in between these two, achieving the required loads within the center web plate substructure itself.

In order to fixate the center web plate substructure according to the load case specified in *3.1 Fatigue loads for the three selected spreader components*, the substructure is rotated 180 degrees and fixated through both the slots to the bottom of the test rig. This solution made it possible to achieve the desired load case with only two hydraulic cylinders applying its load between the two I-beams.

Due to the non-linear load case over the center web plate substructure, the lower part of the second slot needs to be secured to the bottom of the test rig, while it would otherwise lift from the test rig due to the deflection in the center web plate substructure. A third beam is therefore placed through the slot and mounted to the bottom of the test rig. The reacting forces in the third beam, during testing at the highest load, are determined by an FEA of the sub-model, see *Appendix G*.

The fixation tool for the center web plate substructure consists of several different parts: Two I-beams, a U-beam, two holders for the hydraulic cylinders, two spacer plates, as well as the hydraulic cylinders with the load cells (Figure 4.16).

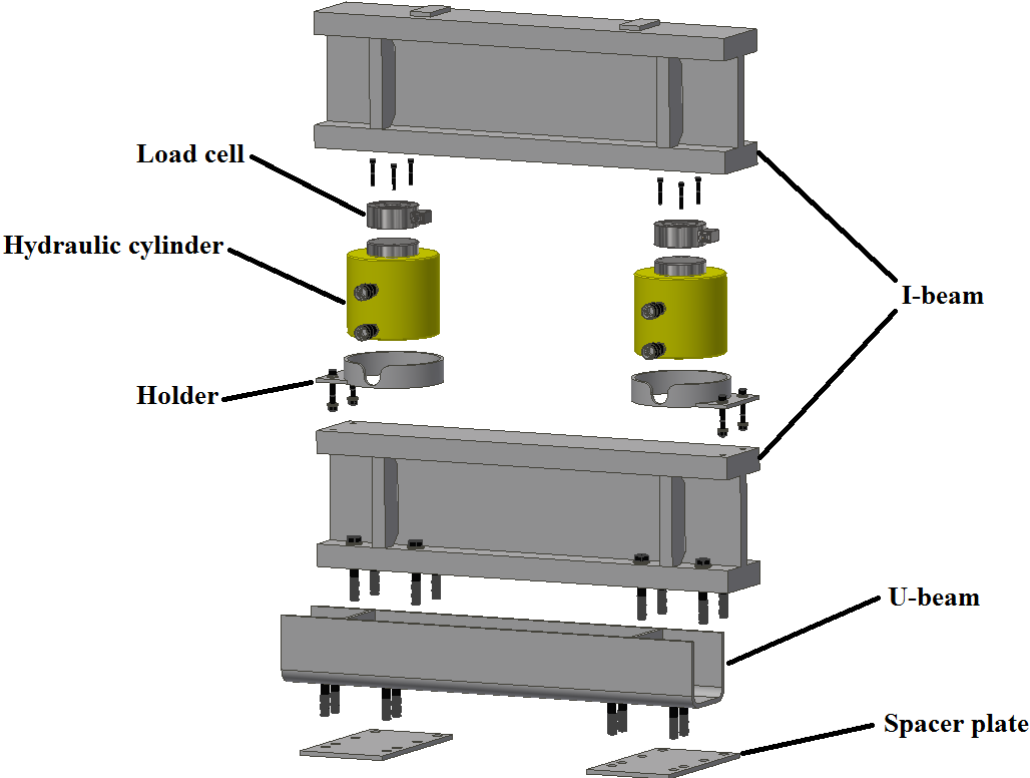


Figure 4.16. The fixation tool for the center web plate sub structure

The I-beams are the two main load bearing components within the fixation tool. They are later in the chapter further described and dimensioned.

The U-beam is selected for fixating the second slot of the center web plate substructure instead of e.g. an I-beam, while the U-beam gives better accessibility when tightening the mounting bolts for both the lower I-beam as well as the U-beam to the test rig. The U-beam is made from 10 mm thick steel plate with a 20 mm radius, giving it a base of 160 mm and a web height of 150 mm.

The spacer plates have the same thickness (10 mm) as the end plate of the center web plate substructure that interfaces with the U-beam and the lower I-beam. They create a flat surface in between where the U-beam and the lower I-beam interfaces with the center web plate substructure and where they mount to the test rig. The spacers acts as the flange to which the mounting bolts to the lower beams can be prestressed against.

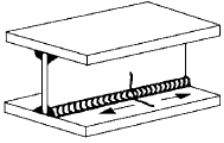
The holders are made out of structural steel tubing that have an outer diameter of 219,1 mm and an inner diameter of 203,1 mm. The inner diameter of the tube is marginally greater than the outer diameter of the hydraulic cylinders, allowing the hydraulic cylinder to sit inside the holder. The tubes are 50 mm high and have a cutout for the lower hydraulic valves on the hydraulic cylinders. An 8 mm steel plate is welded to each holder, according to Figure 4.15, and fitted with M12 mounting bolts, which mounts to each upper flange end of each end of the lower I-beam.

Dimensioning of the I-beams

The two load bearing I-beams are dimensioned to withstand the fatigue from all the intended fatigue testing on the center web plate substructure. Due to the limited space within the slot of the center web plate substructure and the high loads that the beam will be subjected to, the I-beams have to be custom made.

The allowed stress range for the custom made I-beam is calculated according the calculation method in 4.1.2 *Fatigue dimensioning with several load cases*. Since the I-beam will be welded together with fillet welds on both sides of the web, the FAT-class, *FAT*, and the exponent of the S-N curve, *m*, are chosen for the structural detail described in Table 4.4.

Table 4.4. Dimensioning values for continuous manual longitudinal fillet weld (Hobbacher, 2007)

No.	Structural Detail	Description (St.= steel; Al.= aluminium)	FAT St.	FAT Al.	Requirements and Remarks
323		Continuous manual longitudinal fillet or butt weld (based on stress range in flange)	90	36	

The dimensioning number of cycles, N_f for this calculations is the total number of cycles for all the fatigue testing of the center web plate substructure. The maximum allowed stress range for the I-beam is $\Delta\sigma_{Rd} \approx 70$ MPa.

After an iterative process of dimensioning the I-beam, while still enabling space for the hydraulic cylinder and load cell as well as enabling it to fit within the slot of the center web plate substructure, the following dimensions could be established: Length $L = 1$ m, height $h = 300$ mm and width $b = 160$ mm, with a flange thickness of $t_f = 50$ mm and a web thickness of $t_w = 30$ mm. The distance between the two applied loads from the hydraulic cylinders on the I-beam is $F_{load} = 0,7$ m.

When dimensioning the custom designed I-beam, the area moment of inertia I_y can be calculated according to Equation (57) (Sundström, 1999).

$$I_y = \frac{bh^3}{12} - \frac{b(h-2\cdot t_f)^3}{12} + \frac{t_w(h-2\cdot t_f)^3}{12} \quad (57)$$

The subjecting load on the I-beams can't just be seen as a point load in the middle of the beam, as done in the initial calculations in 3.5.2 *Strength analysis of the main plate*. The reacting force from the center web plate substructure will be distributed over a larger part of the I-beam where the two parts interfaces. The calculations for the dimensioning of the I-beam must take into consideration the load case of an equally distributed load for a beam that's simply supported (Figure 4.17).

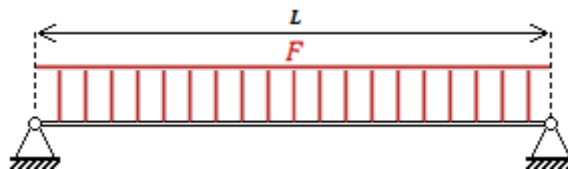


Figure 4.17. Load case for simply supported beam with equally distributed load.

where the subjecting load is the highest load that the center web plate substructure will be tested with, i.e. $F = 1130$ kN.

The maximum torque in the beam with a distributed load, $M_{max\,dist}$, is shown in Equation (58). The maximum torque in the beam with a point load, $M_{max\,point}$, is shown in Equation (59). (Björk, 2013)

$$M_{max\,dist} = \frac{FL_{load}}{8} \quad (58)$$

$$M_{max\,point} = \frac{FL_{load}}{4} \quad (59)$$

Because the load is neither just a single point load nor a fully distributed load over the entire beam, a 50:50 ratio of these two load cases are used in order to calculate the stress in the beam. Since the maximum allowed stress range in the I-beam is based on the stress in the flange, the calculated stress in Equation (60) is the stress in the center of the flange.

$$|\sigma|_{center\,flange} = 0,5 \cdot \frac{M_{max\,dist}}{I_y} \cdot |z|_{center\,flange} + 0,5 \cdot \frac{M_{max\,point}}{I_y} \cdot |z|_{center\,flange} \quad (60)$$

where $z = \frac{(h-t_f)}{2}$, the distance from the center line of the I-beam to the center of the flange.

The stress in the center of the flange in the I-beam is $\sigma_{center\,flange} \approx 68$ kN. During the iterative process of determining the dimensions for the custom made I-beam, as well as determining the length between the hydraulic cylinders where the force is applied, the stress in the I-beam is plotted as a function of the effective length of the I-beam (Figure 4.18). This is done in order to visualize the results and quickly determine if the I-beam fulfills the dimensioning requirement.

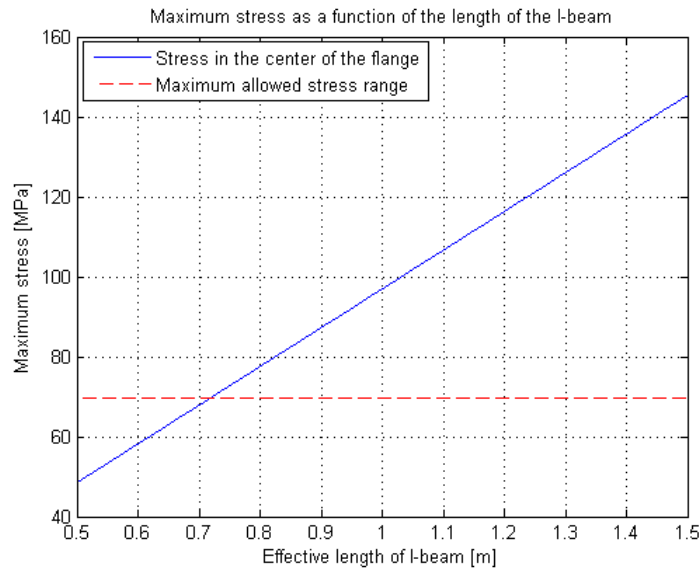


Figure 4.18 Stress in the I-beam as a function of the effective length

The calculation for the diagram in Figure 4.18 is performed in MATLAB and can be seen in Appendix F.

Hydraulic cylinder setup

The selected hydraulic cylinder is a double acting compact standard cylinder from Enerpac, model “RR-1502” (Enerpac, 2013). The cylinder has a cylinder diameter of $d_1 = 158,8$ mm, a piston rod diameter of $d_2 = 114,3$ mm and a stroke of 57 mm. A low profile compression load cell from RPD group, model “RSL0720, 120K”, is mounted on the piston rod end (RDP_group, 2013). In order to fit the load cell on the piston rod end, it must be drilled and threaded with three M8-threads according to the same hole-pattern as for the load cell. The load cell can thereafter be bolted secure to the hydraulic cylinder. This setup makes it possible to measure the actual applied load during the fatigue testing. The hydraulic cylinder with the load cell is shown in Figure (4.19).

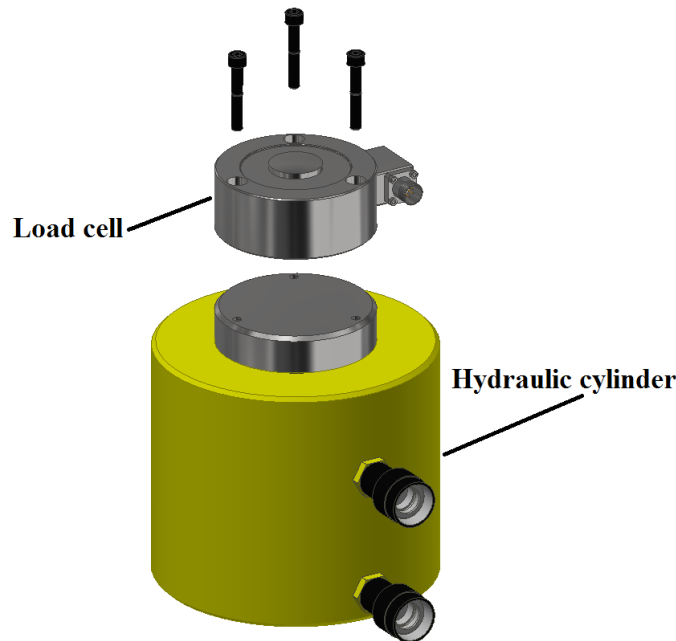


Figure 4.19. Hydraulic cylinder setup for testing the center web plate substructure

When testing the center web plate substructure, two sets of hydraulic cylinders are needed to achieve the desired loads. Each hydraulic cylinder can deliver a pushing force of $F_{push} = 565$ kN at a pressure of $P_1 \approx 290$ bar, when calculated according to the calculation method in *4.1.4 Dimensioning of hydraulic cylinders*.

The selected hydraulic cylinder from Enerpac doesn't have a built in linear sensor that can measure the displacement of the stroke of the cylinder (unlike the selected cylinder from PMC group). A separate LVDT can therefore be placed between the top of the center web plate substructure and the test rig, in order to measure the vertical deflection of the center web plate substructure. Such a solution for the model of the test rig has not been further investigated in this thesis.

4.4 Final dimensioning

When all the interacting surfaces between the main steel structure and the fixations tools for the three selected spreader components are determined, a more accurate final dimensioning of the fatigue testing rig can be performed.

A more basic but still representative model of the main steel structure of the fatigue testing rig is imported into the FEA program, ANSYS, where the subjecting forces and fixations from the fixation tools are applied at each specific point of contact to the test rig for each load case. The FEA is performed with a shell model where each part is illustrated as a plane, which thickness is set in the FEA program. By choosing this modeling type, the FEA calculations can be performed faster as well as enabling the opportunity to easily change the plate thickness of the fatigue testing rig by changing only one parameter. The determined loads and fixation points for each load case are further described and illustrated in *Appendix H*.

The subjecting forces and torques that are actually applied to the test rig, via the fixation tools, are shown in Table 4.5. The dimensioning forces for the center web plate substructure are derived from the FEA performed on the sub-model of the center web plate substructure fixation tool in *Appendix G*. The lower loads in the 2nd, 3rd and 4th tests are scaled down from the obtained value in the 1st test, with the same ratio as between the initial loads for the center web plate substructure.

In order to perform the calculations to establish the maximum stress that the test rig will be subjected to when testing the three selected spreader components, the subjecting forces as well as the estimated amount of cycles for the twistlock assembly needs to be determined. In consensus with Bromma, an estimate is made that the twistlock assembly will be tested with the same amount of cycles as the gearbox housing, and that the lower loads in the 2nd and 3rd test will be scaled down in the same ratio as between the loads for the gearbox housing.

Table 4.5. The actual subjecting forces to the test rig

		1st test	2nd test	3rd test	4th test	Subtotal number of cycles
Reacting forces Center Web Plate Substructure	Force [kN]	34	27	21	17	
	Cycles [<i>n</i>]	30494	60988	121976	243952	457410
Twistlock assembly	Force F_{ver} [kN]	250	201	140		
	Force F_{lat} [kN]	25	20	14		
	Cycles [<i>n</i>]	50000	150000	300000		500000
Gearbox housing	Torque [kNm]	46	37	32		
	Cycles [<i>n</i>]	50000	150000	300000		500000
Summed number of cycles, $N_{t_{sum}}$						1457410
Total number of cycles (x 20), N_t						29148200

The maximum principal stress for the highest load in each load case is determined from the FEA. The FEA for each load case gives the following results: Center web plate substructure $\sigma_{CWPS_{max}} \approx 20$ MPa, Twistlock assembly $\sigma_{TLA_{max}} \approx 43$ MPa, Gearbox housing $\sigma_{GH_{max}} \approx 18$ MPa. The principal stresses for the entire test rig for each load case, obtained from the FEA, are shown in *Appendix H*.

In order to calculate the combined maximum stress that the test rig will be subjected to from each load in each load case, an equivalent constant amplitude stress range, $\Delta\sigma_{eq,S,d}$ can be determined according to Equation (61), which is derived from the IIW Fatigue Recommendations. (Hobbacher, 2007)

$$\Delta\sigma_{eq,S,d} = \sqrt[m]{\sum \tau \cdot \sigma^m} \tag{61}$$

where σ corresponds to the maximum principal stress for each load in each load case and τ corresponds to the ratio of each estimate amount of cycles for each load in each load case, n_i , divided by the sum of the estimated amount of cycles for all loads in all load cases, $N_{t_{sum}}$, i.e. $\tau = \frac{n_i}{N_{t_{sum}}}$.

The maximum principal stress for the lower loads in each load case can be scaled to the same ratio as between the lower load and the highest, while the stress is linear relative to the applied load. An example for the maximum principal stress for the 2nd test for the center web plate substructure is shown in Equation (62).

$$\sigma_{CWPS_{2nd\ test}} = \frac{27}{34} \cdot \sigma_{CWPS_{max}} \tag{62}$$

The equivalent constant amplitude stress range can't be calculated by just using the value of the maximum principal stress from each load of each load case. In order for Equation (61) to be valid, the maximum principal stresses must occur in the same place on the test rig, which they don't as shown in Appendix H.

By applying Equation (61) into ANSYS, the FEA program can calculate the equivalent constant amplitude stress range for all elements in the test rig for all loads in all load cases. The results in Figure (4.20) bases on the results from each FEA for the highest load for each load case.

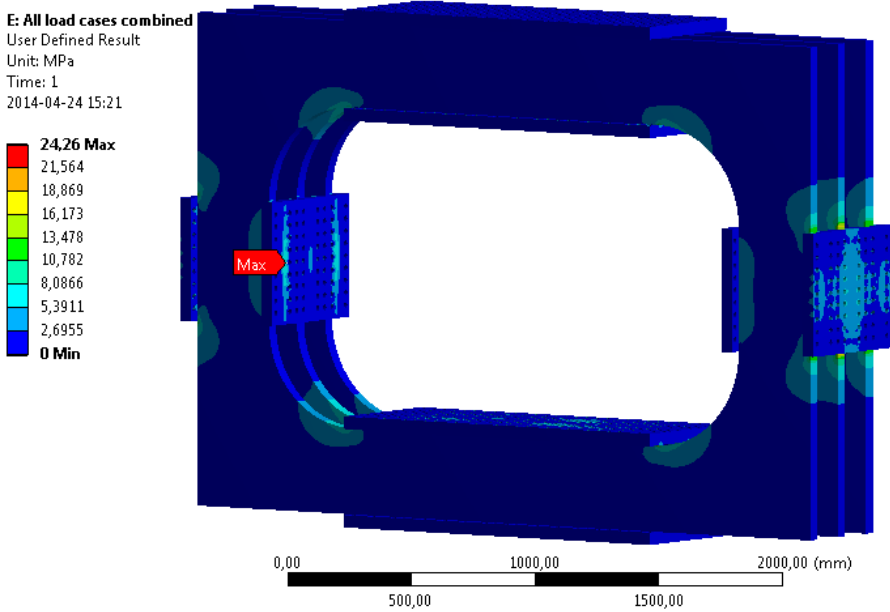


Figure 4.20. The equivalent constant amplitude stress range for all loads in all load cases

The maximum equivalent constant amplitude stress range is $\Delta\sigma_{eq,S,d_{max}} \approx 24$ kN and situated as a stress concentration on the edge of a mounting hole on the inner mounting plate on the side box. The general stress concentrations within the test rig are subjected to a stress of around 15 kN.

The maximum allowed stress range, for the test rig have to be greater than the maximum equivalent constant amplitude stress range, in order for the test rig to withstand the fatigue it's subjected to from the fatigue testing.

$$\Delta\sigma_{Rd} > \Delta\sigma_{eq,S,d,max} \quad (63)$$

Because all the loads in all load cases have been taken into account for the maximum equivalent constant amplitude stress range, the stress intensity factor can be set to $k_m = 1$ when calculating the maximum allowed stress range. This can be done while the results for the maximum allowed stress range will be in direct comparison with the maximum equivalent constant amplitude stress range, as in Equation (63).

The equation for calculating the maximum allowed stress range can be simplified by inserting $k_m = 1$ and Equation (35) into (38) from 4.1.2 *Fatigue dimensioning with several load cases*, giving Equation (64).

$$\Delta\sigma_{Rd} = \frac{FAT}{\gamma_m \cdot m \sqrt[2]{2 \cdot 10^6}} = \frac{125}{1,21 \cdot \sqrt[3]{\frac{29,1482 \cdot 10^6}{2 \cdot 10^6}}} = 48 \text{ kN} \quad (64)$$

where N_t is the total amount of cycles for all the fatigue testing.

When comparing the maximum equivalent constant amplitude stress range to the maximum allowed stress range, it's clear that the test rig is dimensioned to withstand twice the amount of stress as what it's subjected to (for the total amount of cycles for all the fatigue testing).

Since the model in the FEA program allowed for changing the thickness of the steel plates in the test rig by just changing one parameter, some additional FEA were performed to determine the maximum equivalent constant amplitude stress range when using thinner standard size plates for the test rig (Figure 4.21). This information can be useful in order to see if thinner steel plates can be used, thus lowering the weight of the test rig as well as reducing the cost for the base material.

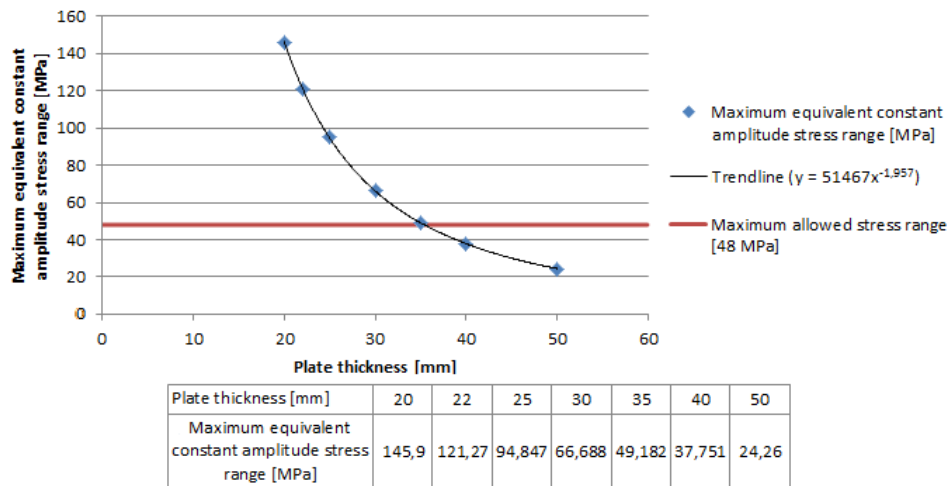


Figure 4.21. The maximum equivalent amplitude stress range as a function of the main steel structures plate thickness

When studying the diagram in Figure 4.21, it's clear that the test rig could be manufactured with 40 mm thick plate, and still withstand the fatigue from all the fatigue testing. If the partial factor of safety, γ_m , would be slightly lowered, thus increase the approximate risk of failure, the plate thickness of the steel plates in the fatigue testing rig could be reduced to 35 mm.

5 DISCUSSION AND CONCLUSIONS

This chapter presents a discussion concerning the design and dimensioning of the fatigue testing rig, as well as conclusions drawn regarding the outcome of the thesis.

5.1 Discussion

The factors used for the concept selection, especially those concerning the manufacturability of the fatigue testing rig, may be a bit biased in the thesis. The final concept rely on having a manufactory plant that have big automated cutting machines that can easily cut bigger sheets of steel plate, which is the case for Bromma. Compared to concept 4, which was the second best scoring concept, it only requires more rudimentary tools that can be found in smaller workshops when manufacturing that test rig. It should be noted that concept 4 still relies on having a foundation, which is not the case for concept 3.

In *4.1.1 Initial design input* it's stated that Bromma wants to use standard components for the test rig from their already well established suppliers. When designing the final concept to these suggestions, certain compromises had to be made to the design of the test rig.

- One of the outer dimensions of the main plates can only be 2 m, while that's the limit of a standard steel plate. Because the cut out in the middle of the main plates had to be enlarged, to allow space for the three selected spreader components within the test rig, the cross section for the O-shape of the main plate had to be reduced, thus weakening the test rig.
- The hydraulic cylinders used in the final concept are not fatigue-rated, while the decision was made to use standard cylinders rather than more complex fatigue-rated ones. This choice significantly reduces the reliability of the test rig and could in worst case compromise the results of the fatigue testing.
- The selected sensors are also not fatigue-rated. The main reason for this is due to the geometric conditions where the load cells needs to be fitted for each fixation tool. Similar fatigue-rated load cells have been looked at, but couldn't be incorporated to the design, while the load cells larger size made them unable to be used due to geometrical constraints.

There are also further hydraulic concerns, regarding the hydraulic cylinders used for the center web plate substructure fixation tool. Because the system relies on two hydraulic cylinders to achieve the desired load, it's recommended that a control valve is used in between the two cylinders in order to get uniform lifting of load.

The frequency at which the hydraulic cylinder can run at for each load case have not been established, while it would require further dimensioning of the complete hydraulic system, which have been disregarded in the thesis.

Concerning the safety aspects when using the fatigue testing rig, some extra safety measures should be incorporated to the test rig. Larger sheets of viable transparent plexiglas can be added to the front and back of the test rig, so that the operator can visually inspect the selected spreader component during the fatigue testing. To further enclose the test rig, durable finely meshed nets can be added around the rest of the test rig. These precautions are made to ensure that the operator or any other personnel nearby doesn't gets hurt if a part or component would suddenly rupture and fly off during the fatigue testing. Additional supports for stabilizing the bottom of the test rig can also be added in order to ensure that the test rig don't topple over if it's subjected to an external force from e.g. a forklift that backs in to it.

All the dimensioning of the fatigue testing rig presented in the thesis are made partly on estimated elementary load cases from mechanics of solids and partly on assumptions and

simplifications done in order to perform FEA. When the failure probability in the equations used to achieve the final results are also taken into consideration as well as the accuracy in the values the test rig is dimensioned against, it's virtually inevitable that some inherent error factors may be contained within the final dimensioning results. For example the results in *4.2.2 Initial dimensioning of the fatigue testing rig* are very misleading, while the true load cases on the test rig are highly dependent on were the fixation tools interfaces with the main steel structure of the test rig.

Because the hydraulic cylinders in the test rig will run at a certain frequency during the fatigue testing, a concern was raised regarding the natural frequency of the test rig. If the frequency of the hydraulic cylinders would coincide with the natural frequency of the main steel structure of the test rig, it could lead to oscillations that could damage the test rig. With the help of ANSYS the natural frequency for the test rig could be obtained from the results of the final dimensioning. The first natural frequency for the main steel structure of the test rig occurs at 16 Hz.

Due to the scale of the thesis, only the most load bearing parts of the test rig and the fixation tools have been fully dimensioned, while other parts have been over dimensioned with the help of engineering assumptions. During the end of the thesis it has been observed that additional FEA of the adaptor plate and shaft for the fixation tool for the gearbox housing would be appropriate to perform, in order to verify their fatigue strength.

During the end of the thesis, concerns were raised regarding the M20 threaded rods that clamp the main- and side boxes to the main plate substructure. When these are subjected to tensile loading, e.g. a force that pulls in towards the center of the test rig, it's uncertain whether or not these can withstand the fatigue. Because they clamp on each side of the main plates and therefore don't have a flange to be properly prestressed against, they can't be dimensioned according to *4.1.3 Dimensioning of prestressed bolted joints*. The design of the main- and side boxes are intentionally made with several holes around their outer mounting plates, thus allowing additional bolted joints to be added to the main- and side boxes.

5.2 Conclusions

The drawn conclusions from the thesis are shown as bullet point below.

- The test rig is geometrically designed to fit the three selected spreader components.
- The test rig is dimensioned to withstand the fatigue for an infinite life, relative to the load cases for the three selected spreader components.
- No welds are present in the assembly of the main steel structure of the test rig.
- Two hydraulic cylinders are used in the test rig, which can easily be disabled from the test rig and changed.
- Two different types of hydraulic cylinders are used in the test rig, depending on the fixation tool used in the test rig. Both hydraulic cylinders are dimensioned to achieve the required loads for each of their load cases.
- With a geometrical size of 3 m wide, 2 m high and 550 mm in depth, the test rig fulfills the geometrical requirement.
- The main steel structure of the test rig weigh 5,5 metric tons, which is less than the maximum weight determined in the requirement specification.
- The test rig with its fixation tools are designed so that sensors for measuring the applied loads, as well as the displacement either already are or can be incorporated into the test rig.
- The test rig has a modular mounting system with mounting points equally spread apart, but due to its enclosed testing space for spreader components it can't be seen as fully modular.

6 FURTHER DEVELOPMENT AND FUTURE WORK

The chapter for further development and future work presents the additional work needed in order to realize the test rig, as well as describing some further modifications that can be done to the test rig in order to get an even more modular design.

6.1 Further development

In order to realize the fatigue testing rig, as Bromma intends to, additional systems and components needs to be design and dimensioned.

Because the thesis has been concentrated on the design of the main steel structure of the test rig and dimensioning of the most critically stressed components, some additional dimensioning and possibly some redesigning of minor stressed components needed. It's also advisable that an experienced structural analysis goes through the fatigue calculations and dimensioning carried out in the thesis to ensure that no errors have been made. After desirable changes have been made to the design of the final concept of the test rig, detailed drawings, assembly drawings and manufacturing documentation can be made.

When the design of the main steel structure is determined the complete hydraulic system, that will power the hydraulic cylinders in the test rig, have to be designed and dimensioned. This system needs to fulfill the required pressure and a required flow to power the hydraulic cylinders so they can apply the maximum desired loads for all the load cases, as well as be able to reach a satisfying cycle time in order to keep the testing time down.

A control system has to be established, where both the hardware and the software need to be incorporated in to the fatigue testing rig. This system will link together with the selected sensors that are already incorporated in to the fixation tools for the selected spreader components. The system will mainly be controlled by measuring the applied load and displacement, via the sensors, during the fatigue testing. Additional strain gauges can be added to the test objects if further information has to be retrieved. The software for the control system can either be a custom made program in e.g. Labview or standard software program that can be bought in. The setup for the software, especially concerning how the program should respond during unforeseen events, can be programed according to the examples mentioned in 2.3.2 *Recommendations for design of a fatigue testing rig* under the paragraph "Sensors, control system, detection methods and safety".

6.2 Future work

The final concept that's been developed in the thesis is based on solid main plates as the main load bearing parts of the test rig. Because standard components have been used throughout the whole design of the test rig, one of its outer dimensions have been restricted to a maximum of 2 m due to the selection of using standard size steel plates. This makes it a compromise between allowing enough space for the test objects within the test rig and the size of the cross section area of the main plates, which gives the test rig its stiffness.

During the design of the final concept, different ideas for an adjustable main plate were thought out, as seen in Figure 6.1. These concepts allowed the test rig to be built bigger than the restrictions when using a solid main plate, while still using standard size plates. It should however be emphasized that these concepts relies on load bearing pins that would be highly stressed in the test rig, as well as the area surrounding the holes where they mount. The pins would also allow each beam in the substructure of the main plate to rotate around the pin, thus reducing the stiffness of the main plate.

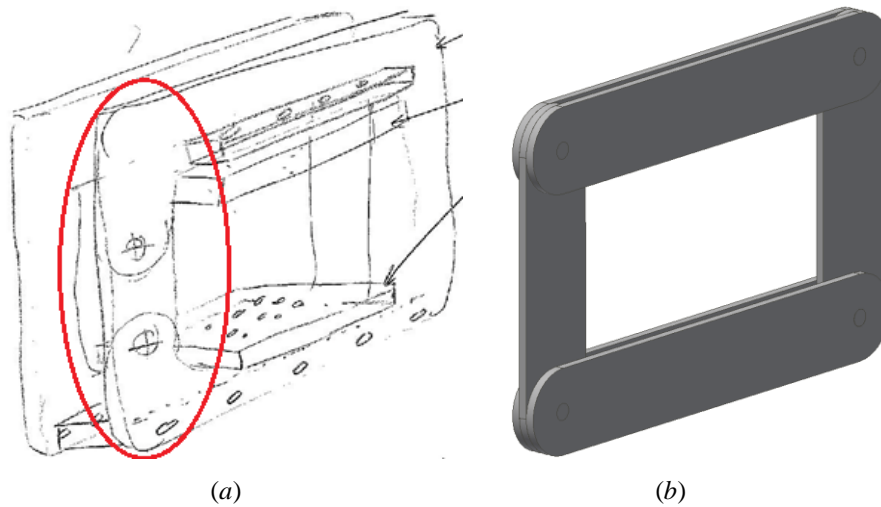


Figure 6.1. Adjustable main plate substructures

The red circle in Figure 6.1a shows the first initial sketched concept of adapting a solid main plate substructure, so that the height of the test rig can be adjusted. This concept uses an upper and a lower part of the main plate that is cut in a U-shape. The height of the main plate is regulated by selecting a suitable length of the mid-section parts that mounts to each end of the U-shape. Due to the U-shape of the upper and lower beam for this concept, stress concentrations will occur in the inner radiuses of these beams in a similar way as for the solid main plate. A second simplified concept (Figure 6.1b) was therefore thought of that is easier to manufacture, while its parts can be cut to a more basic geometry and directly to the preferred dimensions of the fatigue testing rig. It uses steel plate that are cut as straight beams and mounted together with pins in each corner of the main plate. This concept would however have greater deformations compared to the other concept, which is not preferable in a fatigue testing rig.

It should be noted that when using pins in a fatigue testing rig, excessive play can occur in the mounting points where the pins are located. This excessive play can in turn affect the fatigue testing, giving misleading results from the fatigue testing, as well as weakening the test rig and reducing its estimated fatigue life.

To further develop the steel structure in the final concept of the test rig to an even more modular design, which dimensions aren't restricted in the same way as for the solid main plate, further studies have to be made.

7 REFERENCES

AG, B., 2013. http://www.brosa.net/uploads/media/Datasheet_for_inquiry-Load_pin_V2013.pdf. [Online]

Available at: http://www.brosa.net/uploads/media/Datasheet_for_inquiry-Load_pin_V2013.pdf [Accessed 30 4 2014].

And, 2010. *Hydraulic Servo Valves*. [Online]

Available at: <http://www.valvehydraulic.info/creation-and-control-of-fluid-flow/hydraulic-servo-valves.html>

[Accessed 21 1 2014].

Bakhitiari, S., 2013. *Fatigue behaviour of welded components under variable amplitude loading*, Stockholm: KTH Industrial engineering and management.

Berg, H., 2014. *Study visit at Scania, Södertälje* [Interview] (9 1 2014).

Bergman, T., 2007. *Bromma Conquip products - Evaluation of new material for housing*, Hudiksvall: HIAB Development laboratory.

Bergman, T., 2013. *Bromma - Fatigue test Guide Neck*, Hudiksvall: HIAB Development laboratory.

Bergman, T., 2013. *Study visit at HIAB, Hudiksvall* [Interview] (13 11 2013).

Björk, K., 2013. HÅLLFASTHETSLÄRA. In: K. Björk, ed. *Formler och tabeller för mekanisk konstruktion*. Spånga: Karl Björks Förlag HB, pp. 24-31.

Boardman, B., 1990. Fatigue resistance of steels. In: *ASM Handbook Volume 01: Properties and Selection: Irons, Steels, and High-Performance Alloys*. s.l.:ASM International, pp. 673-688.

Bromma, 2013. *Bromma, Bromma products*. [Online]

Available at: <http://www.bromma.com/show.php?id=1192542> [Accessed 4 12 2013].

Bromma, 2013. *Company presentation*. [Online]

Available at: <http://www.bromma.com/show.php?id=1017198> [Accessed 14 11 2013].

Bromma, 2013. *Introduction program, Module 2*. Stockholm: Bromma.

Bromma, 2014. *Material list*. Stockholm: Bromma.

Colly, 1995. 4. Beräkning och dimensionering. In: C. C. AB, ed. *Handbok om skruvförband*. Stockholm: Sundell Reklam & Tidningsproduktion AB, pp. 21.22, 32-33, 44.

Credit1Coach, 2012. *Bromma spreader sts 45*. [Online]

Available at: <http://credit1coach.com/wp-includes/images/smilies/bromma-spreader-sts-45> [Accessed 27 11 2013].

- eFunda, 2014. *eFunda*. [Online]
Available at: http://www.efunda.com/formulae/solid_mechanics/fatigue/fatigue_highcycle.cfm
[Accessed 06 01 2014].
- Enerpac, 2013. *RR-Series, Double-Acting Cylinders*. [Online]
Available at: http://www.enerpac.com/sites/default/files/rr_326e_gb.pdf
[Accessed 30 4 2014].
- ESDEP, 2014. *SystemX*. [Online]
Available at:
<http://www.systemx.fr/meca/cm/ESDEP/Volume%2012/Lecon%2008/Francais/L12-8.pdf>
[Accessed 07 01 2014].
- Esteve, 2012. *Esteve, Harbour mobile crane Gottwald HMK 260E*. [Online]
Available at: http://www.esteve.ee/gottwald_eng.html
[Accessed 2 12 2013].
- Fatemi, A., 2013. *eFatigue*. [Online]
Available at: https://www.efatigue.com/training/Chapter_4.pdf
[Accessed 16 12 2013].
- François, D., 2008. 6.2. High-cycle fatigue tests – endurance limit. In: D. François, ed. *Structural Components: Mechanical Tests and Behavioral Laws*. London: ISTE Ltd and John Wiley &, p. 131.
- Frank Cervone, H., 2009. Applied digital library project management: Using Pugh matrix analysis in complex decision-making situations. *OCLC Systems & Services*, 25(4), pp. 228 - 232.
- Galín, G., 2010. *Institute of aviation*. [Online]
Available at: <http://ioa.edu.pl/about-2/msrc/>
[Accessed 14 01 2014].
- Geis, G., 2013. The approach to the fully electric spreader. *Port technology international*, Volume 38, p. 68.
- Hedegård, J. & Östling, H., 2013. *Study visit to Swerea/KIMAB* [Interview] (25 11 2013).
- Hobbacher, A., 2007. 3. Fatigue resistance. In: A. Hobbacher, ed. *Recommendations for fatigue design of welded joints and components*. Paris: International insitute of welding, pp. 41- 47, 93, 111.
- Hyco, A., 2013. *Hyco Alabama - Introduction to Hydraulic Cylinders*. [Online]
Available at: <http://www.hycoalabama.com/introductiontocylinders.php>
[Accessed 21 1 2014].
- Konecranes, 2013. *Konecranes, Ship-to-shore Gantry Cranes*. [Online]
Available at: <http://www.konecranes.com/equipment/container-handling-cranes/ship-to-shore-gantry-cranes>
[Accessed 2 12 2013].
- KTH, 2008. Dimensionering av flänsförband. In: I. f. maskinkonstruktion, ed. *Maskinelement Handbok*. Stockholm: Institutionen för maskinkonstruktion, pp. 66-67, 77.

Lindström, J., 2010. *Test equipment specification - STS45E Main beam roller test jig*. Ipoh: Bromma.

Mrden, N., 2013. *Study visit at Volvo Construction Equipment, Eskilstuna* [Interview] (5 12 2013).

MTS, 2014. *MTS, Test Componnets, Actuators & Hydraulic Components*. [Online]
Available at: <http://www.mts.com/en/products/producttype/test-components/actuators-hydraulic-components/actuators/index.htm>
[Accessed 29 03 2014].

Nachtwey, P., 2006. *machine design - Guidelines for sizing servohydraulics*. [Online]
Available at: <http://machinedesign.com/archive/guidelines-sizing-servohydraulics>
[Accessed 21 1 2014].

Nord-Lock, 2014. En jämförelse av vanliga skruvåtdragningsmetoder. *Bolted, Number 10*, p. 19.

Olsson, C., 2007. 7 Uttmattningsbelastade svetsförband. In: C. Olsson, ed. *Konstruktionshanbok för svetsade konstruktioner*. Stockholm: Lieber AB, pp. 140-143.

PMC_group, 2013. *Dubbelverkande hydraulcylinder LHA 25*. [Online]
Available at:
<http://www.pmcgroup.se/PageFiles/6093/PMC%20Cylinders%20LHA%2025.pdf?epslanguage=sv>
[Accessed 30 4 2014].

Rao, J., 2011. In: *History of Rotating Machinery Dynamics*. Bangalore: Springer Science, pp. 327-328.

RDP_group, 2013. *Series RSL0720*. [Online]
Available at: <http://www.rdpe.com/pdfs/rsl0720.pdf>
[Accessed 30 4 2014].

Roymech, 2013. *Roymech*. [Online]
Available at: http://www.roymech.co.uk/Related/Hydrostatics/Hydraulic_Calcs.html
[Accessed 03 04 2014].

Shigley, J. E., Mischke, C. R. & Budynas, R. G., 2003. Fatigue failure resulting from variable loading. In: *Mechanical Engineering Design*. New York: McGraw-Hill, pp. 305-393.

SORT+STORE, 2004/2005. *SORT+STORE, Advanced Container Handeling*. [Online]
Available at: <http://www.sort-and-store.com/media/pdf/press-gps04.pdf>
[Accessed 2 12 2013].

SSAB, 2010. 5. Uttmattning. In: SSAB, ed. *Plåthandboken*. Borlänge: Höglund Design AB.

SSAB, 2010. 5.6.6 Beräkningsgång. In: *Plåthandboken*. Borlänge: Österbergs Sörmlandstryck AB.

Sundström, B., 1999. Materialtabell för kolstål, stållegeringar och ståljutgods. In: B.

Sundström, ed. *Handbok och formelsamling i Hållfasthetslära*. Stockholm: Institutionen för hållfasthetslära KTH, pp. 372-379.

Sundström, B., 1999. Tvärsnittdata för massiva tvärsnitt och tunnväggigt rör. In: B. Sundström, ed. *Handbok och formelsamling i Hållfasthetslära*. Stockholm: Institutionen för hållfasthetslära KTH, pp. 322-337.

Sundström, B., 1999. Utmattning. In: B. Sundström, ed. *Handbok och formelsamling i Hållfasthetslära*. Stockholm: Institutionen för hållfasthetslära KTH, pp. 283-308.

Terex, 2013. *Terex, Rubber-Tyred Gantry Cranes*. [Online]
Available at: <http://www.terex.com/port-solutions/en/products/new-equipment/stacking-cranes/rubber-tyred-gantry-cranes/index.htm>
[Accessed 2 12 2013].

Ulrich, K. T. & Eppinger, S. D., 2012. Concept development: The front-end process. In: *Product design and development 5th edition*. New York: McGraw Hill, pp. 16-18.

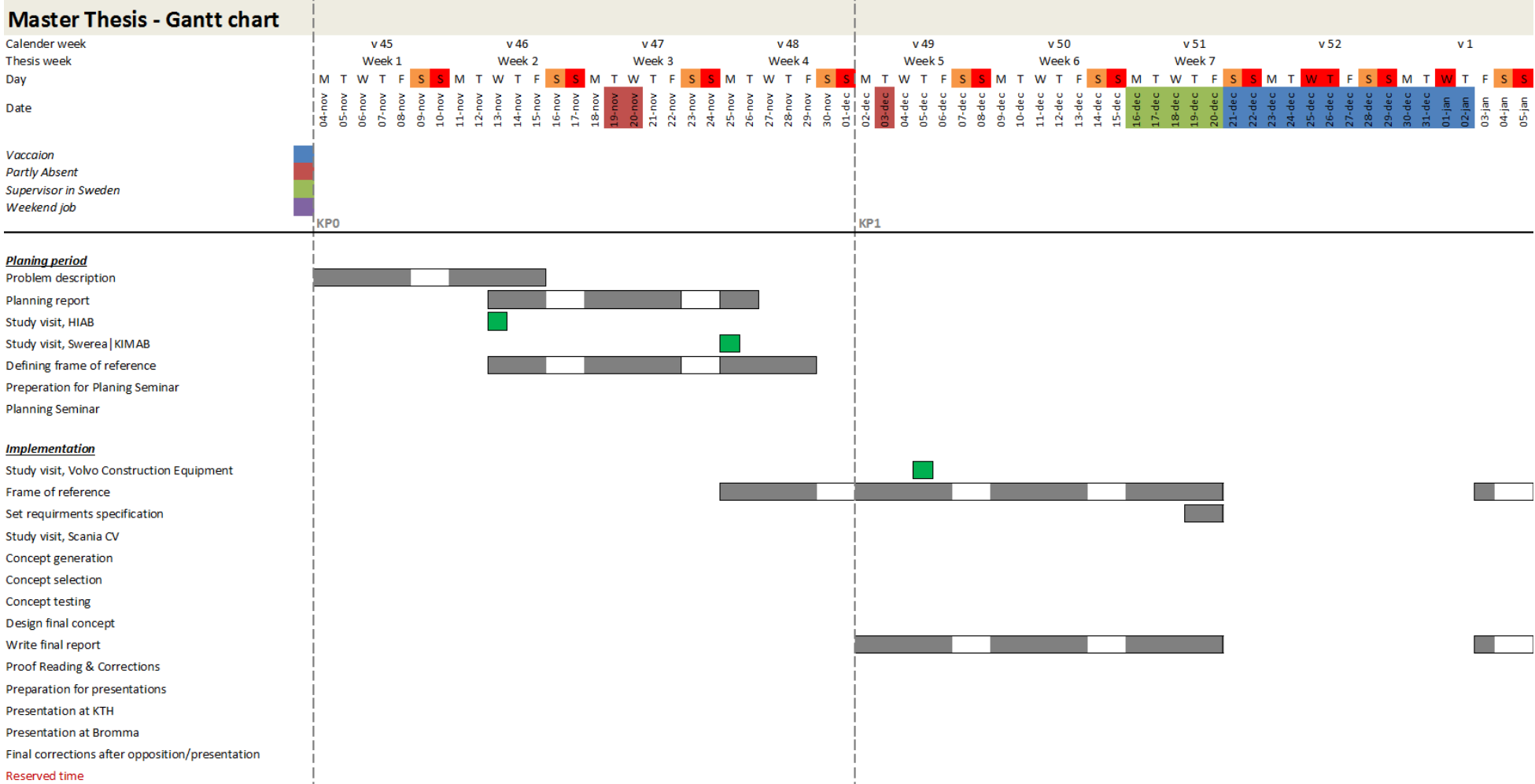
Vervoort, D. -I. S. & Wurmman, D.-I. G., 2014. *ATZonline*. [Online]
Available at:
<http://www.atzonline.com/index.php;do=show/site=a4e/sid=GWV/alloc=38/id=61/special=Special+Simulation>
[Accessed 07 01 2014].

Wiber, 2013. *Wiber - Tryckskruv DIN6332*. [Online]
Available at: <http://www.wiberger.se/templates/din6332.htm>
[Accessed 1 5 2014].

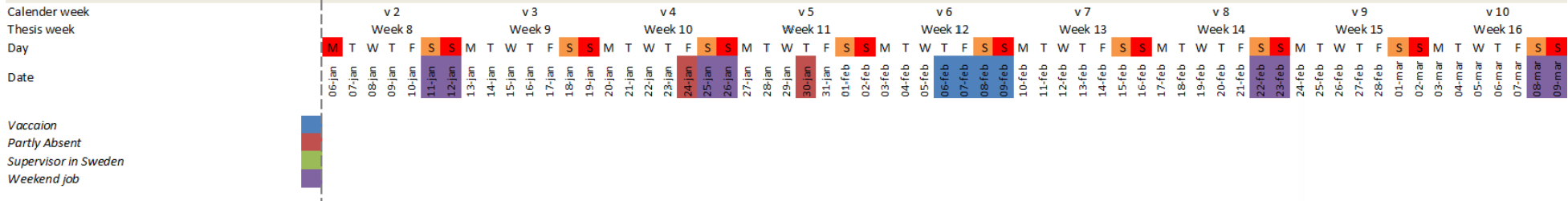
Wimer, N., 2013. *Basic Fatigue Analysis - Neil Wimer*. [Online]
Available at: <http://neilwimer.weebly.com/basic-fatigue-analysis.html>
[Accessed 20 12 2013].

APPENDIX A: GANTT CHART

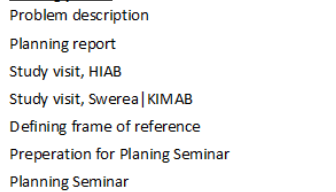
Appendix A shows the detailed Gantt-chart, with its highlighted mile stones, that was used during the master thesis. The chart was regularly updated during the thesis depending on the actual required time for a task, as well as taking into account certain absences and vacations.



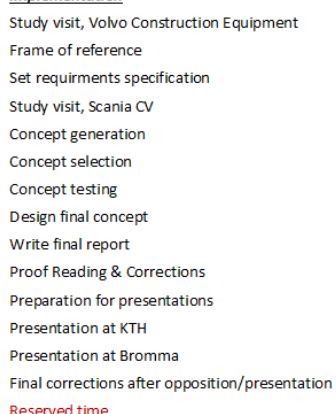
Master Thesis - Gantt chart



Planing period

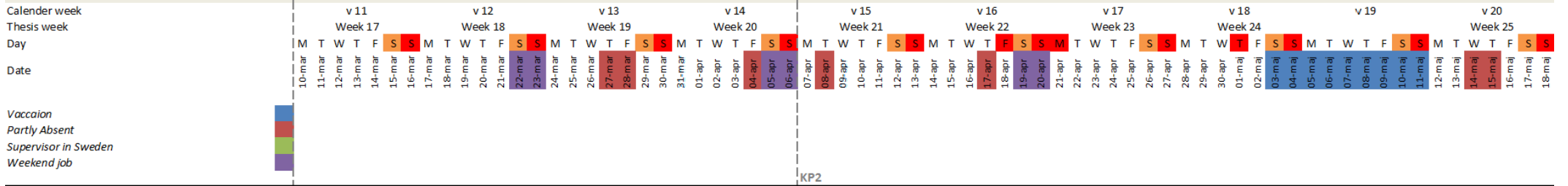


Implementation



Reserved time

Master Thesis - Gantt chart



Planing period

- Problem description
- Planning report
- Study visit, HIAB
- Study visit, Swerea | KIMAB
- Defining frame of reference
- Preperation for Planing Seminar
- Planning Seminar

Implementation

- Study visit, Volvo Construction Equipment
- Frame of reference
- Set requirments specification
- Study visit, Scania CV
- Concept generation
- Concept selection
- Concept testing
- Design final concept
- Write final report
- Proof Reading & Corrections
- Preparation for presentations
- Presentation at KTH
- Presentation at Bromma
- Final corrections after opposition/presentation

Reserved time

APPENDIX B: CALCULATIONS OF LOAD CASES FOR THE THREE SELECTED SPREADER COMPONENTS

Appendix B shows the test values and load cases given by Bromma (in Swedish), to which the test rig and the fixation tools are designed and dimensioned.

Testförutsättningar

20 st centerwebplates.

1. 500.000
2. 1.000.000
3. 2.000.000
4. 4.000.000

Guideblock. 20 st

Testas med 245kN som max, tre test per guideblockdesign =60 tester totalt

Växelhus. 20 st

1. 50.000
2. 150.000
3. 300.000

Test 1, center webplate

Krafter på undre lyftplattan

$$T := \frac{5 \text{ tonne} \cdot g}{4} \cdot 1.61 = 201 \text{ kN}$$

Last på en TB (förenklad, skevhet i end beam ej beaktad)

$$L_1 := 5847 \text{ mm} \quad L_2 := 1653 \text{ mm}$$

$$R_{45} := T \cdot \frac{L_1}{L_2}$$

$$R_{40} := T \cdot \frac{L_1}{L_2 + 2.5 \text{ ft}}$$

$$R_{20} := T \cdot \frac{L_1}{L_2 + 12.5\text{ft}}$$

$$R_{\text{Twin45}} := R_{45} \cdot \frac{32.5\text{tonne}}{51\text{tonne}}$$

$$R_{\text{Twin40}} := R_{40} \cdot \frac{32.5\text{tonne}}{51\text{tonne}}$$

$$R_{45} = 712 \cdot \text{kN}$$

$$R_{40} = 487 \cdot \text{kN}$$

$$R_{20} = 215 \cdot \text{kN}$$

$$R_{\text{Twin45}} = 454 \cdot \text{kN}$$

$$R_{\text{Twin40}} = 311 \cdot \text{kN}$$

$$R := (R_{20} \ R_{\text{Twin40}} \ R_{\text{Twin45}} \ R_{40} \ R_{45})^T$$

$$R_1 := \max(R) = 712 \cdot \text{kN}$$

Fördelning mellan olika typ av lyft:

$$S := (25 \ 12.5 \ 12.5 \ 45 \ 5)^T \% \quad 20 \text{ ft, twin 40ft, twin 45ft, 40ft, 45ft}$$

Lastspektrumsfaktor map på containervikt: $k_{\text{mass}} := 0.25$

Spänningsspektrumfaktor: $k_{\text{stress}} := k_{\text{mass}} \cdot \sum_{i=0}^4 \left[S_i \cdot \left(\frac{R_i}{R_1} \right)^3 \right]$

$$k_{\text{stress}} = 0.061$$

Antal cykler vid maxlast som motsvarar 2 milj cykler variabel last:

$$N_1 := k_{\text{stress}} \cdot 2 \cdot 10^6 = 1.22 \times 10^5 \quad \text{dvs klarar vi } N_1 \text{ cykler med last } R_{\text{max}} \text{ så klarar vi 2 milj cykler i verkligheten.}$$

Last som behövs för brott vid 1 milj cykler: $R_2 := \sqrt[3]{2} \cdot R_1 = 897.14 \cdot \text{kN}$

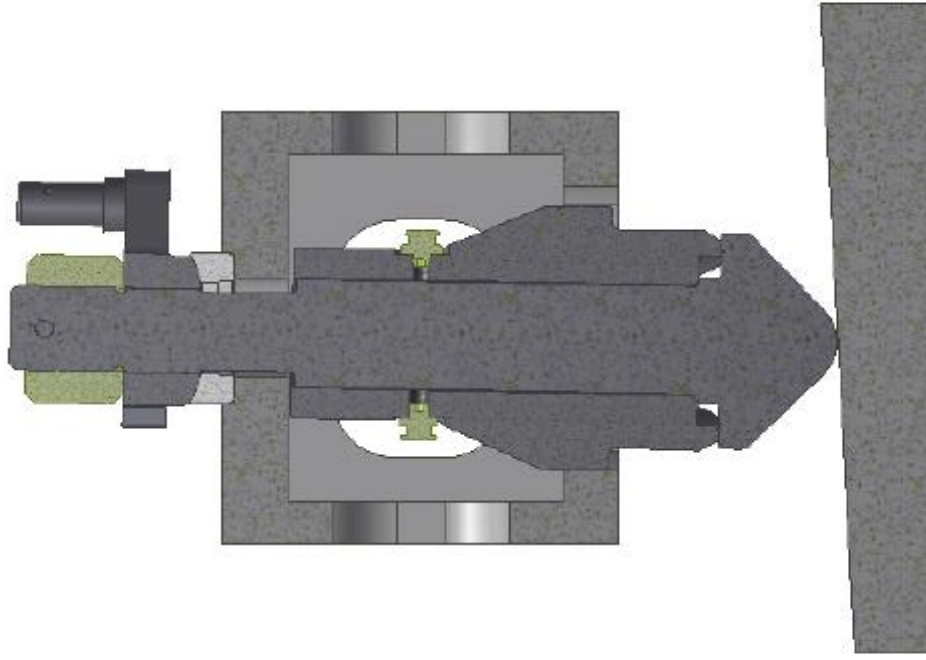
Last som behövs för brott vid 0,5 milj cykler: $R_3 := \sqrt[3]{4} \cdot R_1 = 1.13 \times 10^3 \cdot \text{kN}$

Last som behövs för brott vid 4 milj cykler: $R_4 := \sqrt[3]{0.5} \cdot R_1 = 565.163 \cdot \text{kN}$

Sammanfattning lastfall centerwebplate:

Antal cykler för spreader	500000	1000000	2000000	4000000
Motsvarande cykler i test	30494	60988	121976	243952
Last [kN]	1130	897	712	565

Lastfall guideblock



Lasten appliceras på ovsidan av testboxen med innehållande twistlock assembly. Testboxen styrs i sidled. Den nedre träffytan har tillräcklig lutning så att twistlocken snedställs vid belastning.

$$F_{2,\max} := 12.5\text{tonne} \cdot g \cdot 2 = 245.166 \text{ kN}$$

Anta att varje guideblockdesign testas vid tre testnivåer, 1 milj cykler, 500.000 cykler och 100.000 cykler.

$$F_2 := \left(F_{2,\max} \sqrt[3]{0.5 \cdot F_{2,\max}} \sqrt[3]{0.1 \cdot F_{2,\max}} \right)^T$$

$$F_2^T = (245.166 \quad 194.589 \quad 113.796) \text{ kN} \quad \text{Lastnivåer för guideblock test}$$

Lastfall växelhus

$$M_V := 2.200\text{mm} \cdot 25\text{kN} = 10 \cdot \text{kN} \cdot \text{m}$$

$$\text{FAT} := 160\text{MPa} \quad (\text{Osäker på detta värde})$$

$$\sigma := 72.4\text{MPa} \quad \text{Spänning vid } M_V$$

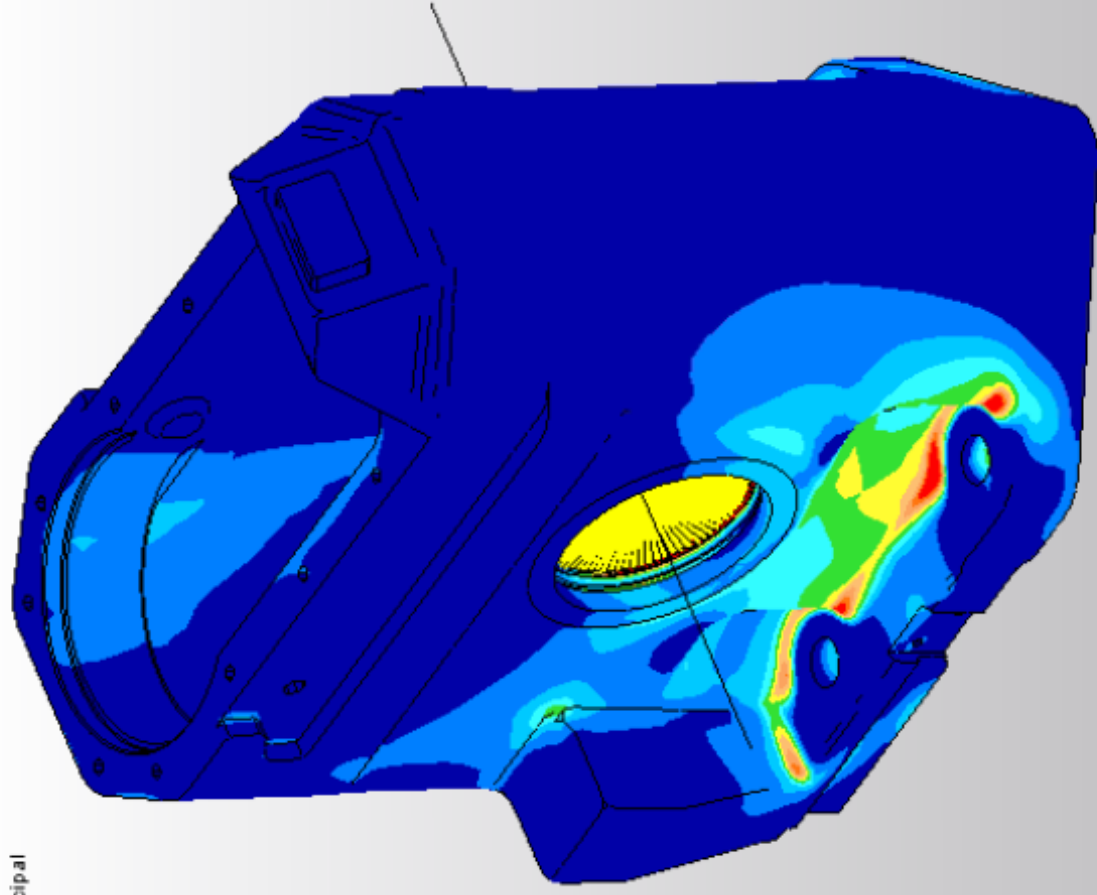
$$A := \frac{\sigma}{M_V} = 7.24 \cdot \frac{\text{MPa}}{\text{kN} \cdot \text{m}}$$

$$M_{V50} := \frac{\text{FAT}}{\sqrt[5]{\frac{1}{50000} \cdot A}} = 46 \cdot \text{kN} \cdot \text{m} \quad \sigma_{50} := M_{V50} \cdot A = 335 \cdot \text{MPa}$$

$$M_{V150} := \frac{\text{FAT}}{\sqrt[5]{\frac{1}{150000} \cdot A}} = 37 \cdot \text{kN} \cdot \text{m} \quad \sigma_{150} := M_{V150} \cdot A = 269 \cdot \text{MPa}$$

$$M_{V300} := \frac{\text{FAT}}{\sqrt[5]{\frac{1}{300000} \cdot A}} = 32 \cdot \text{kN} \cdot \text{m} \quad \sigma_{300} := M_{V300} \cdot A = 234 \cdot \text{MPa}$$

Stress
Maximum Principal
N/(mm²)



Sammanfattning växelhus

Antal cykler	50000	150000	300000
Last [kNm]	46	37	32

Exempel på spänningsspektrumsfaktor:

Anta att spänningarna på en viss punkt i testriggen blir:

$\Delta\sigma_0 := 200\text{MPa}$ för centerwebplate test med största lasten för centerwebplate test

$\Delta\sigma_1 := 150\text{MPa}$ för guideblock test på 245kN

$\Delta\sigma_2 := 100\text{MPa}$ för växelhustest med högsta växelhuslasten

De individuella spänningsspektrumsfaktorerna blir då (om vi antar att punkten vi tittar på är svetsad):

För centerwebplate testet:

$$R_1 = 712.061 \text{ kN} \quad R_2 = 897.14 \text{ kN} \quad R_3 = 1.13 \times 10^3 \text{ kN}$$

laster för centerwebplatetest

$$R_4 = 565.163 \text{ kN}$$

$$F_1 := (R_1 \ R_2 \ R_3 \ R_4)^T$$

$$F_{1,\max} := \max(R_1, R_2, R_3, R_4) = 1.13 \times 10^3 \text{ kN}$$

$$n_1 := \left(1.22 \times 10^5 \ 6.099 \times 10^4 \ 3.049 \times 10^4 \ 2.44 \times 10^5 \right)^T$$

$$n_{\text{tot}0} := \sum_{i=0}^3 n_{1_i} \quad n_{\text{tot}0} = 4.575 \times 10^5$$

$$kQ_0 := \sum_{i=0}^3 \left[\frac{n_{1_i}}{n_{\text{tot}0}} \cdot \left(\frac{F_{1_i}}{F_{1.\text{max}}} \right)^3 \right] = 0.267$$

För guideblock testet.

$$F_{2.\text{max}} := 245 \text{ kN}$$

Anta att varje guideblockdesign testas vid tre testnivåer, 1 milj cykler, 500.000 cykler och 100.000 cykler.

$$F_2 := \left(F_{2.\text{max}} \sqrt[3]{0.5 \cdot F_{2.\text{max}}} \sqrt[3]{0.1 \cdot F_{2.\text{max}}} \right)^T$$

$$F_2^T = (245 \quad 194.457 \quad 113.719) \text{ kN}$$

$$n_2 := (100000 \quad 500000 \quad 1000000)^T$$

$$n_{\text{tot}1} := \sum_{i=0}^2 n_{2_i} \quad n_{\text{tot}1} = 1.6 \times 10^6$$

$$kQ_1 := \sum_{i=0}^2 \left[\frac{n_{2_i}}{n_{\text{tot}1}} \cdot \left(\frac{F_{2_i}}{F_{2.\text{max}}} \right)^3 \right] = 0.281$$

För växelhustestet

$$M_V := (M_{V50} \quad M_{V150} \quad M_{V300})^T$$

$$M_{Vmax} := \max(M_V)$$

$$M_{Vmax} = 46.216 \text{ kN}\cdot\text{m}$$

$$n_3 := (50000 \quad 150000 \quad 300000)^T$$

$$n_{tot_2} := \sum_{i=0}^2 n_{3_i} \quad n_{tot_2} = 5 \times 10^5$$

$$kQ_3 := \sum_{i=0}^2 \left[\frac{n_{3_i}}{n_{tot_2}} \left(\frac{M_{V_i}}{M_{Vmax}} \right)^3 \right] = 0.46$$

Sammanräknad spänningsspektrumfaktor:

$$N_{TOT} := 20 \cdot \left(\sum_{i=0}^2 n_{tot_i} \right) = 5.115 \times 10^7 \quad \text{totalt antal lastcykler som riggen ska dimensioneras för}$$


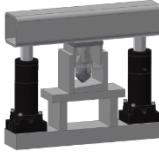
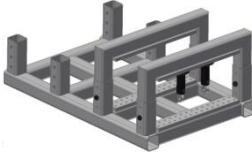
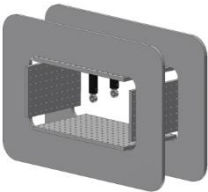
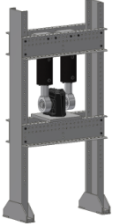

$$\Delta\sigma_{max} := \max(\Delta\sigma) = 200 \text{ MPa}$$

$$k_{tot} := \sum_{i=0}^2 \left[\frac{n_{tot_i}}{N_{TOT}} \cdot kQ_i \left(\frac{\Delta\sigma_0}{\Delta\sigma_{max}} \right)^3 \right] = 0.011 \quad \text{spänningsspektrum faktor för testriggen.}$$

$$B := \begin{pmatrix} 50000 & 150000 & 300000 \\ \frac{M_{V50}}{\text{kN}\cdot\text{m}} & \frac{M_{V150}}{\text{kN}\cdot\text{m}} & \frac{M_{V300}}{\text{kN}\cdot\text{m}} \end{pmatrix}$$

APPENDIX C: PUGH'S MATRIX

The scored Pugh's matrix with weighted factors.

Factors	Weight	HIAB's test rig	Concept 1	Concept 2	Concept 3	Concept 4	Concept 5
Picture							
Geometrically dimensioned to fit the three selected spreader component	5	B A S E L I N E	1	2	2	3	1
Modular mounting solution for hydraulic cylinders	3		0	1	3	2	1
Easily disable one hydraulic cylinder under normal setup	2		-3	1	1	1	1
Ability to manufacture the test rig at Bromma's own manufacturing facility	2		0	0	2	0	2
Use of readily available material and components at Bromma's manufacturing facility	2		0	0	2	-1	-1
Use of standard parts and components to reduce complexity	2		0	0	-1	2	1
Reduce the amount of welds	3		1	-2	3	2	3
Reduce the amount of subcomponents	2		2	-1	2	-2	-1
Modular design	4		0	1	2	3	1
Accessibility and general ease of mounting and dismounting test objects	1		2	1	1	2	2
Ability to move the test rig	3		2	-2	0	-1	1
Ease of maintenance, service and repair	3		3	0	1	3	2
Ability to perform multi-axial fatigue testing	2		0	0	3	1	0
General safety aspects concerning user safety during fatigue testing	4		-2	0	1	0	0
Long life time on subcomponents that are effected to wear	3		1	0	1	-1	-1
Cost of operation	4		n/a	n/a	n/a	n/a	n/a
Manufacturing cost	2		n/a	n/a	n/a	n/a	n/a
Total +		0	12	6	24	19	15
Total -		0	-5	-5	-1	-5	-3
Overall total		0	7	1	23	14	12
Weighted total		0	18	6	65	46	33

APPENDIX D: FEA OF MAIN PLATE FOR CONCEPT TESTING

FEA performed for determining the maximum principal stresses as well as the total deflection in one main plate.

All of the results from the FEA of the main plate in 3.5 Concept testing are illustrated and presented in Figure 1-6. The FEA was performed with a subjecting force F of 250 kN, 500 kN, 1000 kN.

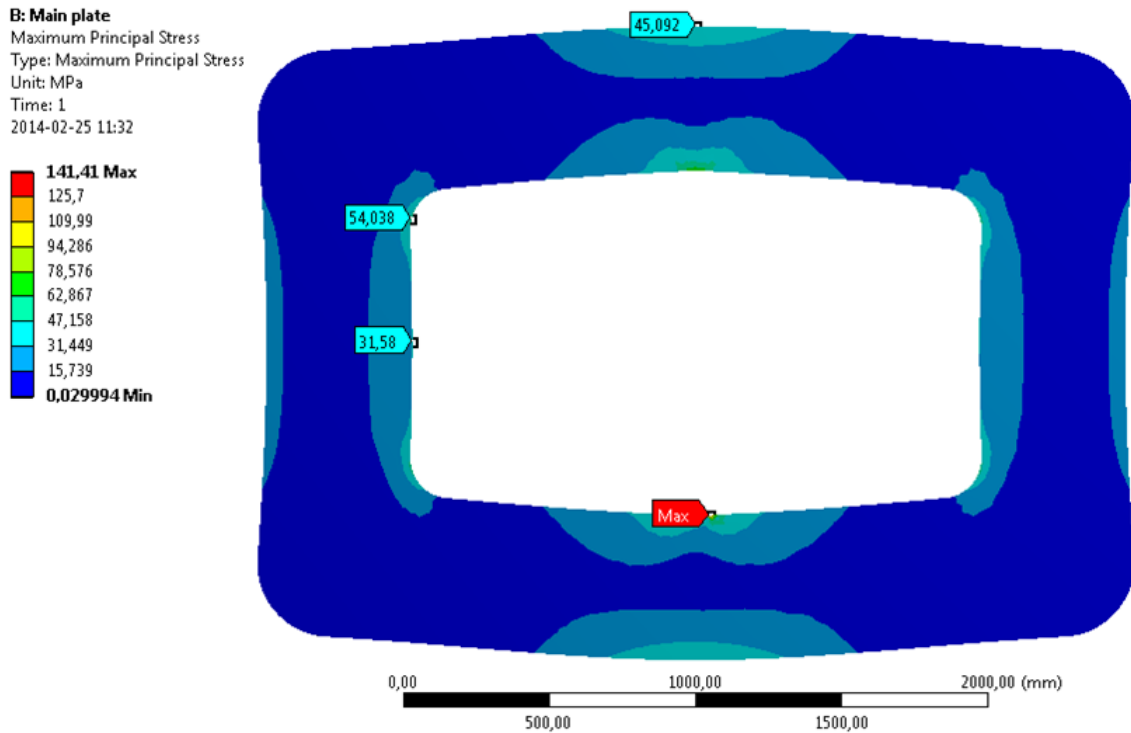


Figure 1. The maximum stresses for the main plate at a force of 250 kN

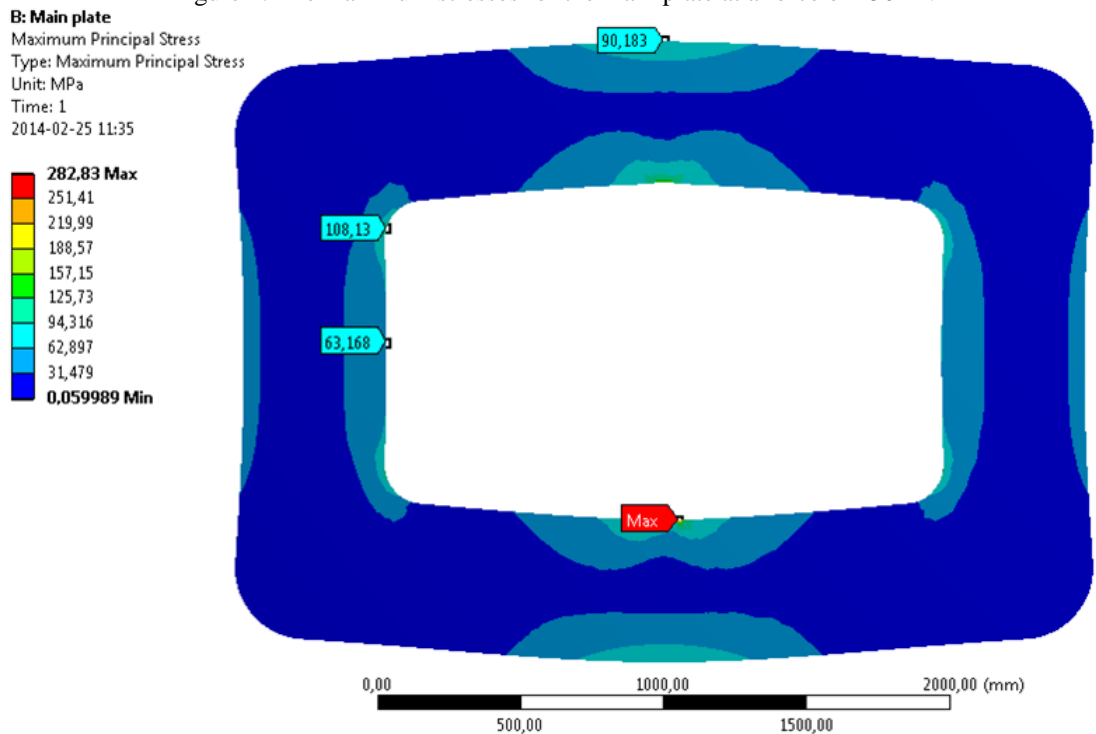


Figure 2. The maximum stresses for the main plate at a force of 500 kN

B: Main plate
 Maximum Principal Stress
 Type: Maximum Principal Stress
 Unit: MPa
 Time: 1
 2014-02-25 11:41

565,65 Max
 502,82
 439,98
 377,14
 314,31
 251,47
 188,63
 125,79
 62,957
 0,11998 Min

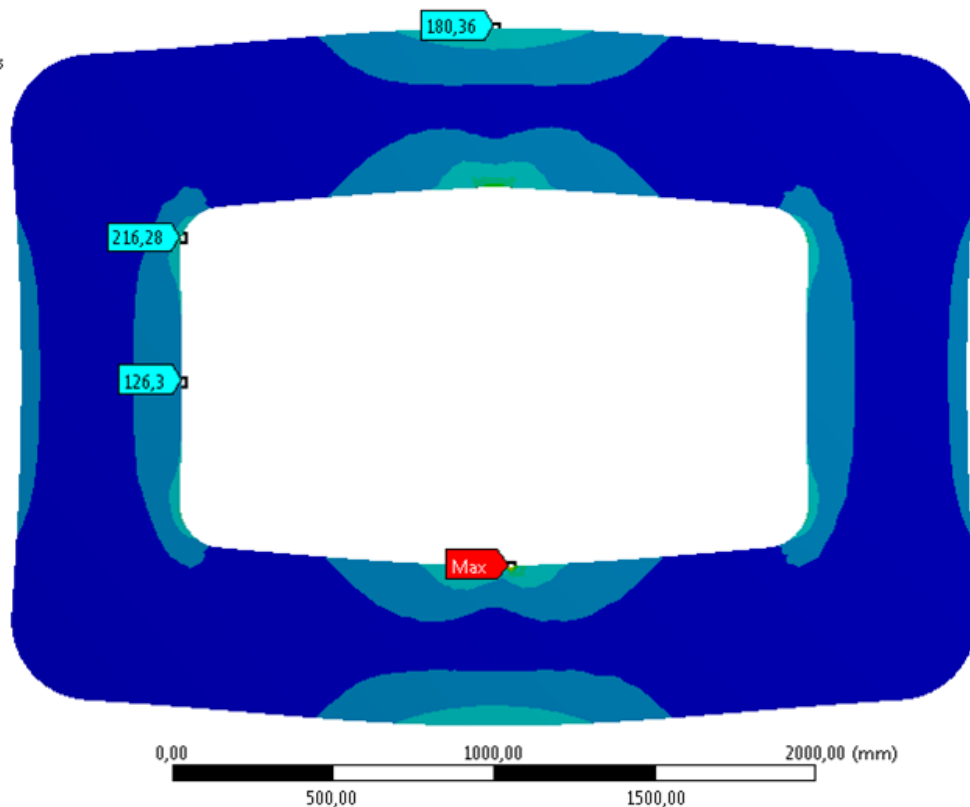


Figure 3. The maximum stresses for the main plate at a force of 1000 kN

B: Main plate
 Total Deformation
 Type: Total Deformation
 Unit: mm
 Time: 1
 2014-02-25 11:30

0,90594 Max
 0,80528
 0,70462
 0,60396
 0,5033
 0,40264
 0,30198
 0,20132
 0,10066
 0 Min

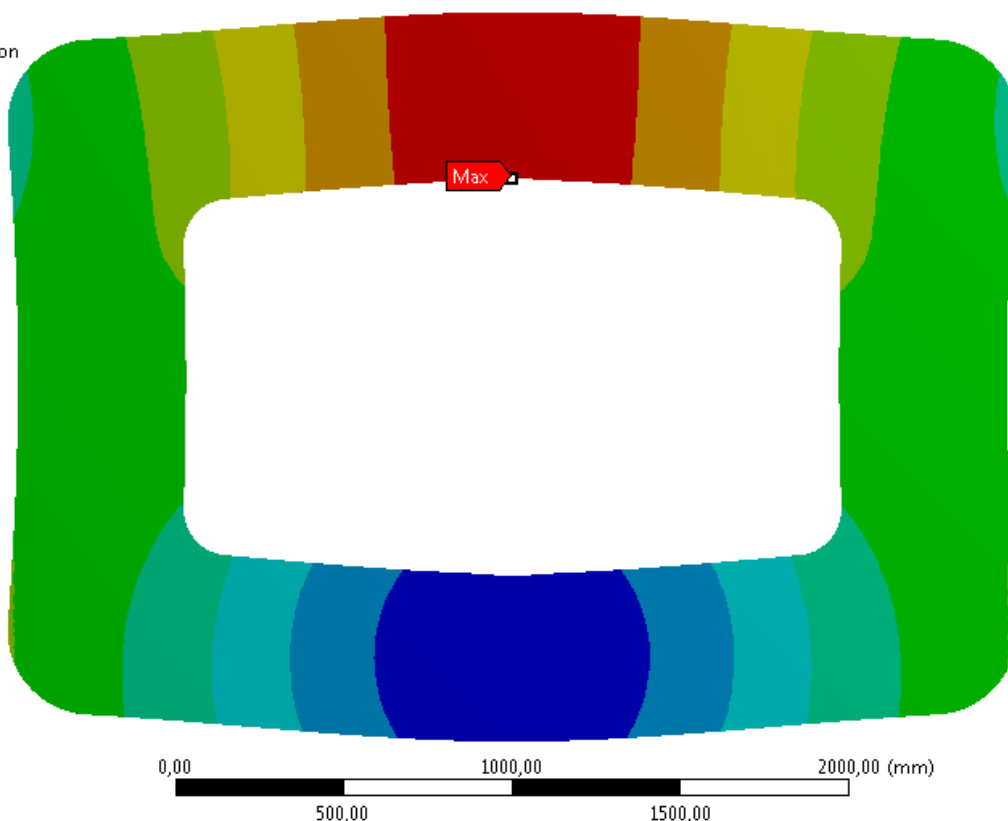


Figure 4. The total deflection in the center for the main plate at a force of 250 kN

B: Main plate
Total Deformation
Type: Total Deformation
Unit: mm
Time: 1
2014-02-25 11:34

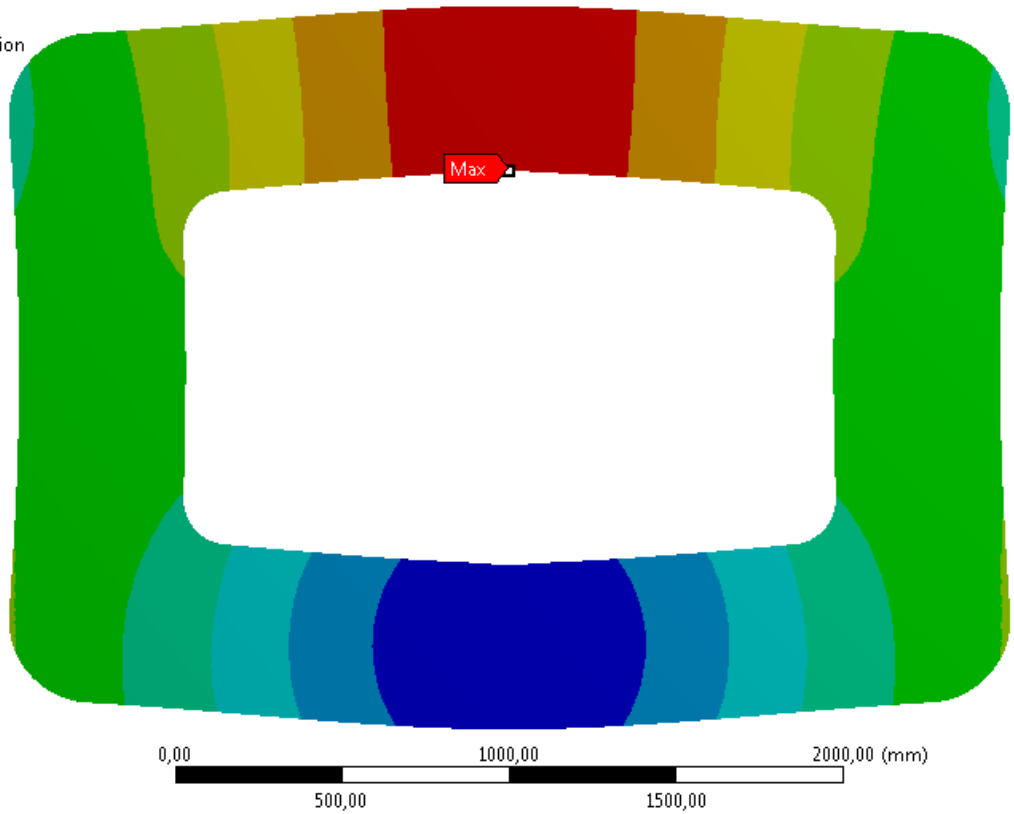
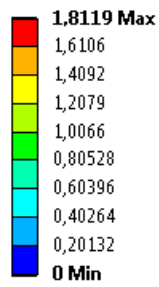


Figure 5. The total deflection in the center for the main plate at a force of 500 kN

B: Main plate
Total Deformation
Type: Total Deformation
Unit: mm
Time: 1
2014-02-25 11:39

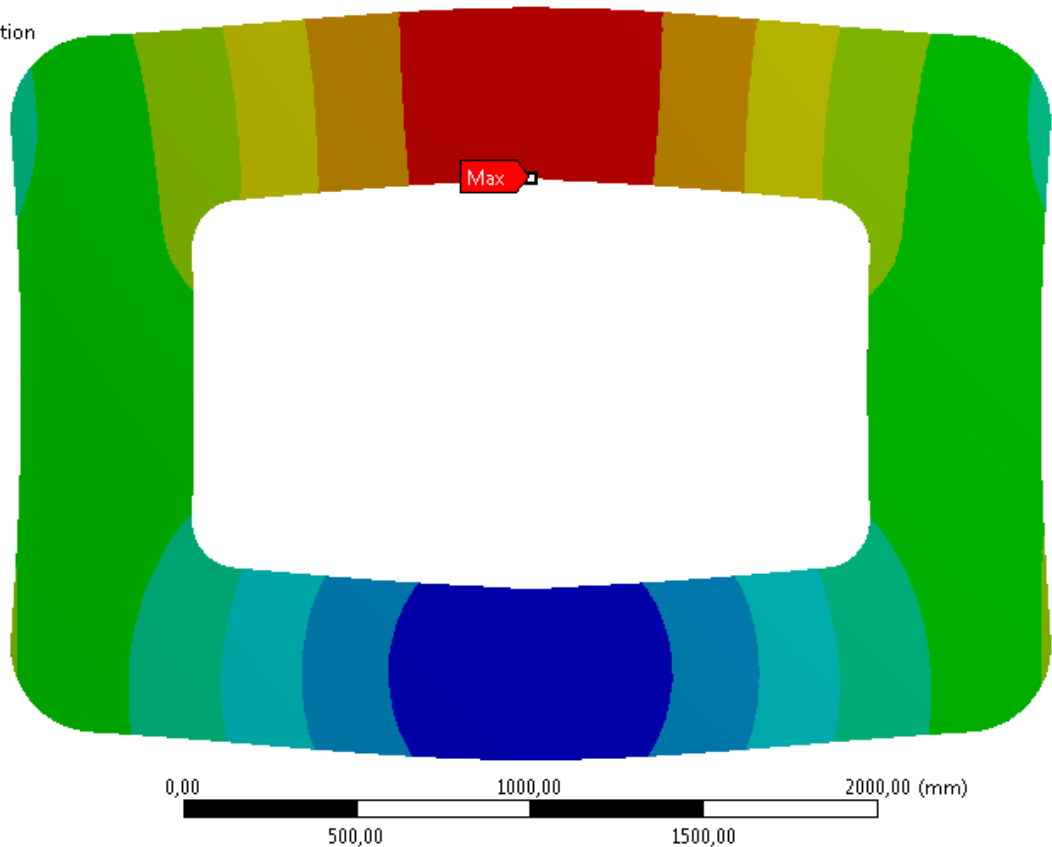
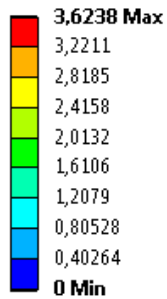


Figure 6. The total deflection in the center for the main plate at a force of 1000 kN

APPENDIX E: MATLAB CODE FOR THE INTITAL TESTING

MATLAB-code for determining the maximum stresses as well as the deflection for both Section A and Section B in one main plate, as well as for the lever arm solutions.

MATLAB code for calculating the main plate

```
clc
clear all

%% Single main plate calculations for Concept 3

% SECTION A

b = 50e-3; % Width of the "beam"
h = 500e-3; %Height of the "beam"
E = 208e9 ; %Young's modulus for the material of the beam. [Pa]

Iy = (b*h^3)/12; % For solid beam, the upper part of the main plate 500x50mm

Lm = 2.5; % Length of horizontal "beam" of main plate

x = 0.25; % Ratio between simply supported and fixed support

fatot = [];
fbtot = [];
sigmaatot1 = [];
sigmaatot2 = [];
Ftot = [];

for F = 0:50e3:1000e3

    % Simply supported
    fa = (F*Lm^3)/(48*E*Iy); % Deflection in the center of the "beam" [m]
    Mmax1 = (F*Lm)/4; % Maximum torque in the "beam" [Nm]
    sigmaa1 = (Mmax1/Iy)*(h/2); % Maximum stress in the "beam" [MPa]

    % Fixed support
    fb = (F*Lm^3)/(192*E*Iy); % Deflection in the center of the "beam" [m]
    Mmax2 = (F*Lm)/8; % Maximum torque in the "beam" [Nm]
    sigmaa2 = (Mmax2/Iy)*(h/2); % Maximum stress in the "beam" [MPa]

    Ftot = [Ftot F];
    fatot = [fatot fa];
    fbtot = [fbtot fb];
    sigmaatot1 = [sigmaatot1 sigmaa1];
    sigmaatot2 = [sigmaatot2 sigmaa2];

end

sigmaatot = sigmaatot1.*x + sigmaatot2.*(1-x);
ftot = fatot.*x + fbtot.*(1-x);

% SECTION B

A = b*h; % Area of cross section
Ln = 1.5; % Length of vertical "beam" of main plate

deltatot = [];
sigmabt1 = [];
```

```

sigmabt2 = [];

for F = 0:50e3:1000e3

    % Simply supported
    delta = ((F/2)*Ln)/(E*A);
    sigmab1 = (F/2)/A;

    %Fixed supported
    M = (F*Lm)/8; % Reacting bending moment from the upper part of the main
plate
    Mmax = M; % Due to constant torque over the whole beam
    sigmab2 = (Mmax/Iy)*(h/2) + sigmab1; % Maximum stress, Bending AND
tensile [MPa]

    deltatot = [deltatot delta];
    sigmabt1 = [sigmabt1 sigmab1];
    sigmabt2 = [sigmabt2 sigmab2];

end

sigmabt = sigmabt1.*x + sigmabt2.*(1-x);

% Total deflection in y-axis of the main plate
totdef = ftot.*2 + deltatot;

% Plotting the deflection
figure(1)
plot (Ftot*10^-3, ftot*10^3, Ftot*10^-3, deltatot*10^3, Ftot*10^-3,
totdef*10^3);
title('The deflection as a function of the subjecting force')
xlabel('Subjecting force [kN]');
ylabel('The deflection in the center [mm]');
legend('Section A', 'Section B', 'Total deflection of the main plate (y-
axis)');
grid on

% Plotting the maximum stress
figure(2)
plot (Ftot*10^-3, sigmaatot*10^-6, Ftot*10^-3, sigmabt*10^-6);
title('Maximum stress as a function of the subjecting force')
xlabel('Subjecting force [kN]');
ylabel('Maximum stress [MPa]');
legend('Section A', 'Section B');
grid on

% BUCKELING
Iz = (h*b^3)/12; % For solid beam, the vertical part of the main plate
500x50mm (weak side)

Pk = ((pi^2)*E*(2*Iz))/(Ln^2);

disp(' ')
disp(['The buckeling force is ', num2str(Pk*10^-3), ' kN']);

% ANSYS values

Ff = [0 250 500 1000]; % Force [kN]

ASecA = [0 45.092 90.183 180.36]; % Maximum stress in section A [MPa]
ASecB = [0 31.58 63.168 126.3]; % Maximum stress in section B [MPa]

```

```

ARadius = [0 54.038 108.13 216.28]; % Maximum stress in Radius [MPa]
Adefltot = [0 0.90594 1.8119 3.6238]; % Maximum deflection [MPa]

% Plotting the maximum stress
figure(3)
plot (Ftot*10^-3, sigmaatot*10^-6, Ftot*10^-3, sigmabt*10^-6, 'LineWidth',
3);
hold on
plot (Ff, ASecA, Ff, ASecB, Ff, ARadius)
hold off
title('Maximum stress as a function of the subjecting force')
xlabel('Subjecting force [kN]');
ylabel('Maximum stress [MPa]');
legend('Section A (Calculated)', 'Section B (Calculated)', 'Section A (FEA)',
'Section B (FEA)', 'Inner radius (FEA) ');
grid on

% Plotting the deflection
figure(4)
plot (Ftot*10^-3, totdef*10^3, 'r', 'LineWidth', 3);
hold on
plot (Ff, Adefltot, 'r')
hold off
title('The total deflection of the main plate as a function of the subjecting
force')
xlabel('Subjecting force [kN]');
ylabel('The deflection in the center [mm]');
legend('Total deflection of the main plate (Calculated)', 'Total deflection
of the main plate (FEA)');
grid on

if ASecA(end) > (sigmaatot(end)*10^-6)
    devSecA = (ASecA(end)-(sigmaatot(end)*10^-6))/(sigmaatot(end)*10^-6);
else
    devSecA = ((sigmaatot(end)*10^-6)-ASecA(end))/ASecA(end);
end

if ASecB(end) > (sigmabtot(end)*10^-6)
    devSecB = (ASecB(end)-(sigmabtot(end)*10^-6))/(sigmabtot(end)*10^-6);
else
    devSecB = ((sigmabtot(end)*10^-6)-ASecB(end))/ASecB(end);
end

if Adefltot(end) > (totdef(end)*10^3)
    devdef = (Adefltot(end)-(totdef(end)*10^3))/(totdef(end)*10^3);
else
    devdef = ((totdef(end)*10^3)-Adefltot(end))/Adefltot(end);
end

disp(' ')
disp(['The devation in Section A is ', num2str(devSecA*100), ' %']);
disp(' ')
disp(['The devation in Section B is ', num2str(devSecB*100), ' %']);
disp(' ')
disp(['The devation for the total deflection is ', num2str(devdef*100), '
%']);

```


MATLAB code for calculating the lever arm solutions

```
clc
clear all

%% Lever arm solution

% AREA MOMENT OF INERTIA FOR AN H- OR I-BEAM

h = 330e-3; %height [m]
b = 160e-3; %width [m]
t1 = 7.5e-3; %thickness of web [m]
tf = 11.5e-3; %thickness of flange [m]

Iy = ((t1*(h-tf)^3)/12)+(1/2)*tf*b*(h-tf)^2; %For IPE 330 (dimensions
330mmx160mm)
Iys = (b*h^3)/12; % For solid beam with dimensions 330x160mm

% Deflection of beam

Fsubject = 520e3; %Subjecting force [N]
ratio = 2.2; %Ratio [m]
E = 208e9 ; %Young's modulus for the material of the beam. [Pa]
Fapplied = Fsubject/ratio; %Applied force at the end of the beam [N]

ftot = [];
btot = [];
sigmatot = [];

% I-beam
for b = 1:0.001:2 %Total length of the beam [m]
    L = b/(ratio+1); %Distance between the supports [m]
    a = b-L; %Distance from force to the none-fixating support [m]

    f = (Fapplied*(a^2)*b)/(3*E*Iy); % Deflection of I-beam [m]

    Mmax = Fapplied * a; % Maximum torque in the I-beam [Nm]
    sigma = (Mmax/Iy)*(h/2); % Maximum stress in the I-beam [MPa]

    btot = [btot b];
    ftot = [ftot f];
    sigmatot = [sigmatot sigma];
end

f2tot = [];
sigma2tot = [];

%Solid beam
for b = 1:0.001:2 %Total length of the beam [m]
    L = b/(ratio+1); %Distance between the supports [m]
    a = b-L; %Distance from force to the none-fixating support [m]

    f = (Fapplied*(a^2)*b)/(3*E*Iys); % Deflection of solid beam [m]

    Mmax = Fapplied * a; % Maximum torque in the solid beam [Nm]
    sigma = (Mmax/Iys)*(h/2); % Maximum stress in the solid beam [MPa]

    f2tot = [f2tot f];
    sigma2tot = [sigma2tot sigma];
end
```

```

% Plotting the deflection as a function of the length of the beam
figure(1)
plot (btot, ftot*10^3, btot, f2tot*10^3);
title('The deflection as a function of the total length of the lever arm')
xlabel('Total length of the lever arm [m]');
ylabel('The deflection at the end of the lever arm [mm]');
legend('I-beam', 'Solid beam');
grid on
% ylim([0 50])

% Plotting the maximum stress as a function of the length of the beam
figure(2)
plot (btot, sigmatot*10^-6, btot, sigma2tot*10^-6);
title('Maximum stress as a function of the total length of the lever arm')
xlabel('Total length of the lever arm [m]');
ylabel('Maximum stress in the lever arm [MPa]');
legend('I-beam', 'Solid beam');
axis ([1 2 0 750])
grid on

%% Short beam

Ls = 0.5:0.001:1.5; % Length of short beam [m]

H = 240e-3; % [m]
B = 160e-3; % [m]
bb = 2; % Amount of beams [N]

Iysb = (B*H^3)/12;

Mmax = ((CWPS_F(1)/bb).*Ls)/4; % Maximum torque in the solid beam [Nm]
sigmaS = (Mmax./Iysb)*(h/2); % Maximum stress in the beam [MPa]

% Plotting the maximum stress as a function of the length of the beam
figure(3)
plot (Ls, sigmaS*10^-6);
title('Maximum stress as a function of the length of the beam')
xlabel('Length of beam [m]');
ylabel('Maximum stress [MPa]');
grid on

```

APPENDIX F: MATLAB CODE FOR LOAD BEARING I-BEAM FOR THE CENTER WEB PLATE SUBSTRUCTURE

MATLAB-code for iteratively determining the design of the load bearing I-beam.

```
clc
clear all

%% Beam at CWPS

CWPS_F = [1130e3 897e3 712e3 565e3]; % Subjecting forces [N]
CWPS_N = [30494 60988 121976 243952]; % Number of cycles [N]
Ls = 0.5:0.001:1.5; % Length of short beam [m] MAX in model 1.2m

% -----
Fi = CWPS_F;
ni = CWPS_N * 20; % 20 stands for the amount of times the tests are going to
be performed
Fmax = max(Fi);
Nt = sum(ni);
FAT = 90; m = 3; % Dimensioning values for continuous manual longitudinal
fillet weld
gammam = 1.21; % Partialkoefficient med hänsyn till brottrisk

km = sum((Fi./Fmax).^m.*(ni./Nt)); % Kollektivfaktorn
Sm = (Nt/(2*10^6))*km; % Spänningsförloppsparametern
deltaSRd = FAT/(gammam * nthroot(Sm, m)); % Tillåten spänningsvidd
deltaSRdv = ones(1,length(Ls))*deltaSRd; % Vector med samma värde
% -----

H = 300e-3; % [m]
B = 160e-3; % [m]
t1 = 50e-3; % Flange [m]
t2 = 30e-3; % Web [m]
c = 125e-3; % Distance from center plane to underside of flange [m]
bb = 1; % Amount of beams [N]

Iy = (B*H^3)/12 - (B*(H-2*t1)^3)/12 + (t2*(H-2*t1)^3)/12;

% Mmax = ((CWPS_F(1)/bb).*Ls)/4; % Maximum torque in the solid beam [Nm]
% sigmaS = (Mmax./Iy)*(H/2); % Maximum stress in the beam [MPa]
Mmax1 = ((CWPS_F(1)/bb).*Ls)/4; % Simply supported, force in middle, Maximum
torque in the beam [Nm]
Mmax2 = ((CWPS_F(1)/bb).*Ls)/8; % Simply supported, Even load over over beam,
Maximum torque in the beam [Nm]
sigmaS1 = (Mmax1./Iy)*(c); % Stress in under side of the flange
sigmaS2 = (Mmax2./Iy)*(c); % Stress in under side of teh flange

sigmaS = 0.5*sigmaS1 + 0.5*sigmaS2;

% Ploting the maximum stress as a function of the length of the beam
figure(1)
plot(Ls, sigmaS*10^-6, Ls, deltaSRdv, '--r');
title('Maximum stress as a function of the length of the I-beam')
xlabel('Effective length of I-beam [m]');
ylabel('Maximum stress [MPa]');
grid on
legend('Stress in the center of the flange', 'Maximum allowed stress range')
```

APPENDIX G: FEA OF MAIN LOAD BEARING BEAMS FOR THE CENTER WEB PLATE SUBSTRUCTURE

FEA performed for determining the reacting forces of the load bearing beams in the center web plate substructure.

While the custom designed and dimensioned I-beams will be the main load bearing part in the center web plate substructure, an FEA was performed in order to establish the reacting forces in Figure 1 (illustrated in purple). These reacting forces occur due to the non-linear load case over the center web plate substructure relative to its fixations. These obtained reaction forces from the FEA are used for the overall dimensioning of the fatigue testing rig. The load case in Figure 1 is with an applied force of $F = 1130 \text{ kN}$ over the center web plate substructure.

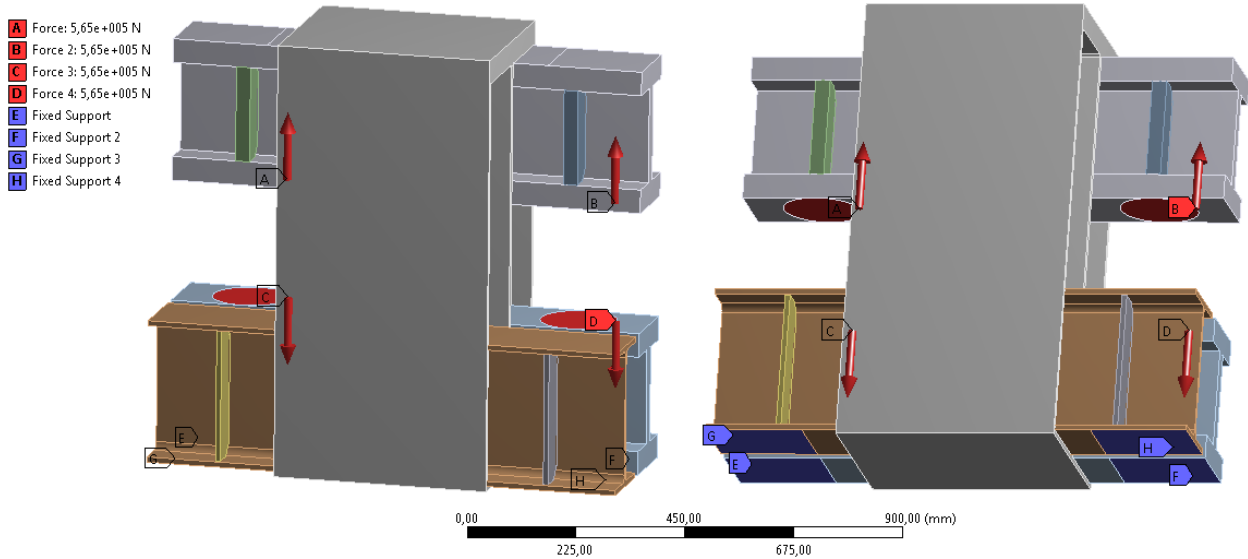


Figure 1. Applied loads on the main load bearing beams for the center web plate substructure

The thinner I-beam in Figure 1 (illustrated in brown) was only used as during the FEA. After the FEA was performed the I-beam was changed for a U-beam, while that type of beam allowed for better access to the bolts, i.e in order to tightening the mounting bolts to the desired prestress. Even though this change have been made for the fixation tool for the center web plate substructure, the reacting force in the U-beam will be equal with the one for the I-beam in Figure 1. The reacting forces in the mounting points of the beams are illustrated in Figure 2.

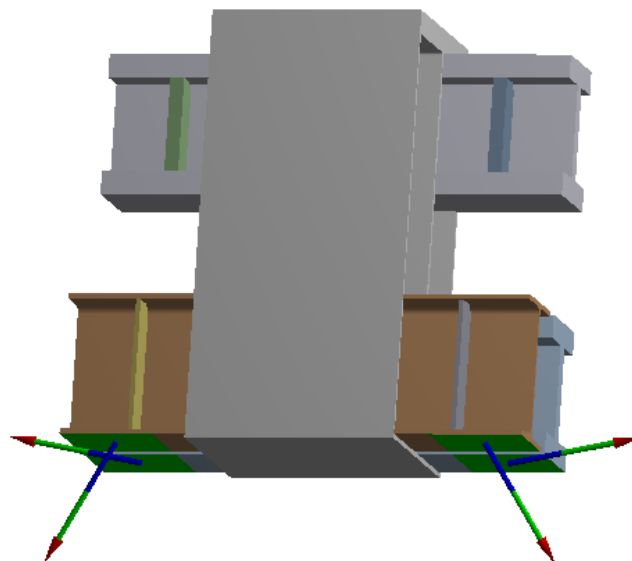


Figure 2. Illustrated reacting forces in the mounting points of the beams

The reacting force in area E and F, the mounting points for the custom designed and dimensioned I-beam, will be subjected to a compressional load of 34 kN according to the FEA, i.e the I-beam will be pushing down on to the fatigue testing rig. The reacting force in area G and H, the mounting points for the thinner I-beam, will in turn be subjected to a tensile load of 34 kN. The bolted joints for this beam therefore needs to be further dimensioned.

APPENDIX H: FEA OF THE MAIN STEEL STRUCTURE OF THE FATIGUE TESTING RIG

FEA performed for determining maximum equivalent stress in the complete fatigue testing rig.

After importing the shell model of the main steel structure of the fatigue testing rig to the FEA, a 50 mm plate thickness is added to all the parts in the model. The threaded rods that clamp the main and side box to the main plate subassembly are removed in this simplified model. All the contacts in the model are seen as bonded edge-edge contacts.

The meshing of the model is seen in Figure 1. A fine even mesh is used on the entire model, with further refined mesh on the inner mounting plates where the subjecting forces will be applied to the test rig.

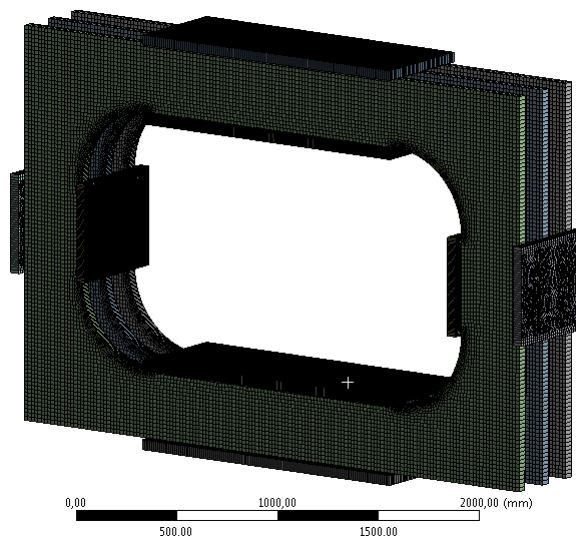


Figure 1. Meshed model of the main steel structure of the fatigue testing rig

All the subjecting loads for the different load cases, illustrated below, are for the highest load for each load case. The results of the maximum equivalent stresses for the lower loads for each load case can be scaled down from the results of the highest applied load, while the stresses are linear relative to the applied loads.

The subjecting loads (in this case the reacting forces obtained from *Appendix G*) and fixations for the fixation tool for the center web plate substructure are illustrated in Figure 2.

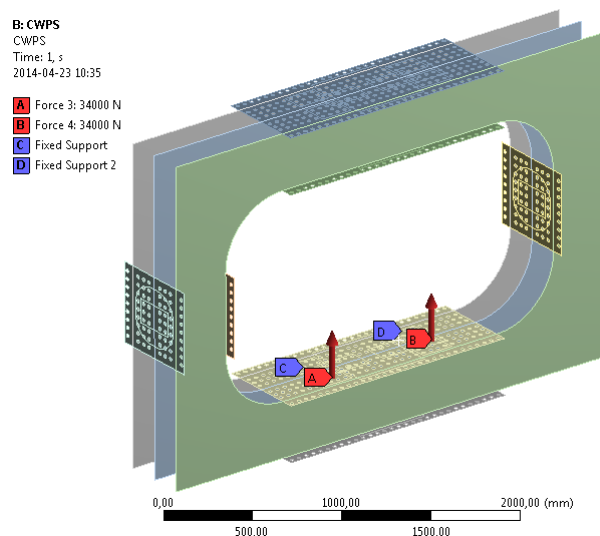


Figure 2. Subjecting loads and fixations when testing the center web plate substructure

The subjecting loads and fixations for the fixation tool for the twistlock assembly are illustrated in Figure 3.

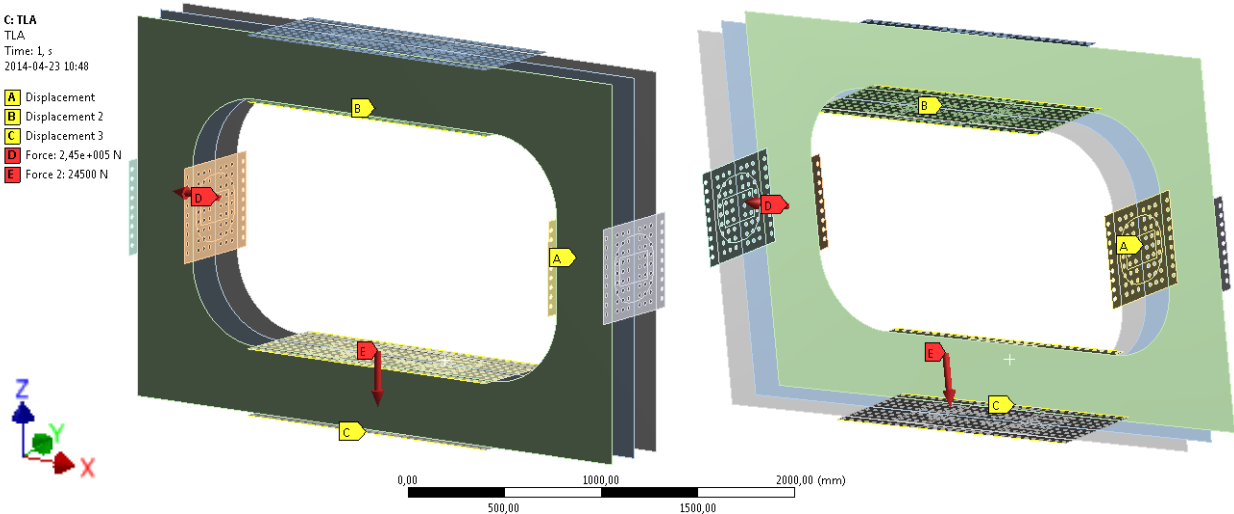


Figure 3. Subjecting loads and fixations when testing the twistlock assembly

The subjecting load in E is set to 10 % of the subjecting load in D, while it's the reacting lateral force that occurs due to the angulated plate that is used when applying the load (see Equation in 4.3.1 *Twistlock assembly*). In order to fixate the test rig so that no unwanted forces or moments will occur next to the fixations, three displacements are used to lock the test rig in each axis. Displacement A locks the interfacing plane on test rig in x-axis, displacement B locks the interfacing plane in z-axis and displacement C locks the edge of the outer mounting plate in y-axis.

The subjecting loads and fixations for the fixation tool for the gearbox housing are illustrated in Figure 4.

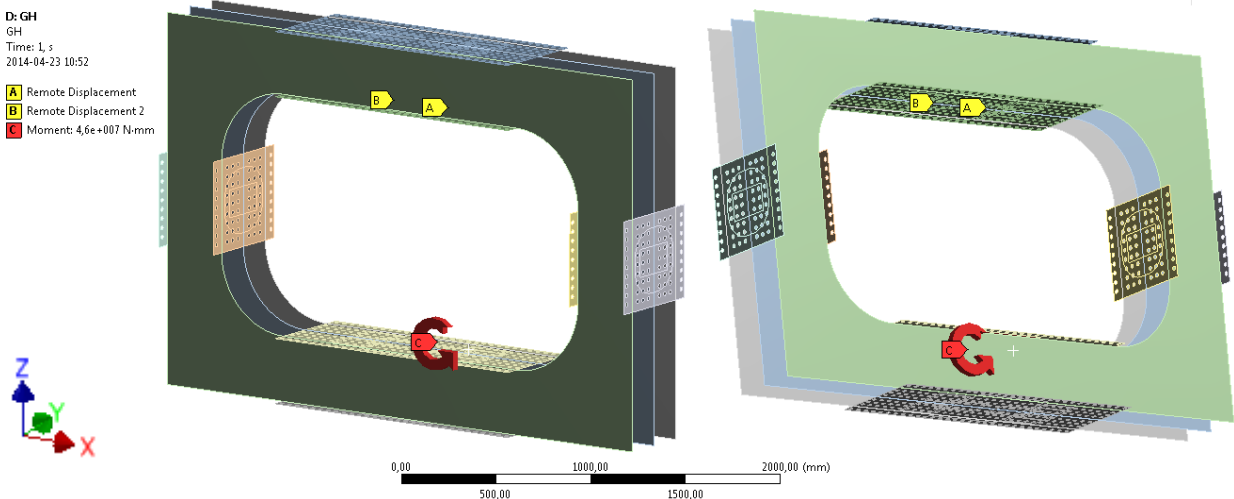


Figure 4. Subjecting loads and fixations when testing the gearbox housing

The subjecting torque (46 kNm) applies on the surface of the lower inner mounting plate where the adaptor plate for the gearbox housing interfaces with the test rig. The remote displacements A and B linearly lock the test rig in the center point of each of the two interfacing surfaces. This allows the surfaces in A and B to rotate in y-axis and follow the natural movement of the test rig when the torque is applied.

The maximum principal stresses for the highest load for each load case is obtained by running the FEA with the previously explained setups. The stresses for each load case are illustrated in Figure 5-7. The deformations shown in the Figures are magnified in order to observe how the rig deforms for each load case.

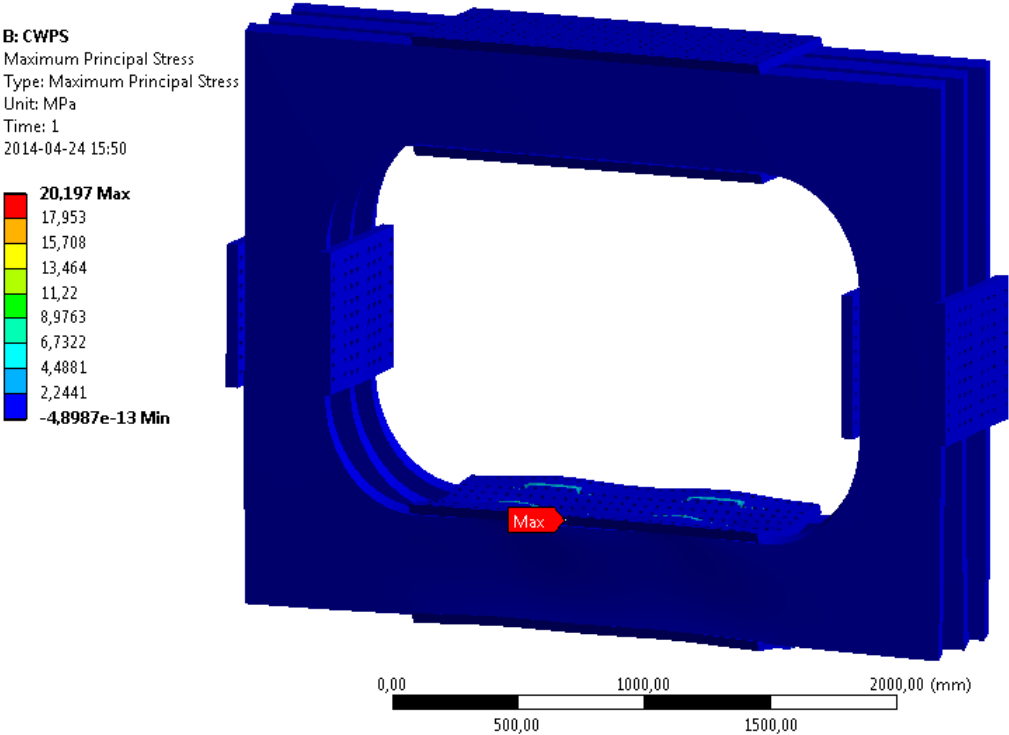


Figure 5. Maximum principal stresses in the test rig, when testing the center web plate substructure

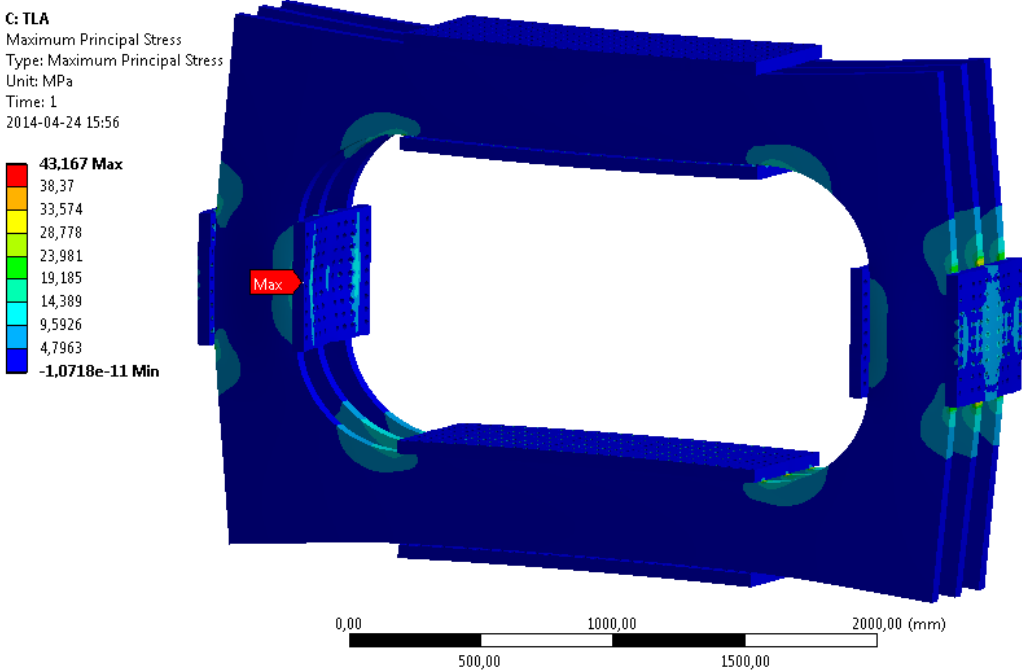


Figure 6. Maximum principal stresses in the test rig, when testing the twistlock assembly

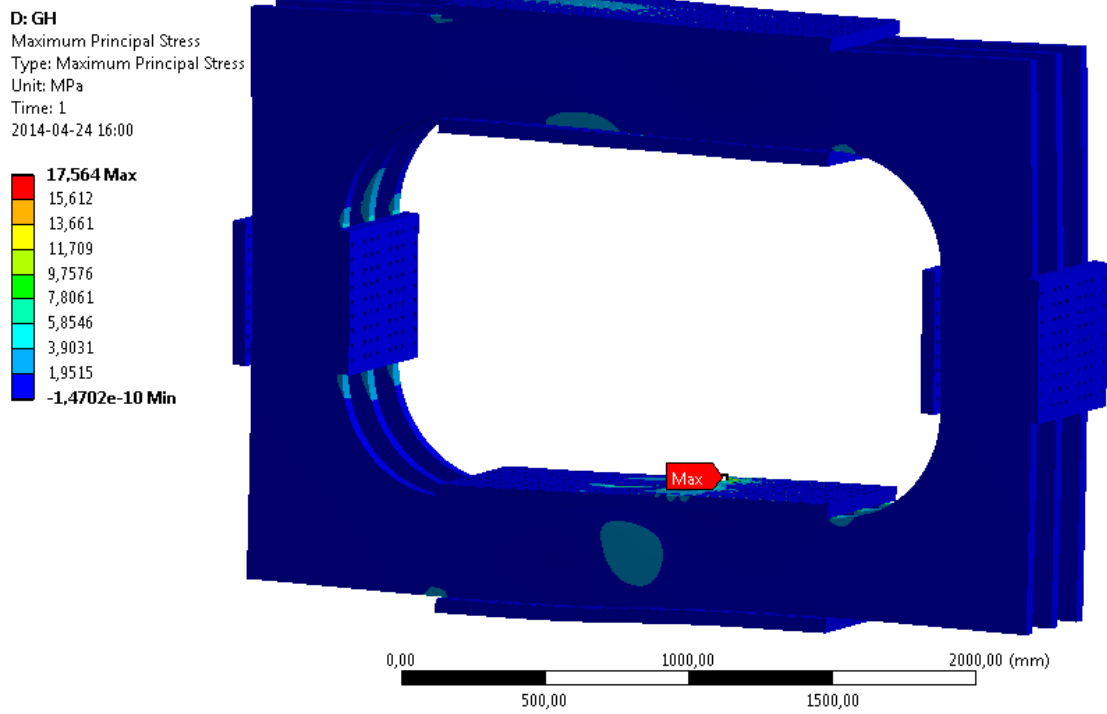


Figure 7. Maximum principal stresses in the test rig, when testing the gearbox housing